

ULTRA GAIN BOOST CONVERTER FED BLDC MOTOR FOR FCEV APPLICATIONS

A Major Project Report

Submitted in partial fulfillment of the
requirements for the award of the Degree of

BACHELOR OF TECHNOLOGY

IN

ELECTRICAL AND ELECTRONICS ENGINEERING

by

G. VINAY KUMAR (20P65A0222)

B. JHANSI (19P61A0218)

B. VINAY KUMAR (19P61A0217)

B. SANDEEP (20P65A0205)

Under the esteemed guidance of

Dr. B. NAGI REDDY M.Tech, Ph. D, MIEEE, MISRD

Associate Professor

DEPARTMENT OF ELECTRICAL & ELECTRONICS ENGINEERING

Counselling Code : **VBIT**



(A UGC Autonomous Institution, Approved by AICTE, Accredited by NBA & NAAC-A Grade, Affiliated to JNTUH)

VIGNANA BHARATHI INSTITUTE OF TECHNOLOGY

(An Autonomous Institution, Accredited by NBA and NAAC, New Delhi)

Aushapur(V), Ghatkesar (M), Medchal Dist, Telangana-501301

2019-23



(A UGC Autonomous Institution, Approved by AICTE, Accredited by NBA & NAAC-A Grade, Affiliated to JNTUH)

Aushapur (V), Ghatkesar (M), Medchal Dist, Telangana -501301
DEPARTMENT OF ELECTRICAL AND ELECTRONICS ENGINEERING

CERTIFICATE

This is to certify that major project report entitles, “**ULTRA GAIN BOOST CONVERTER FED BLDC MOTOR FOR FCEV APPLICATIONS**”, done by G. VINAY KUMAR (20P65A0222), B. JHANSI (19P61A0218), B. VINAY KUMAR (19P61A0217), B. SANDEEP (20P65A0205) submitted to the faculty of Electrical and Electronics Engineering in partial fulfillment of the requirements for the Degree of BACHELOR OF TECHNOLOGY from VBIT, Aushapur, Hyderabad.

Project Guide

Dr. B. NAGI REDDY M.Tech, Ph. D, MIEEE, MISRD
Associate Professor

Head of the Department

Dr. K. Neelima M.Tech, Ph. D, MISTE
Professor & HoD

EXTERNAL EXAMINER



(A UGC Autonomous Institution, Approved by AICTE, Accredited by NBA & NAAC-A Grade, Affiliated to JNTUH)

Aushapur (v), Ghatkesar (m), Medchal Dist., Telangana -501301

DEPARTMENT OF ELECTRICAL AND ELECTRONICS ENGINEERING

DECLARATION

We hereby declare that the project entitled “**ULTRA GAIN BOOST CONVERTER FED BLDC MOTOR FOR FCEV APPLICATIONS**” is carried out during 2019-2023 in a partial fulfillment for the award of **Bachelor of Technology** Degree in Electrical and Electronics Engineering. We have not submitted this dissertation to any other University or Organization for the award of any other Degree.

by

G. VINAY KUMAR	(20P65A0222)
B. JHANSI	(19P61A0218)
B. VINAY KUMAR	(19P61A0217)
B. SANDEEP	(20P65A0205)

ACKNOWLEDGEMENT

We take the opportunity to acknowledgement with thanks and deep sense of gratitude towards our Principal **Dr. P.V.S. SRINIVAS**, who extended his whole hearted cooperationand encouragement in the successful completion of our project.

We express our sincere thanks to **Dr. K. NEELIMA**, HoD, Department of Electrical and Electronics Engineering who has given her invaluable suggestions and encouraging support and guidance in carrying out the project.

We were very much thankful to our guide **Dr. B. NAGI REDDY**, Associate Professor, who extended invaluable suggestions, encouragement and guidance in carrying out the project.

We hereby, one and all who extended helping hand in the accomplishment of our project.

by

G. VINAY KUMAR **(20P65A0222)**

B. JHANSI **(19P61A0218)**

B. VINAY KUMAR **(19P61A0217)**

B. SANDEEP **(20P65A0205)**

ABSTRACT

Due to the more vigorous regulations on carbon gas emissions and fuel economy, Fuel cell electric vehicles (FCEV) are becoming more popular in the automobile industry. This article presents a 1.26-kW proton exchange membrane fuel cell (PEMFC), supplying electric vehicle powertrain through a Ultra voltage-gain dc–dc boost converter. High switching-frequency and high voltage-gain dc–dc converters are essential for the propulsion of FCEV. In order to attain high voltage-gain, a Ultra voltage-gain boost converter is also designed for FCEV system. The main principle of this converter is to operate in a continuous conduction mode under steady-state analysis and it makes use of switched Inductors for obtaining high voltage gain. This converter includes two diodes, three inductors, two capacitors and three switches. Even with the small values of duty ratios, higher voltage gain can be obtained with the help of proposed converter. The traditional boost converter has the minimum boosting capability, while the proposed converter has the higher voltage gain among the different topologies. The proposed converter provides high voltage-gain while at the same time, imposing small voltage stresses on the switches. Such features make the proposed converter to suitable well for electric vehicle applications. A stack of PEMFC produces an unregulated low DC output voltage. A Ultra gain Boost converter regulates the PEMFC output voltage. Boost converter is extensively used as a front-end power conditioner for the fuel cell. The output voltage of the proposed converter is given to the electric motor through an inverter for propulsion of the vehicle. The electric motor plays an important role in FCEVs. An adequate motor considerably reduces the cost and size of the fuel cell. Adversely, DC motors have high maintenance cost and low efficiency due to the brushes and rotating devices. At present, permanent magnet BLDC motor is mostly using in FCEV applications due to simple control, high reliability and high ruggedness. The Proposed configuration is simulated using MATLAB software and verified theoretically.

CONTENTS

LIST OF CONTENTS	PAGE NO
ACKNOWLEDGEMENT	i
ABSTRACT	ii
TABLE OF CONTENTS	iii
LIST OF FIGURES	vi
LIST OF TABLES	ix
ABBREVIATIONS	x
CHAPTER 1: INTRODUCTION	1
1.1 Introduction	1
1.2 DC-DC Converters for Fuel Cell Electric Vehicles	3
1.2.1 Buck Converter	4
1.2.2 Boost Converter	5
1.2.3 Buck – Boost Converter	5
1.2.4 DC/DC converters for electric vehicles	7
1.3 Fuel Cell	7
1.3.1 Key Components of a Hydrogen FCEV	8
1.4 Electric vehicle converters requirements	9
1.5 Brushless DC Motors	10
1.5.1 Working principle of BLDC Motor	11
1.5.2 Comparison of DC motors	12
1.6 Literature Review	14
1.7 Problem Formulation	16
1.8 Objective of the project	17
1.9 Organization of the Project	17
1.10 Summary	17
CHAPTER-2: PROPOSED HIGH STEP – UP	18
CONVERTER	
2.1 Introduction	18
2.2 Fuel Cell Modelling	18

2.3 Proposed Ultra Gain Boost Converter	20
2.4 Modes of operation	21
2.4.1 Mode 1	21
2.4.2 Mode-2	21
2.5 BLDC Motor Modelling	23
2.6 Summary	25
CHAPTER-3: DESIGN OF PROPOSED	26
CONVERTER	
3.1 Introduction	26
3.2 Inductor L_x Design	26
3.3 Inductor L_Y and L_Z	27
3.4 Capacitor C_Y Design	28
3.5 Capacitor C_X Design	28
3.6 Fuel Cell Modelling	30
3.7 VSI and BLDC motor	31
3.8 BLDC motor Controller and commutation	32
3.9 Speed control system	32
3.10 The Back Electro Motive Force (BEMF)	33
3.11 Summary	35
CHAPTER-4: RESULTS AND DISCUSSIONS	36
4.1 Introduction	36
4.2 Simulation Waveforms of proposed converter	37
4.3 Characteristics of Proposed Converter with Different Topologies	41
4.4 Simulation results of proposed configuration	44
4.5 Summary	50
CHAPTER-5: CONCLUSION & FUTURE SCOPE	51
5.1 Conclusion	51
5.2 Future Scope	51
5.3 POs & PSOs attainment	51
REFERENCES	52

LIST OF FIGURES

FIGURE NO	NAME OF THE FIGURE	PAGE NO
1.1	Operational block diagram of DC/DC converter	3
1.2	Buck converter	4
1.3	Boost converter	5
1.4	Buck-Boost converter	6
1.5	Block diagram of fuel cell electric vehicle	10
1.6	Construction of BLDC Motor	11
1.7	Interaction between magnetic field lines	12
1.8	Rotational motion of permanent magnet	12
1.9	Brushed DC motor	13
1.10	Brushless DC motor	13
1.11	BLDC motor with different pole configurations	14
2.1	Electrical Equivalent circuit of fuel cell	19
2.2	Operation of fuel cell	19
2.3	The proposed configuration circuit	20
2.4	The ideal key waveforms of the converter	21
2.5	The configuration of mode I	22
2.6	The configuration of mode 2	22
2.7	Circuit Diagram of Stator Winding	24
2.8	Block Diagram of proposed converter topology	25
3.1	Inductor L_X current	26
3.2	The inductors L_Y and L_Z currents	27
3.3	The capacitor C_Y output voltage	28
3.4	The capacitor C_X current and voltage	29
3.5	Block Diagram of BLDC Motor Speed Control	33

3.6	Back EMF of Decoder for MATLAB Drive	34
3.7	Inverter Switching for MATLAB Drive	34
3.8	Proposed converter with BLDC Motor	34
4.1	Simulation diagram of the proposed converter	37
4.2	Simulation diagram of whole proposed system	37
4.3	Simulated waveform of input capacitor voltage (V_{CX})	38
4.4	Simulated waveform of Diode voltage (V_{DX})	38
4.5	Simulated waveform of Diode voltage (V_{DY})	39
4.6	Simulated waveform of Diode current (I_{DX})	39
4.7	Simulated waveform of Diode current (I_{DY})	40
4.8	Input power Pin, Output power Pout, Losses	40
4.9	Output voltage (V_o)	43
4.10	Voltage Gain	44
4.11	Fuel cell voltage vs time	44
4.12	Fuel cell current vs Time	45
4.13	Boost Converter voltage vs Time	45
4.14	Boost converter Current vs Time	46
4.15	Decoder- EMF pulses of A, B & C Hall signals	46
4.16	Gate Pulses Provided by Inverter- Switching Block	47
4.17	Inverter Output Voltage	47
4.18	Hall Signals vs Time	48
4.19	Speed Vs time	48
4.20	Torque vs Time	49
4.21	Stator Current vs Time	49
4.22	Stator Back emf signals Vs Time	50

LIST OF TABLES

TABLE NO	NAME OF THE TABLE	PAGE NO
2.1	The voltage stresses of the Switching devices	23
2.2	The current stresses of the switching devices	23
3.1	1.26kW PEMFC parameter specifications	31
3.2	Truth Table for BLDC drive with Hall Sensor	32
4.1	Simulation component values	36
4.2	Comparison values of proposed converter with different converter topologies	42

ABBREVIATIONS

PEMFC	Proton Exchange Membrane Fuel Cell
EV	Electric Vehicle
FCEV	Fuel Cell Electric Vehicle
IC	Integrated Circuit
CCM	Continuous Conduction Mode
DCM	Discontinuous Conduction Mode
DC	Direct Current
BLDC	Brushless Direct Current
VSI	Voltage source inverter

CHAPTER 1

INTRODUCTION

1.1 Introduction

The environmental pollution is enlarging due to the existence of a greater number of gasoline vehicle. To mitigate pollution, the electric vehicles are very essential, and it is a best choice compared to traditional vehicles. Recently electric vehicles have gained more recognition compared to gasoline vehicles, due to environmental and economic concerns. With the advancement of technology related to motor and battery, the electric vehicles will become the favorable substitute to gasoline vehicles. Brushless DC motors are good choice for electric vehicles, since they have increased power densities, better speed-torque characteristics, top efficiency, wide speed ranges and less maintenance. But it needs complex electronics for control. In battery powered electric vehicle, the energy storage system is electrochemical batteries such as NiMH or Lithium based batteries. In applications involving electric vehicle, the discussion is with the life span of battery and driving range achieved, since battery may be acceptable in steady long duration.

The main concern in electric vehicles for efficient operation is in successful utilization of battery and improved motor control. Chemical batteries are prime energy storage in various industrial applications. Gel cell batteries are a type of lead acid batteries which are maintenance free and they are also known as sealed batteries. To utilize energy from battery effectively is an important challenge in electric vehicles. In traditional control system braking energy is dissipated at braking resistances in the form of heat. The energy wasted during braking in gasoline vehicles can be efficiently harvested by means of regenerative braking mechanism in vehicles. Hence the dependence on fuel can be reduced, improved fuel economy and reduced fuel emission can be obtained. When the vehicle is moving on a declining surface, the speed which is regulated in an inclining surface, supply the energy to the storage device; here it is battery, which is acting as a load during that condition. Normally regenerative braking can be deployed using an additional converter that converts the back emf to the suitable level to charge the battery. In this paper a bidirectional chopper is proposed such that depending upon the direction of power flow two operation modes are possible- boost

ULTRA GAIN BOOST CONVERTER FED BLDC MOTOR FOR FCEV APPLICATIONS

and buck mode. Here boost action is performed during normal driving such that the flow of power is from battery to BLDC motor and buck action during regenerative braking.

Due to the environmental pollution and finite reserves of fossil fuels, automobile industries are showing more interest in Fuel Cell Electric Vehicles (FCEV). The rapid advancements in power electronics and fuel cell technologies have empowered the significant development in FCEVs. Fuel cells have the advantages of clean power generation, high reliability, high efficiency and low noise. Depending on the type of electrolyte substance fuel cells are categorized into different types such as Proton Exchange Membrane Fuel Cell (PEMFC), Alkaline Fuel Cell (AFC), Phosphoric Acid Fuel Cell (PAFC), Solid Oxide Fuel Cell (SOFC) and Molten Carbonate Fuel Cell (MCFC). Among all of these, PEMFCs are dominating the automobile industry due to their low operating temperature and the quick startup. The output voltage of fuel cell depends on membrane water content and cell temperature. Notably, fuel cells have non-linear voltage-current characteristics.

The fuel cell stack produces low DC voltage at its output. To produce higher DC voltages, more fuel cells have to be added to the stack or a step-up converter has to be used. In this configuration, a basic boost converter cascaded with switched inductor circuit is used instead of using more fuel cells. A stack of PEMFC produces an unregulated low DC output voltage. So, a boost or step-up DC-DC converter is required to boost and regulate the PEMFC output voltage. Boost converter is extensively used as a front-end power conditioner for the fuel cell. For low power applications, the conventional boost converter is used as a power electronic interface whereas for high power applications boost converter might not be compatible because of its low current handling capability and thermal management issues. So, this project proposes an Ultra voltage gain Boost converter for fuel cell applications to attain low switching stress and high voltage gain.

The output voltage of the proposed converter is given to the electric motor through an inverter for propulsion of the vehicle. The electric motor plays an important role in FCEVs. An adequate motor considerably reduces the cost and size of the fuel cell. In past, most automakers are used DC motors for electric vehicle applications. Adversely, DC motors have high maintenance cost and low efficiency due to the

brushes and rotating devices. At present, permanent magnet BLDC motor is mostly using in FCEV applications due to simple control, high reliability and high ruggedness. It consists of a PEMFC, Ultra voltage gain boost converter, voltage source inverter (VSI) and a BLDC motor. The ultra-voltage gain boost converter operates as an interface between PEMFC and VSI. Ultra-voltage gain boost converter supplies power to the BLDC motor through VSI. The switches of the VSI are controlled by using electronic commutation of BLDC motor. The motor shaft is connected to vehicle wheels for the propulsion.

1.2 DC-DC Converters for Fuel Cell Electric Vehicles

A DC-to-DC converter is an Power Electronic device that converts a source of direct current (DC) from one voltage level to another. Power levels range from very low to very high (high-voltage power transmission). DC-DC converters are also referred to as linear or switching regulators, depending on the method used for conversion. There is a broad range of operating voltages for various electronic devices, such as ICs and MOSFETs, which necessitates providing voltage for each. A Buck Converter provides a lower voltage than the original voltage, while a Boost Converter supplies a higher voltage.

From fig 1.1 a DC-DC converter is an electronic circuit that facilitates the conversion of direct current from one voltage level to another based on the requirements. This electric power converter is capable of operating at a wide range of power levels from very low power, such as in the case of batteries, to very large power, such as in the case of large-scale high voltage power transmission system. The DC-to-DC converter must be able to operate as a step up or down voltage supplier to provide constant load voltage over the entire battery voltage range through the operation.

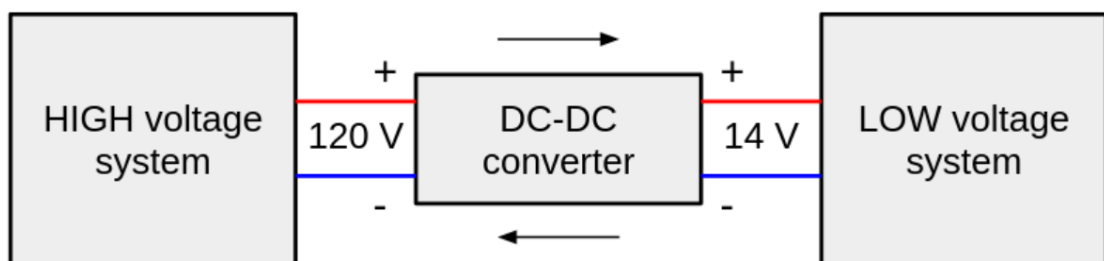


Fig 1.1 Operational block diagram of DC/DC converter

DC-DC converters can be divided into two categories according to whether there is electrical isolation between the input and output: those without electrical isolation are called non-isolated DC-DC converters, and those with electrical isolation are called isolated DC-DC converters. Non-isolated DC-DC converters can be divided into three categories: single-tube, double-tube and four-tube, according to the number of active power devices used.

1.2.1 Buck Converter

From fig 1.2 a buck converter steps down the applied DC input voltage level directly. By directly means that buck converter is non-isolated DC converter. Non-isolated converters are ideal for all board level circuits where local conversion is required. Fax machines, scanners, Cell phones, PDAs, computers, copiers are all examples of board level circuits where conversion may require at any level inside the circuit. Hence, a buck converter converts the DC level of input voltage into other required levels.

Buck converter is having a wide range of use in low voltage low power applications. Multiphases of buck converters can provide high current with low voltage. Therefore, it can be used for low voltage high power applications. This article will discuss both low voltage low power converter and low voltage high power converter. The basic buck converter consists of a controlled switch, a diode, capacitor and controlled driving circuitry. The switch controls the flow of input power into output by turning ON and OFF periodically. The time for which the switch is ON during the whole period is known as Duty cycle. The basic buck converter consists of a controlled switch, a diode, capacitor and controlled driving circuitry.

The value of duty cycle D ranges between 0 and 1. For $D=0$, zero voltage appear across load while for $D=1$, all the input voltage appears across the load. That's why

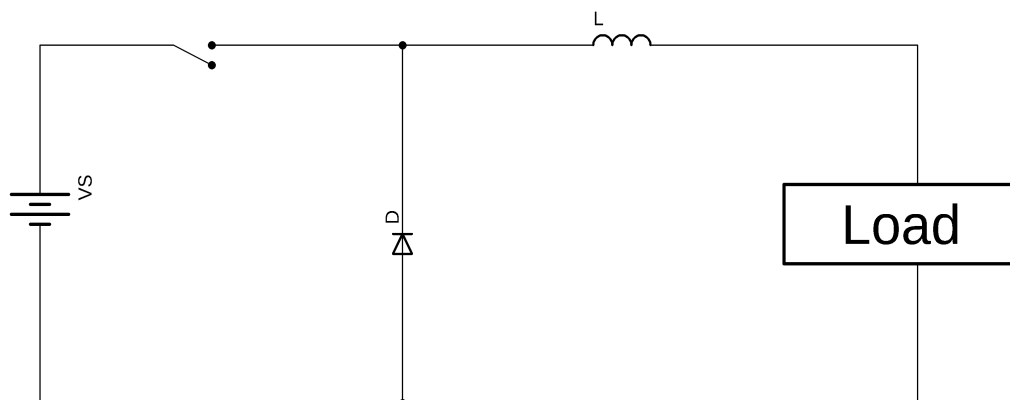


Fig 1.2 Buck converter

buck converter is operated for D greater than 0 and less than 1. The basic circuit diagram of buck converter can be seen below. A buck converter operates in two types of conduction modes i.e., CCM and DCM. In CCM (Continuous Conduction Mode) the inductor current I_L remains positive throughout the switching period. This article will discuss both low voltage low power converter and low voltage high power converter.

1.2.2 Boost Converter

From fig 1.3 also called DC-DC boost converters, they can produce voltage higher than the input voltage. In a typical boost converter, the induction coil receives almost all the current, while the closed diode doesn't let the current charge the capacitor and the load. Due to a higher electric current, the coil accumulates much more magnetic field energy compared to a step-down schematic. When the voltage drops to a certain point, the power key is turned off, while the diode is turned on. The input voltage adds to the energy stored in the coil, which makes the output voltage of boost DC-DC converters higher than the input voltage.

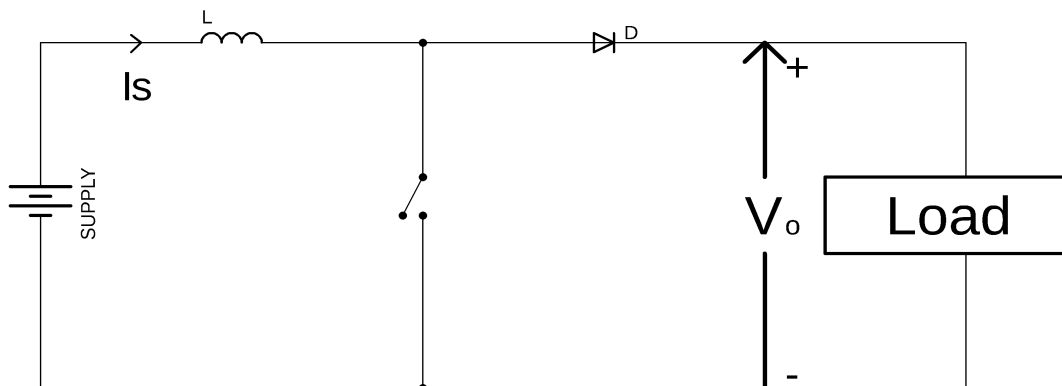


Fig 1.3 Boost Converter

Boost converters are used whenever you can't provide a high enough input voltage with batteries or there's simply not enough room for more batteries. They are typically used in hybrid vehicles, lighting systems that use energy-saving lamps, portable lighting devices, etc.

1.2.3 Buck – Boost Converter

The buck-boost converter is a DC-to-DC converter (also known as a chopper) with an output voltage magnitude that is either greater than or less than the input voltage magnitude. It is used to “step up” the DC voltage, similar to a transformer for AC

circuits. It is equivalent to a flyback converter using a single inductor instead of a transformer. Two different topologies are called buck-boost converter.

DC-DC converters are also known as choppers. Here we will have a look at Buck Boost converter as shown in fig 1.4 which can operate as a DC-DC Step-Down converter or a DC-DC Step-Up converter depending upon the duty cycle, D. An inductor will be connected in parallel with the output terminals and a diode is connected similarly to that as seen in the boost converter. The solid-state device which is basically a semiconductor device will act as the switching device.

The working operation of the DC-DC converter is the inductor in the input resistance has an unexpected variation in the input current. If the switch is ON then the inductor feeds the energy from the input and it stores the energy of magnetic energy. If the switch is closed it discharges the energy. The output circuit of the capacitor is assumed as high sufficient than the time constant of an RC circuit is high on the output stage. The huge time constant is compared with the switching period and make sure that the steady state is a constant output voltage $V_o(t) = V_o(\text{constant})$ and present at the load terminal.

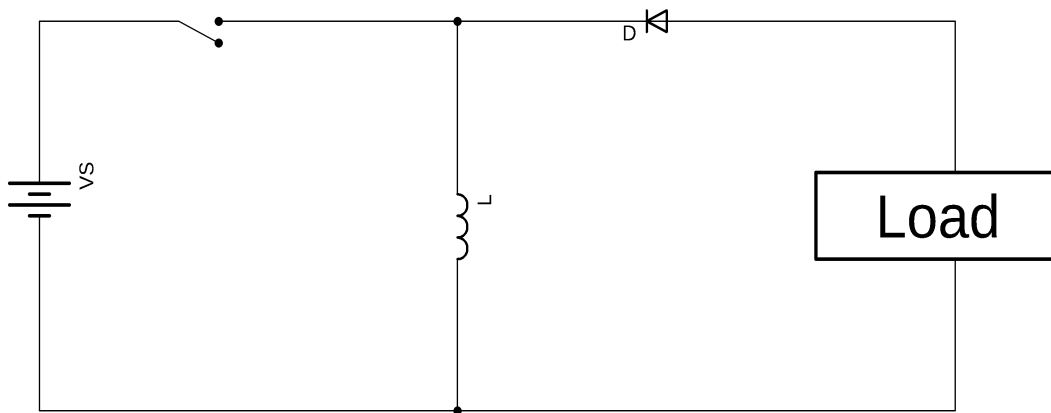


Fig 1.4 Buck-Boost converter

There are two different types of modes in the buck boost converter. The following are the two different types of buck boost converters.

1. Continuous Conduction Mode:

In the continuous conduction mode, the current from end to end of inductor never goes to zero. Hence the inductor partially discharges earlier than the switching cycle.

2. Discontinuous Conduction Mode:

In this mode the current through the inductor goes to zero. Hence the inductor will totally discharge at the end of switching cycles.

1.2.4 DC/DC converters for electric vehicles

The different configurations of EV power supply show that at least one DC/DC converter is necessary to interface the FC, the Battery or the Supercapacitors module to the DC-link.

In electric engineering, a DC-DC converter is a category of power converters and it is an electric circuit which converts a source of direct current (DC) from one voltage level to another, by storing the input energy temporarily and then releasing that energy to the output at a different voltage. The storage may be in either magnetic field storage components (inductors, transformers) or electric field storage components (capacitors).

DC/DC converters can be designed to transfer power in only one direction, from the input to the output. However, almost all DC/DC converter topologies can be made bi-directional. A bi-directional converter can move power in either direction, which is useful in applications requiring regenerative braking.

The amount of power flow between the input and the output can be controlled by adjusting the duty cycle (ratio of on/off time of the switch). Usually, this is done to control the output voltage, the input current, the output current, or to maintain a constant power. Transformer-based converters may provide isolation between the input and the output. The main drawbacks of switching converters include complexity, electronic noise and high cost for some topologies.

1.3 Fuel Cell

A fuel cell uses the chemical energy of hydrogen or other fuels to cleanly and efficiently produce electricity. If hydrogen is the fuel, the only products are electricity, water, and heat. Fuel cells are versatile and power applications across multiple sectors, including transportation, industrial/commercial/residential buildings, and long-term energy storage for grids in reversible systems.

Fuel cells offer several advantages over traditional combustion-based technologies used in many power plants and vehicles today. Fuel cells operate at a higher efficiency than internal combustion engines, converting the chemical energy of fuels directly into electrical energy, with efficiencies exceeding 60%. Fuel cells have low or no emissions compared to internal combustion engines. Hydrogen fuel cells only emit water and no carbon dioxide, addressing a significant climate challenge. There are

no air pollutants that create smog on the job site and cause health problems. Since fuel cells have few moving parts, they are quiet during operation.

Fuel cells work like batteries, but they do not self-discharge and do not require recharging. They generate electricity and heat as long as fuel is provided. A fuel cell consists of two electrodes – a cathode (or anode) and an anode (or cathode) – sandwiched around an electrolyte. Fuel, such as hydrogen, is introduced into the anode and air is introduced into the cathode. In a hydrogen fuel cell, a catalyst at the anode splits hydrogen molecules into protons and electrons, which follow different paths to the cathode. The electrons pass through an external circuit, creating an electric current. The protons move through the electrolyte to the cathode, where they combine with oxygen and electrons to produce water and heat. Fuel cells have low or no emissions compared to internal combustion engines. Up to date, hydrogen is being stored in compressed gas cylinders and liquid tanks. Innovative approaches, including chemical hydrides, carbon systems, and hydrogen absorption through metal hydrides, still require significant improvement in terms of capacity and safety. Even if the storage system design becomes as efficient as expected and affordable, the refueling infrastructure needs to be widespread enough to make hydrogen available to millions of vehicle owners.

1.3.1 Key Components of a Hydrogen Fuel Cell Electric vehicle

- **Battery (auxiliary):** In an electric drive vehicle, the low-voltage auxiliary battery provides electricity to start the car before the traction battery is engaged; it also powers vehicle accessories.
- **Battery pack:** This high-voltage battery stores energy generated from regenerative braking and provides supplemental power to the electric traction motor.
- **DC/DC converter:** This device converts higher-voltage DC power from the traction battery pack to the lower-voltage DC power needed to run vehicle accessories and recharge the auxiliary battery.
- **Electric traction motor (FCEV):** Using power from the fuel cell and the traction battery pack, this motor drives the vehicle's wheels. Some vehicles use motor generators that perform both the drive and regeneration functions.
- **Fuel filler:** A nozzle from a fuel dispenser attaches to the receptacle on the vehicle to fill the tank.

- Fuel tank (hydrogen): Stores hydrogen gas onboard the vehicle until it's needed by the fuel cell.
- Power electronics controller (FCEV): This unit manages the flow of electrical energy delivered by the fuel cell and the traction battery, controlling the speed of the electric traction motor and the torque it produces.
- Thermal system (cooling) – (FCEV): This system maintains a proper operating temperature range of the fuel cell, electric motor, power electronics, and other components.
- Transmission (electric): The transmission transfers mechanical power from the electric traction motor to drive the wheels.

1.4 Electric vehicle converters requirements

As shown in fig 1.5, In case of interfacing the Fuel Cell, the DC/DC converter is used to boost the Fuel Cell voltage and to regulate the DC-link voltage. However, a reversible DC/DC converter is needed to interface the SCs module. A wide variety of DC-DC converters topologies, including structures with direct energy conversion, structures with intermediate storage components (with or without transformer coupling), have been published. However, some design considerations are essential for automotive applications:

- Light weight
- High efficiency
- Small volume
- Less size
- Low electromagnetic interference
- Low current ripple drawn from the Fuel Cell or the battery

The step-up function of the converter, Control of the DC/DC converter power flow subject to the wide voltage variation on the converter input. Each converter topology has its advantages and its drawbacks. For example, The DC/DC boost converter does not meet the criteria of electrical isolation. Moreover, the large variance in magnitude between the input and output imposes severe stresses on the switch and this topology suffers from high current and voltage ripples and also big volume and weight. A basic interleaved multichannel DC/DC converter topology permits to reduce the input and output current and voltage ripples, to reduce the volume and weight of the inductors and to increase the efficiency. These structures, however, cannot work efficiently when

a high voltage step-up ratio is required since the duty cycle is limited by circuit impedance leading to a maximum step-up ratio of approximately.

Hence, two series connected step-up converters would be required to achieve the specific voltage gain of the application specification. A full-bridge DC/DC converter is the most frequently implemented circuit configuration for fuel-cell power conditioning when electrical isolation is required. The full bridge DC/DC converter is suitable for high-power transmission because switch voltage and current are not high. It has small input and output current and voltage ripples. The full-bridge topology is a favourite for zero voltage switching (ZVS) pulse width modulation (PWM) techniques.

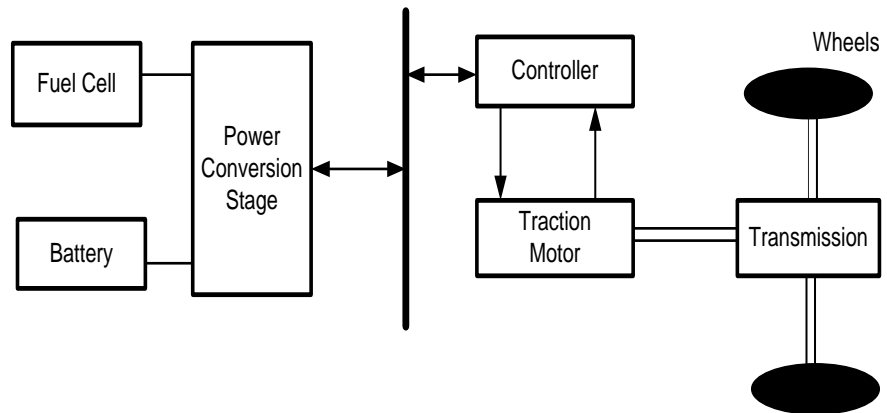


Fig 1.5 Block diagram of fuel cell electric vehicle

From fig 1.5 a basic interleaved multichannel DC/DC converter topology permits to reduce the input and output current and voltage ripples, to reduce the volume and weight of the inductors and to increase the efficiency. Usually, this is done to control the output voltage, the input current, the output current, or to maintain a constant power. The full bridge DC/DC converter is suitable for high-power transmission because switch voltage and current are not high. It has small input and output current and voltage ripples. Transformer-based converters may provide isolation between the input and the output. Hydrogen fuel cells only emit water and no carbon dioxide, addressing a significant climate challenge.

1.5 Brushless DC Motors

A Brushless DC Motor is similar to a Brushed DC Motor but as the name suggests, a BLDC doesn't use brushes for commutation but rather they are electronically commutated. In conventional Brushed DC Motors, the brushes are used to transmit the power to the rotor as they turn in a fixed magnetic field. A BLDC motor uses electronic commutation and thus eliminates the mechanically torn brushes.

Its major components comprise:

- an armature or rotor made of permanent.
- a stator with windings that create a magnetic field when energized.

The rotor's magnets and stator's windings provide the rotation of the motor. They attract each other with opposite poles and repel each other with the same poles. They use opposite poles to attract one another and the same poles to repel each other. Fig 1.6 shows the construction of BLDC motor. A brushed DC motor goes through a similar process. The main distinction is in how the current provided to the wire windings is switched.

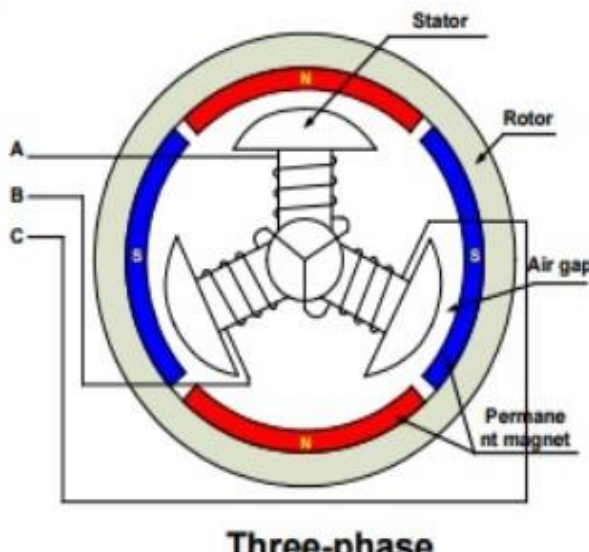


Fig 1.6 Construction of BLDC Motor

1.5.1 Working principle of BLDC Motor

BLDC motor works on the principle of Lorentz force law which states that whenever a current carrying conductor is placed in a magnetic field it experiences a force. As a consequence of reaction force, the magnet will experience an equal and opposite force. A BLDC motor controller controls the motor's speed and torque, as well as starting, stopping, and reversing its rotation. Compared to Brushed Motor, both operate based on a similar principle, in which the rotational motion is generated through the attraction and repulsion of magnetic poles of permanent and electromagnets. However, the way these motors are controlled is very different. BLDCs require a complex controller to convert a single DC power to three-phase voltage, whereas a brushed motor can be controlled by regulating the DC voltage.

Electromagnet

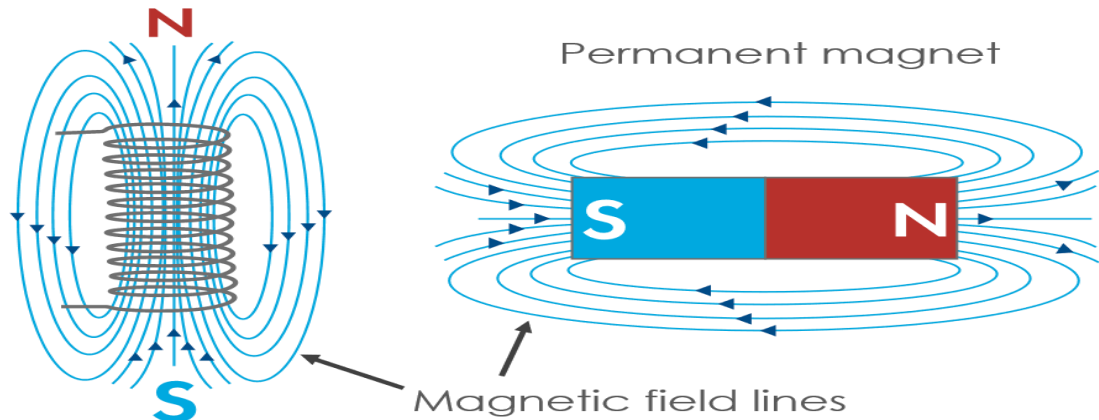


Fig 1.7 Interaction between magnetic field lines

Fig 1.7 shows the interaction between magnetic field lines. A commutator with brushes initiates the mechanical process in a BDC motor. But in a BLDC motor it happens electronically with the use of transistor switches.

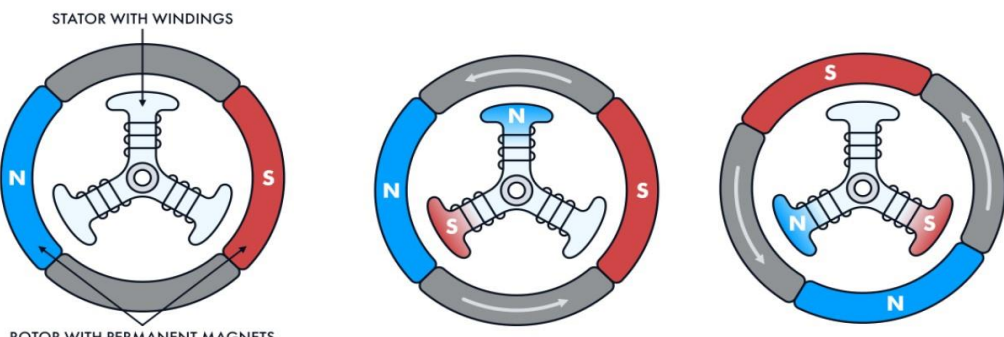


Fig 1.8 Rotational motion of permanent magnet

Fig 1.8 shows the rotational motion of permanent magnet. A BLDC motor controller detects the position of the rotor either by using sensors (for example, a Hall-effect sensor which we used in our project) or sensorless. The sensors measure the rotor's position and send out this data. The controller receives the information and enables the transistors to switch the current and energize the required winding of the stator at the right time.

1.5.2 Comparison of DC motors

Traditional Brushed DC motors have wound coils in the rotor, which are surrounded by magnets contained in the stator. The two ends of a coil are connected to the commutator. The commutator in turn connects to electrodes called brushes, resulting in the flow of direct current electric power through the brushes and coil for as long as the brushes and commutator are in contact. But in BDC motor

- Brushes require frequent replacement due to mechanical wear.
- Brushes transfer current to the commutator, due to which sparking occurs.
- Brushes limit the maximum speed and number of poles the armature can have.

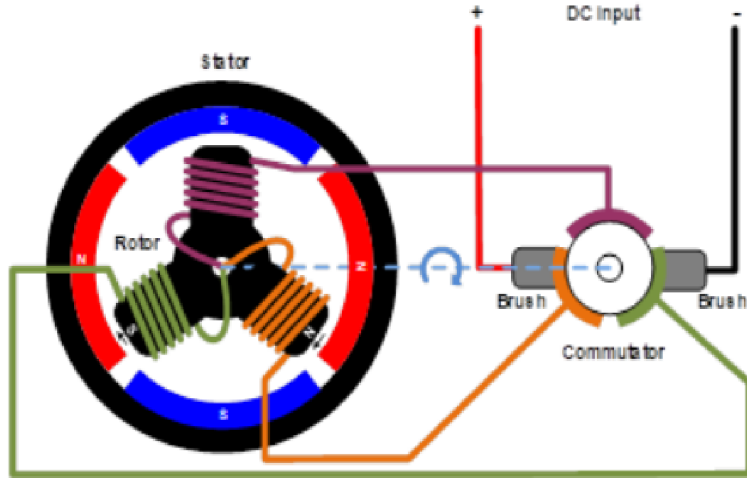


Fig 1.9 Brushed DC motor

Fig 1.9 represents a Brushed DC motor. All the drawbacks discussed above can be prevented in a brushless DC motor. BLDC motors overcome the shortcomings of brushed motors by replacing mechanical commutation with electronic commutation. Electronic control circuit is required in a brushless DC motor for switching stator magnets to keep the motor running. This makes a BLDC motor potentially less rugged. A BLDC motor is a kind of flipped version of a brushed motor because the permanent magnets are installed in the rotor, whereas the coil windings become the stator.

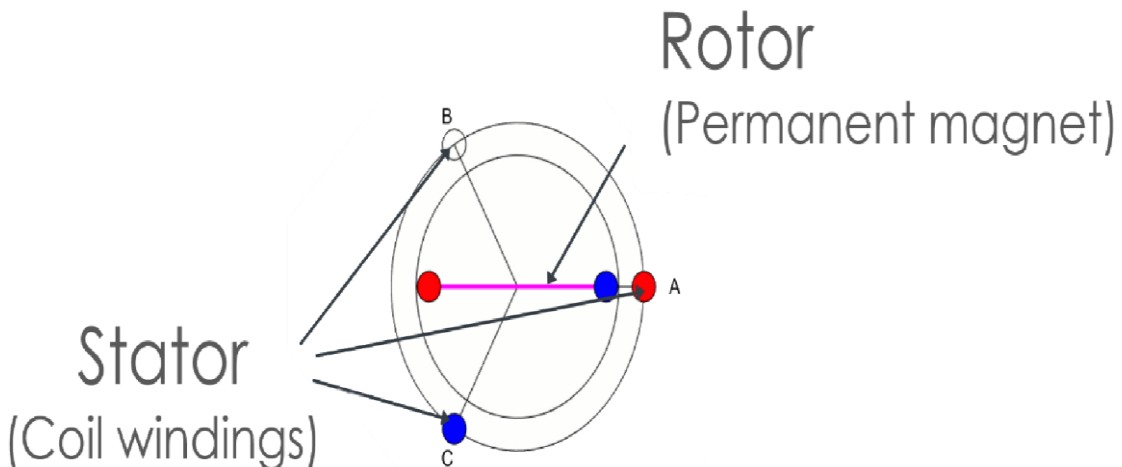


Fig 1.10 Brushless DC motor

Fig 1.10 represents a Brushless DC motor. Though brushless motors can be constructed with different numbers of phases, three phase brushless motors are the most

common. Fig 1.11 shows the BLDC motor with different pole configurations. Motors can also be built with more poles, which requires more magnetic sections in the rotor, and more windings in the stator. Higher pole counts can provide higher performance, though very high speeds are better accomplished with lower pole counts.

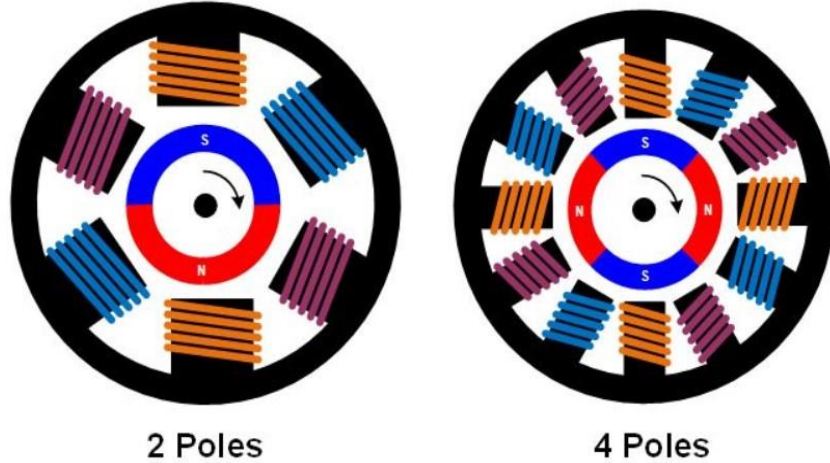


Fig 1.11 BLDC motor with different pole configurations

1.6 Literature Review

In [1] a quadratic boost converter composed of two boost converters is proposed to attain high voltage gain. But, using of two boost converters may reduce the overall efficiency of the system. A new quadratic boost converter with reduced buffer capacitor stress is presented in [1] which consists of one active switch, three passive switches and two LC filters. The proposed quadratic boost converter is capable of converting the input voltage level in higher output voltage level than the traditional boost converter. In addition, its buffer capacitor voltage stress is lower than the conventional quadratic boost converter with the same function. Therefore, it could be designed with smaller and higher efficiency. The main features of the proposed converter include quadratic voltage gain of the traditional boost converter and lower voltage stress on the buffer capacitor.

A cascaded 2-phase interleaved DC-DC boost converter is proposed in [2]. However, this topology suffers from poor reliability and less efficiency. This paper has presented a cascaded converter which allows connecting a low-voltage high-power source to a high-voltage output. An energy control structure has been proposed to manage the transfer of energy in the system based on flatness principle. The proposed converter structure is constituted by a cascade of two sub converters in order to obtain the desired voltage ratio and small power-source current undulations. The choice of an

interleaved boost converter for the first sub converter and a three-level boost converter for the second one leads to a better efficiency of the global conversion structure owing to the use of the MOSFET/Schottky diode technology rather than insulated-gate bipolar transistor/Ultrafast diode technology for the second sub converter.

In [3], a boost converter with voltage multiplier cell is proposed to achieve high voltage gain, but the voltage gain of single multiplier cell is not much enough to drive the powertrain of FCEV. This paper introduces a new family of DC–DC converters based on the three-state switching cell and voltage multiplier cells. It is possible to generate the six novel non isolated dc–dc converters, i.e., buck, boost, buck–boost, Cuk, SEPIC, and Zeta. The analyzed converter can be applied in uninterruptible power supplies, fuel cell systems, and is also adequate to operate as a high-gain Boost stage with cascaded inverters in renewable energy systems. Furthermore, it is suitable in cases where dc voltage step-up is demanded, such as electrical fork-lift, audio amplifiers, and many other applications. It is also expected that non-Isolated converters based on the 3SSC and VMC may be competitive solutions for high-current-high-voltage-step-up applications if compared with some other isolated approaches.

Isolated converters with coupled inductors or high frequency transformers are proposed to achieve high voltage gain in [4]. The concept of winding-cross-coupled inductors (WCCIs) and voltage multiplier cells is integrated to derive a novel Interleaved high step-up converter in this paper. The volt-age gain is extended and the extreme duty cycle is avoided by the WCCIs and the voltage multiplier cells compared with the conventional interleaved boost converter, which can reduce the peak current and voltage stress on the switches to reduce the conduction losses. Moreover, ZCS turn-on for the switch is achieved and the output diode reverse-recovery problem is alleviated by the leakage inductance to reduce the switching losses and EMI noises. Furthermore, the leakage energy is recycled and the voltage spikes on the power MOSFETs are absorbed by the voltage multiplier cells.

In [5], a power factor corrected (PFC) Bridgeless (BL) buck–boost converter-fed brushless direct current (BLDC) motor drive as a cost-effective solution for low-power Applications. An approach of speed control of the BLDC motor by controlling the dc link voltage of the voltage source inverter (VSI) is used with a single voltage sensor. This facilitates the Operation of VSI at fundamental frequency switching by

ULTRA GAIN BOOST CONVERTER FED BLDC MOTOR FOR FCEV APPLICATIONS

using the electronic commutation of the BLDC motor which offers reduced Switching losses.

A PFC based BL-CSC converter fed BLDC motor drive has been proposed in [6] with improved power quality at the AC mains. A bridgeless configuration of a CSC converter has been used for achieving reduced conduction losses in PFC converter. The Speed control of BLDC motor and power factor correction at AC mains has been achieved using a single voltage sensor. The switching losses in the VSI have been reduced by the use of fundamental frequency switching by electronically Commutating the BLDC motor. Moreover, the speed of BLDC motor has been controlled by controlling the DC link voltage of the VSI.

A non-isolated bidirectional DC-DC converter is presented in [7]. This converter consists of two boost converters to enhance the voltage Gain. Four power switches are employed in the proposed converter which their body diodes are also used. Two Inductors and a capacitor are also employed as passive Components. Two of the switches work as power switches and the remaining are applied for the synchronous rectifiers. Voltage gain of the Proposed converter is higher than conventional buck converter.

The three-level hybrid boost dc-dc Converter is discussed in [8], which can be step-up the fuel cell output voltage with high voltage gain. The working principle of present Converter is based on the traditional neutral clamped multi-Level inverter. Fuel cell stack is designed in the place of normal dc battery. Hybrid boost dc-dc converter is Connected to Multi level inverter for AC output to drive EV. The major advantage with this converter, the voltage across the power switches is half of the output voltage of the converter. The output of DC voltage is again converted into AC by using multilevel inverter.

The configuration proposed in [9] deals with the design of a digital current Control applied to a variable-speed low inductance brushless dc (BLDC) motor drive. A robust static full-state feedback control law is determined by means of a convex optimization problem, subject to linear-matrix-inequality constraints. The optimization is used to achieve a fast time response with reduced overshoot under the parametric variation.

The three-phase high voltage gain DC-DC converter is proposed [10] for FCEV applications. The interleaving technique reduces the input current ripple and voltage

stress on the power semiconductor devices. The proposed converter has reduced the fuel cell input current ripples and the voltage stress on the power semiconductor switches. The RBFN based MPPT technique is designed for 1.26 kW PEMFC for extracting the maximum power from the fuel cell at different temperatures.

1.7 Problem Formulation

Fuel cells are the most important sources of energy. There is a problem since the voltages produced by the fuel cell much below acceptable values and are very dependent on factors like temperature. The fuel cell systems need high voltage gain converters. Boost converters, switched-capacitor converters and switched conductors are used to achieve higher voltage gain, efficiency and low voltage stress. In this project an ultra-Voltage gain DC-DC converter is proposed with fuel cell as energy system. High voltage gain is achieved through the proposed converter.

1.8 Objective of the Project

The main objective of this project is to propose a new dc/dc boost configuration with high voltage-gain capability for Fuel cell converters. The proposed converter should have low voltage stress and ripples. The complete analysis is validated by implementing a prototype on Simulink.

1.9 Organization of the Project

1. This chapter mainly deals with the working principle and detailed information about various types of DC-DC converters, Fuel Cell and BLDC motor.
2. This chapter mainly deals with the detailed operation of the proposed High gain step up converter, Fuel cell and BLDC motor.
3. This chapter mainly deals with the design analysis of proposed converter with the implementation of fuel cell and the BLDC motor.
4. This chapter mainly deals with the theoretical analysis and simulation results of Proposed Converter.
5. This chapter mainly deals with the conclusions and future scope of the project.

1.10 Summary

This chapter clearly elaborates the basic introduction of DC – DC converters, Fuel cell BLDC motor and their advantages and disadvantages. The literature survey of the present step-up technologies are also given with recent advancements.

CHAPTER 2

PROPOSED HIGH STEP-UP CONVERTER

2.1 Introduction

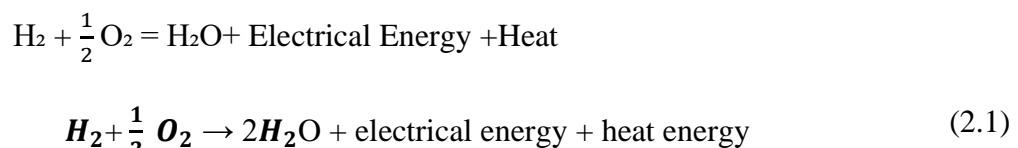
This chapter mainly includes about the basic information about the fuel cell and its chemical reaction with necessary equations. The proposed converter consists of two diodes, three inductors, two capacitors, and three switches. The three switches are triggered on and off simultaneously. BLDC motor is normally powered by conventional three phase inverter which is controlled by the rotor position information obtained from Hall sensors or simply from hall position sensors.

2.2 Fuel Cell Modelling

A fuel cell is an electrochemical device that converts hydrogen fuel into electricity. The inputs to the fuel cell are air and fuel and these are converted into water and electricity through a chemical reaction. From fig 2.2 a single fuel cell consists of two electrodes (anode and cathode) and an electrolyte. The electrolyte separates the positive and negative charged ions of the hydrogen fuel. When the hydrogen and oxygen are fed into the cell, electricity is generated at the output of the cell in the presence of an electrolyte.

Fig 2.1 shows the electrical equivalent circuit diagram of fuel cell.

Overall electrochemical reaction is given by,



The voltage generated from the fuel cell is given by

$$V_{FC} = E_{NERNST} - V_{act} - V_{ohmic} - V_{con} \quad (2.2)$$

Where V_{act} is used for modelling the activation losses and is given by

$$V_{act} = A \cdot I_n \left(\frac{I_{FC} + i_n}{i_0} \right) \quad (2.3)$$

The voltage drop due to Ohmic losses is given as:

$$V_{ohm} = R_m (i_{FC} + i_n) \quad (2.4)$$

The concentrations losses are expressed as:

$$V_{con} = -B \cdot I_n \left(1 - \frac{i_{FC} + i_n}{i_1} \right) \quad (2.5)$$

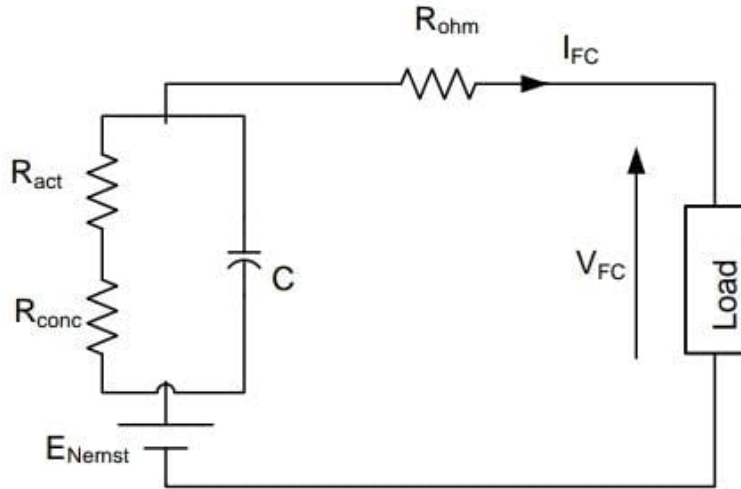


Fig 2.1 Electrical Equivalent circuit of fuel cell

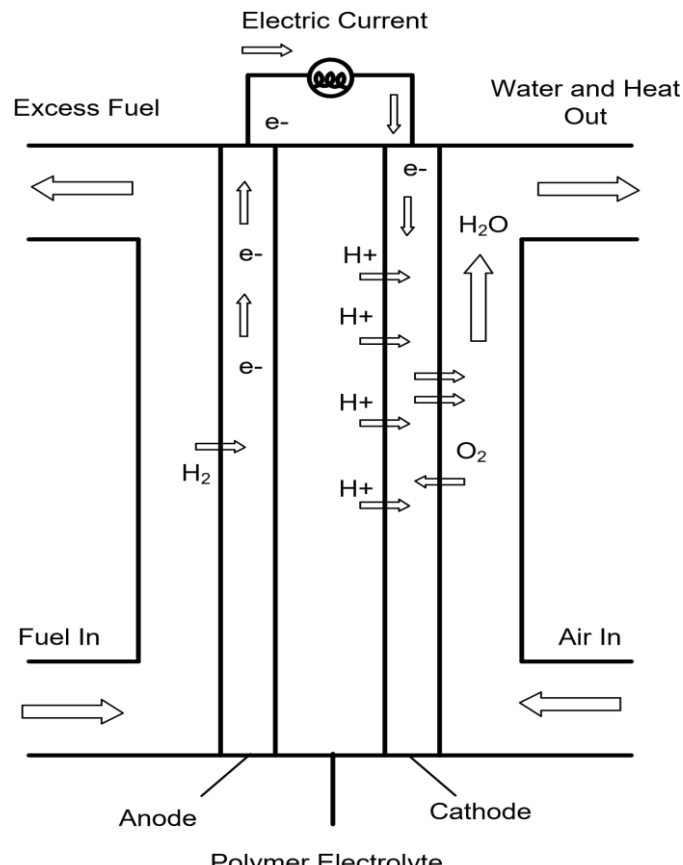


Fig 2.2 Operation of fuel cell

2.3 Proposed Ultra Gain Boost Converter

The configuration of the proposed converter is depicted in figure 2.3. It consists of two diodes, three inductors, two capacitors, and three switches. The three switches are

triggered on and off simultaneously. The two-diodes are operated in a complementary manner to the switches in order to provide a free path for the inductor current. Inductors charge in parallel when the switches are turned on and discharge their energy to the output load once switches are turned off. In the upcoming analysis, the small-ripple approximation is used. The converter is designed to operate in the continuous conduction mode (CCM). The parameters are assumed to be ideal for the upcoming analysis in order to facilitate the analysis of the converter. A graph of the ideal key waveforms of the circuit devices is shown in fig 2.4. The two possible operating modes of the converter are discussed as follows:

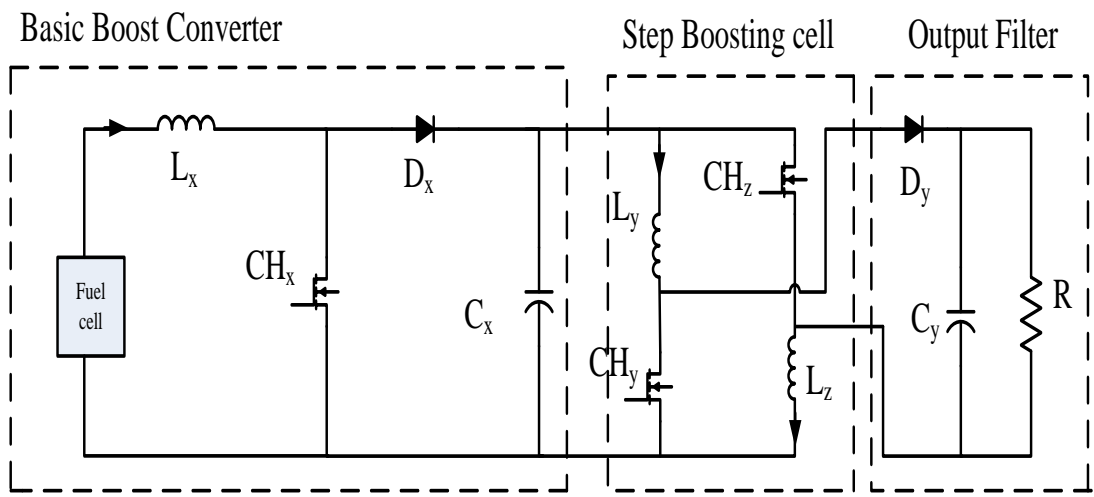


Fig 2.3 The proposed configuration circuit

The Proposed converter has mainly three sections:

- Basic Boost converter
- Step Boosting cell
- Output filter

The combination of the above three sections forms the Proposed converter with high voltage gain, high efficiency, lower voltage stresses and lower current stresses. The converter is designed to operate in the continuous conduction mode (CCM). The Proposed converter operates in two modes.

The characteristic equations that describe this mode of operation in the following. In the upcoming analysis, the small-ripple approximation is used. The converter is designed to operate in the continuous conduction mode . The parameters are assumed to be ideal for the upcoming analysis in order to facilitate the analysis of the converter.

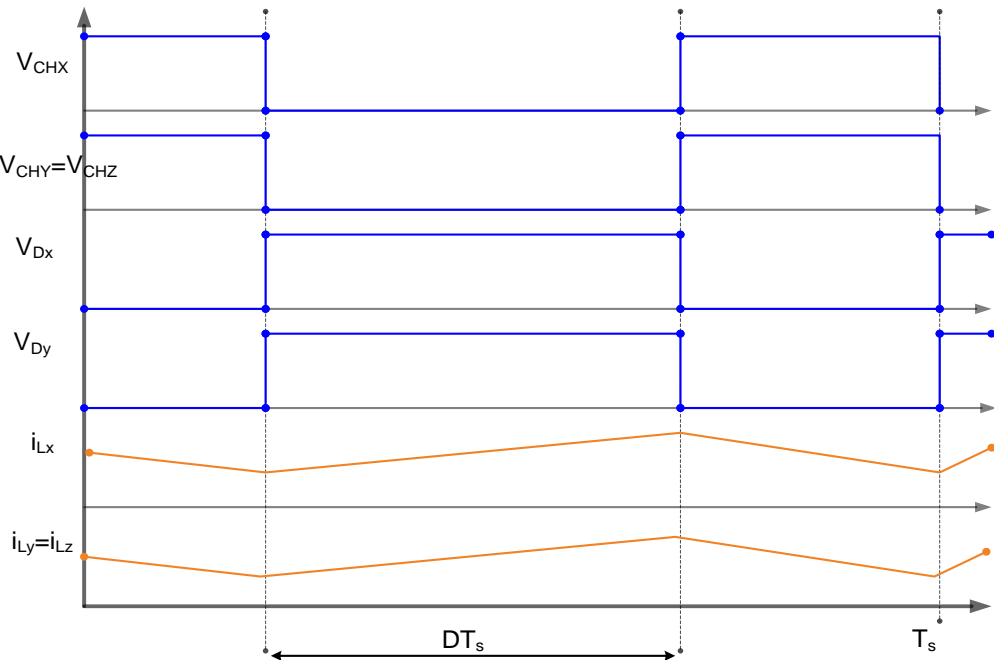


Fig 2.4 The ideal key waveforms of the converter

2.4 Modes of operation

The detailed operation of the proposed converter for various modes is discussed in the following sections.

2.4.1 Mode 1

This mode is activated once the switches are turned on, and the depiction of this mode is illustrated in fig 2.5. The three switches are turned on simultaneously. In this mode, inductor L_x is energized from the input dc-source, while inductors L_y and L_z are energized from capacitor C_x . Diodes D_x and D_y are reversely biased. Output capacitor C_y releases its energy to the load side. The characteristic equations that describe this mode of operation in the following.

2.4.2 Mode-2

This mode is activated once the switches are turned off, and the depiction of this mode is illustrated in fig 2.6. The three switches are turned off at the same time. In this mode, inductor L_x is discharging its energy into capacitor C_x , while inductors L_y and L_z are discharging their energy into output load and output capacitor C_y . In order to maintain a continuous path for the inductor currents, diodes D_x and D_y work as freewheeling diodes when they are turned on. The characteristic equations that describe this mode of operation in the following circuit diagrams and with the proposed converter waveforms.

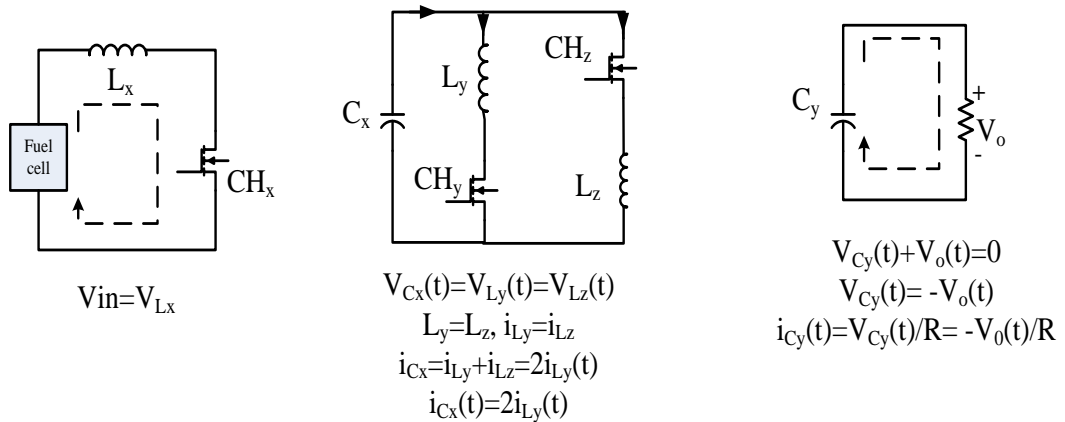


Fig 2.5 The configuration of mode I

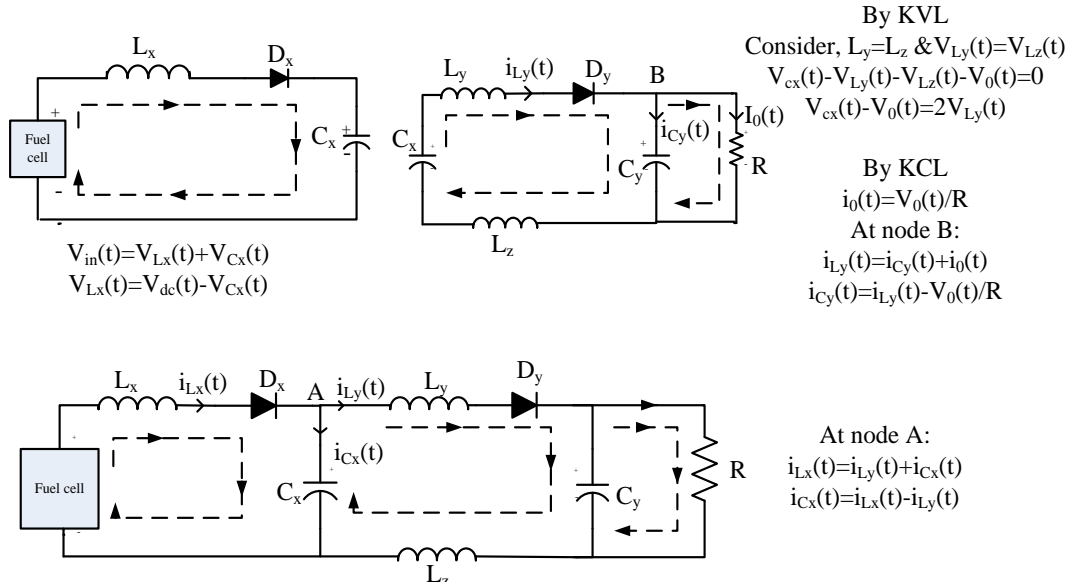


Fig 2.6 The configuration of mode 2

The voltage and current stresses of each component are depicted in Tables 2.1 and 2.2, respectively. All components have a voltage stress lower than the output voltage. This is a distinct advantage of this topology. It enables us to select the devices with low ratings, thus improving the overall efficiency of the system. However, multiple diodes and capacitors are required when the conversion ratio is high. Isolated topologies, such as coupled inductors and flyback converters, use the turns ratio, in addition to the duty cycle, to control the converter voltage gain. As the required step-up ratio is performed at moderate duty cycle, the overall efficiency is increased.

Table 2.1 The voltage stresses of the switching devices.

Switching Device	Peak Voltage Stress
CH_X	$V_o * (1 - D)/(1 + D)$
CH_Y	$V_o/(1 + D)$
CH_Z	$V_o/(1 + D)$
Dx	$V_o * (1 - D)/(1 + D)$
Dy	$2 * V_o/(1 + D)$

Table 2.2 The current stresses of the switching devices.

Switching Device	RMS Current Stress
CH_X	$I_{in} * \sqrt{D}$
CH_Y	$(1 - D) * \sqrt{D} * I_{in}/2$
CH_Z	$(1 - D) * \sqrt{D} * I_{in}/2$
Freewheeling Diodes	Average Current Stress
Dx	$I_{in} * (1 - D)$
Dy	$(1 - D)^2 * I_{in}/2$

Equations from tables 2.1 and 2.2 represents the relationship between the voltage across capacitor C_1 and input/output voltages.

The voltage and current stresses of each component are depicted in tables 2.1 and 2.2, respectively. All components have a voltage stress lower than the output voltage. This is a distinct advantage of this topology. It enables us to select the devices with low ratings, thus improving the overall efficiency of the system.

2.5 BLDC Motor Modelling

The Y-connected, 3-phase motor with a 4-pole permanent magnetic rotor is driven by a PWM inverter. The equivalent circuit diagram of the stator winding is as shown in fig 2.7. The rotor position, which determines the switching sequence of the IGBT transistors, is detected by means of 3 Hall sensors mounted on the stator. The switching scheme implemented in the inverter logic is well-known.

The model equations of a BLDC motor are composed of a voltage equation, a torque equation and a motion equation. The stator of a general BLDC motor has three windings like an induction motor or a permanent magnet synchronous motor.

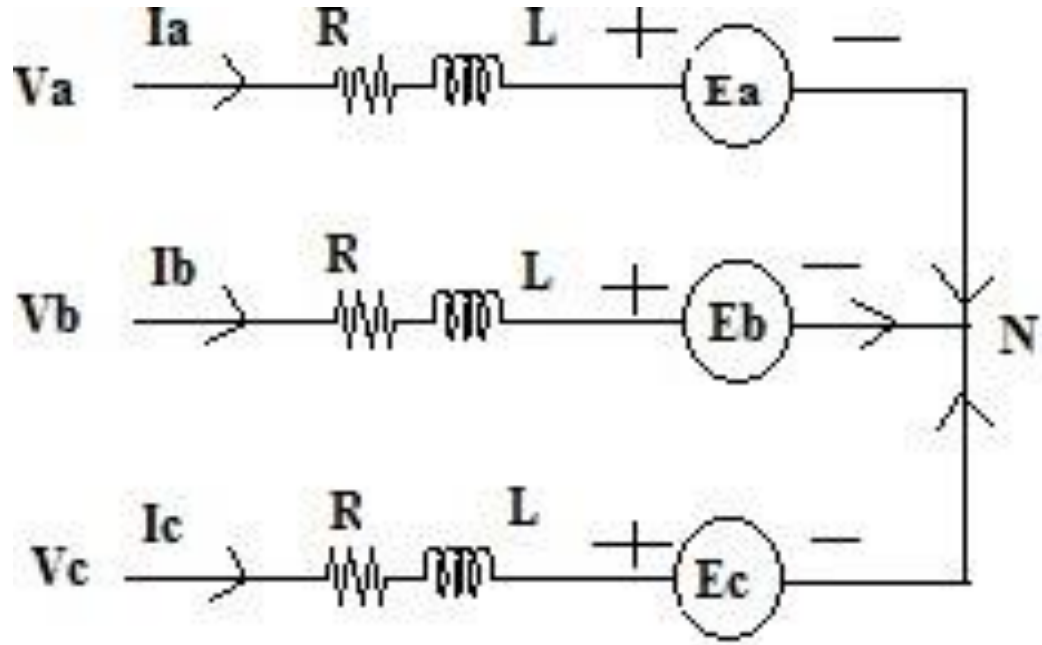


Fig 2.7 Circuit Diagram of Stator Winding

From the fig 2.7 stator winding, the equations of the 3-phase brushless dc machine are as below,

$$V_a = I_a R + L \frac{di}{dt} + E_a \quad (2.6)$$

$$V_b = I_b R + L \frac{di}{dt} + E_b \quad (2.7)$$

$$V_c = I_c R + L \frac{di}{dt} + E_c \quad (2.8)$$

Where V_a , V_b , and V_c are the phase voltages, I_a , I_b , and I_c are the phase currents, R , L are the stator phase resistance, self-inductance and E_a , E_b and E_c are the back emf of phase A, B, and C, respectively. The back emf voltages are functions of the rotor mechanical speed and the rotor electrical angle θ_r , that is the coefficients K_a , K_b , and K_c are dependent on the rotor angle θ_r . The mechanical equations are

$$J \frac{d\omega}{dt} = T_{me} - T_l - B\omega \quad (2.9)$$

Where B is a coefficient, T_l is the load torque, and P is the no. of poles. The coefficient B is calculated from the moment of inertia J and the mechanical time constant T_m as below.

$$B = \frac{J}{T_{em}} \quad (2.10)$$

$$\frac{d\theta_y}{dt} = \frac{P}{2} \omega_m \quad (2.11)$$

Fig 2.8 shows block Diagram of proposed converter topology. BLDC motor is normally powered by conventional three phase inverter which is controlled by the rotor position information obtained from Hall sensors or simply from hall position sensors.

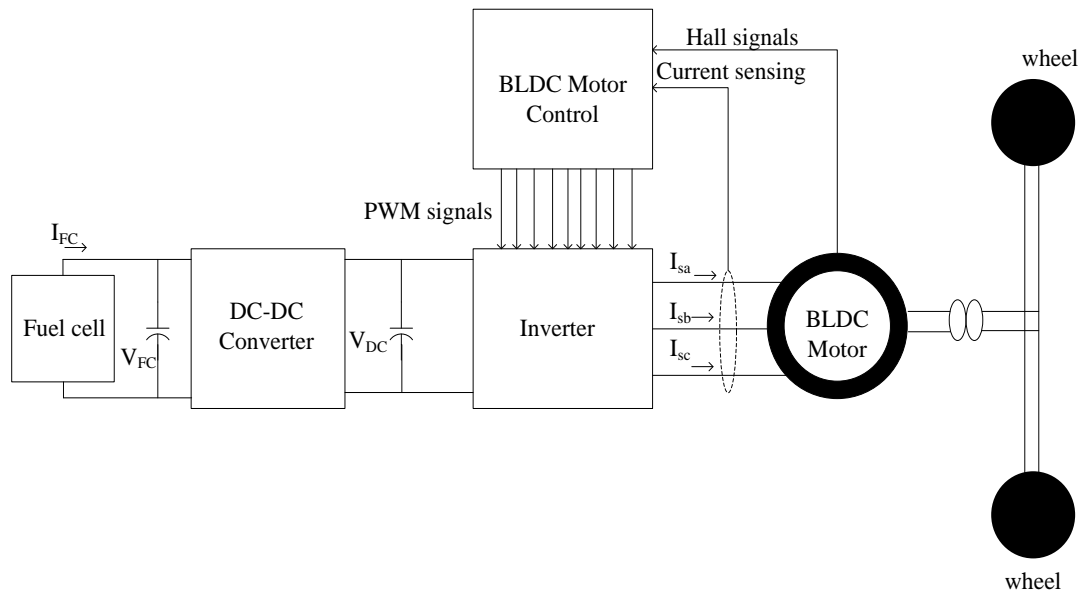


Fig 2.8 Block Diagram of proposed converter topology

In three phase windings, we use one Hall Sensor for each winding to provide three overlapping signals giving a 60° or 120° wide position range. At present, permanent magnet BLDC motor is mostly used in FCEV applications due to simple control, high reliability and high ruggedness. An adequate motor considerably reduces the cost and size of the fuel cell.

2.6 Summary

This chapter clearly elaborates the configuration of the proposed converter and the detailed information about the fuel cell and the BLDC motor. It is also discussed about the modes of operation of the proposed converter with theoretical equations. This section also shows the circuit configurations and waveforms of the different modes. The voltage and current stresses of each component are also depicted.

CHAPTER 3

DESIGN OF PROPOSED CONVERTR

3.1 Introduction

The principle of operation and the steady-state analysis of the converter in the continuous conduction mode are presented. The design and selection of converter parameters, such as inductor and capacitor values, are based on the amount of ripple allowed on each element. The design of the proposed circuit parameters are illustrated in the following sections. The design analysis of Fuel cell and BLDC motor are presented.

3.2 Inductor L_x Design

The inductor L_x current is shown in fig 3.1. The average value of the inductor L_x current is defined as I_1 and the difference between the inductor peak and the average current is Δi_{Lx}

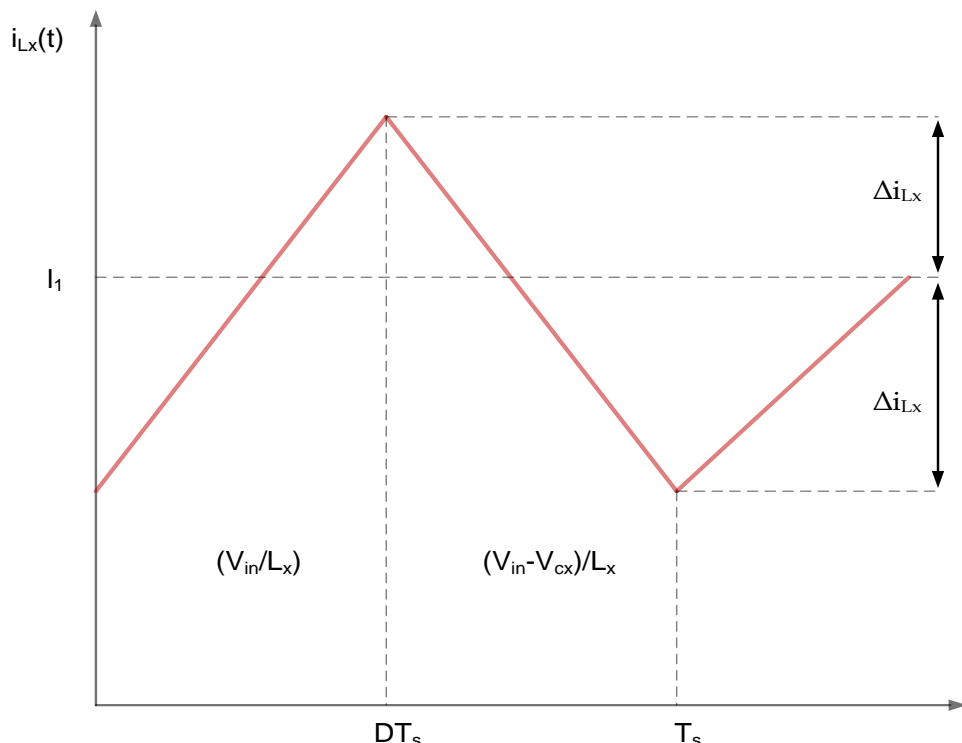


Fig 3.1 inductor L_x current

Considering the first interval of the switching cycle, the ripple of inductor L_x is given by

$$2\Delta i_{LX} = \left(\frac{V_{in}}{L_X}\right) DT_s \quad (3.1)$$

$$L_X = \left(\frac{V_{in}}{2\Delta i_{LX}}\right) DT_s \quad (3.2)$$

As Equation (3.2) describes, the inductance of L_X depends on the input voltage V_{in} , duty cycle D , sample time T_s , and inductor current ripple Δi_{LX} .

3.3 Inductor L_y and L_z Design

The inductor L_y , which is similar to L_z , current is shown in fig 3.2. The average value of the inductor L_y current is defined as I_y and the difference between the inductor peak and the average current is Δi_{Ly} . Considering the first interval of the switching cycle, the ripple of inductor L_y is given by

$$2\Delta i_{Ly} = \left(\frac{V_{in}}{L_y}\right) \left(\frac{DT_s}{1-D}\right) \quad (3.3)$$

$$L_Y = L_Z = \left(\frac{V_{in}}{2\Delta i_{Ly}}\right) \left(\frac{DT_s}{1-D}\right) \quad (3.4)$$

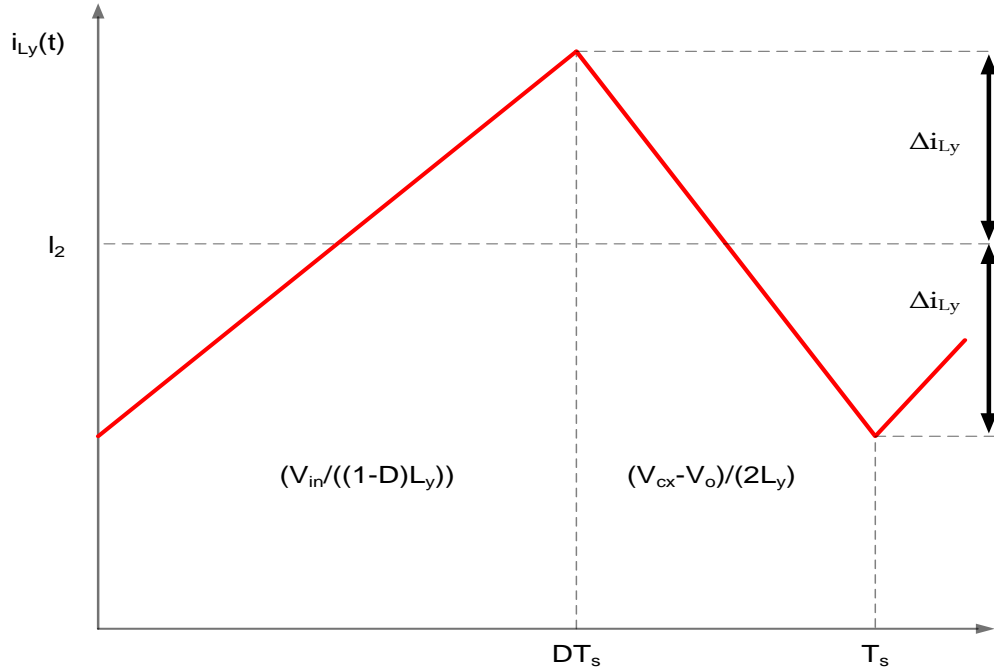


Fig 3.2 The inductors L_y and L_3 currents.

As Equation (3.4) describes, the inductance of inductors L_2 and L_3 depend on the input voltage V_{in} , duty cycle D , sample time T_s , and the inductor current ripple Δi_{L2} . The value of the peak-to-peak ripple of inductor current. The difference between the inductor peak and the average current is Δi_{Ly} .

3.4 Output Capacitor C_y -Design:

The output voltage ripple of the converter is limited by the amount of ripple permitted on the capacitor C_y voltage. Consequently, capacitor C_y should be designed to ensure that the converter output voltage exhibits ripple within the permitted range.

The capacitor C_y voltage is expressed in fig 3.3, where V_o is the capacitor voltage average value and the difference between the capacitor peak and the average voltage is ΔV_o . Considering the first interval of the switching cycle, the ripple of capacitor C_y is given by

$$\Delta v_o = \left(\frac{V_o}{2RC_y} \right) DT_s \quad (3.5)$$

$$C_y = \left(\frac{V_o}{2\Delta v_o} \right) DT_s \quad (3.6)$$

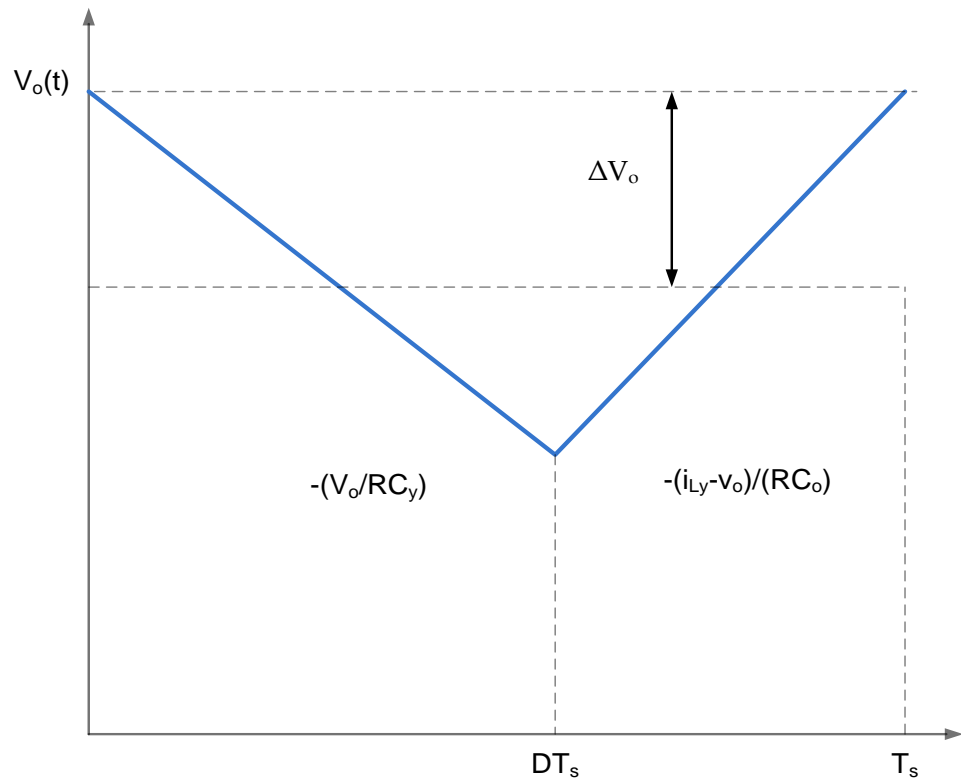


Fig3.3 The capacitor C_y output voltage

As can be seen from Equation (3.6), the value of capacitor C_y depends on the output voltage V_o , duty cycle D , sample time T_s , and the capacitor voltage ripple Δv_o .

3.5 Capacitor C_x Design

ULTRA GAIN BOOST CONVERTER FED BLDC MOTOR FOR FCEV APPLICATIONS

The design of capacitor C_x is not straightforward; similar to capacitor C_y , its current is equal to the inductor L_x current, but without the dc components (see fig 3.4). As seen in fig (3.3) , the capacitor C_x voltage reaches its maximum and minimum limits at the two zero crossing points of is current waveforms.

Let ΔV_{cx} be the difference between the average and max value of the capacitor C voltage value; the relation between the total charge q and the peak-to-peak ripple of the capacitor C_x voltage is

$$q = C_x(2\Delta V_{cx}) \quad (3.7)$$

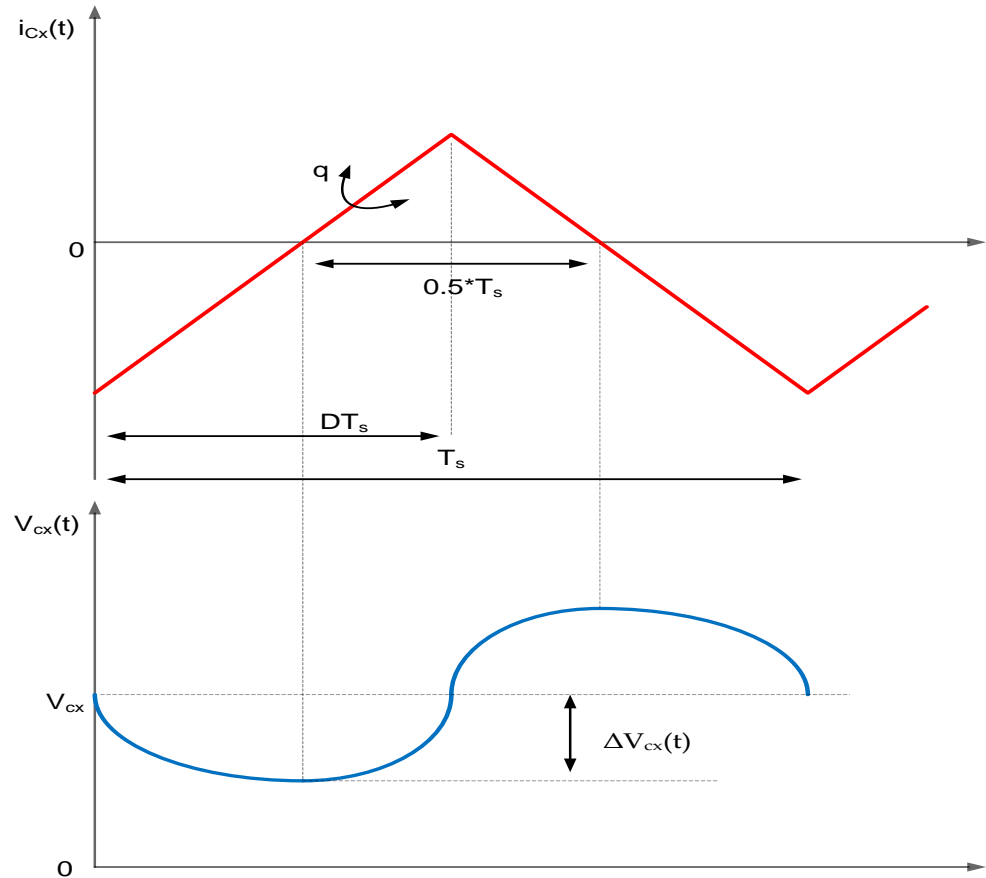


Fig3.4 The capacitor C_x current and voltage.

The value of charge q is obtained by integrating the shaded area of the capacitor C_{1x} current , and due to the symmetry of the capacitor, the current waveform q is given by:

$$q = \frac{1}{2} \Delta i L \frac{T_s}{2} \quad (3.8)$$

Substitute Equation (3.8) into Equation (3.7) and a solution for the voltage ripple peak amplitude yields

$$\Delta v_{C_x} = \frac{\Delta i_L T_s}{8 C_x} \quad (3.9)$$

Hence,

$$C_X = \frac{\Delta i_{LX} Ts}{8\Delta v_{CX}} \quad (3.10)$$

The capacitor value depends upon on the inductor Lx current ripple, sampling time, and the permitted ripple on capacitor Cx.

3.6 Fuel Cell Modelling

A fuel cell is an electrochemical device that converts hydrogen fuel into electricity. The inputs to the fuel cell are air and fuel and these are converted into water and electricity through a chemical reaction. A single fuel cell consists of two electrodes (anode and cathode) and an electrolyte. The electrolyte separates the positive and negative charged ions of the hydrogen fuel. When the hydrogen and oxygen are fed into the cell, electricity is generated at the output of the cell in the presence of an electrolyte. Fuel cell produces only heat and water as the wastage of the chemical reaction.

The cell voltage of PEMFC is given as

$$V_{FC} = E_{Nernst} - V_{act} - V_{ohm} - V_{con} \quad (3.11)$$

Where E_{Nernst} is the open-circuit (or reversible) thermodynamic voltage and is given as

$$E_{NERST} = 1.229 - 8.5 \times 10^{-4}(T - 298.15) + 4.308 \times 10^{-5}T (\ln(P_{H_2}) + 0.5\ln(P_{O_2})) \quad (3.12)$$

Where T is absolute temperature (K), Po2 and Ph2 are oxygen and hydrogen partial pressures (ATM) respectively. Activation voltage V_{act} is the combination of both anode and cathode activation overvoltage and is expressed as

$$V_{act} = -[\delta_1 + \delta_2 + \delta_3 T \ln(CO_2) + \delta_4 T \ln(I_{FC})] \quad (3.13)$$

Where δ_i ($i = 1,2,3,4$) is empirical coefficient for each cell and CO₂ is the dissolved oxygen concentration at the liquid/gas interface and is calculated by using the following expression

$$CO_2 = \frac{P_{O_2}}{(5.08 \times 10^6) \times \exp(-\frac{498}{T})} \quad (3.14)$$

Ohmic overvoltage V_{ohm} is expressed as

$$V_{ohm} = I_{FC}(R_C + R_M) \quad (3.15)$$

Where RM is the electron flow equivalent resistance and R_C is the proton resistance. RC is considered as constant.

$$R_M = \frac{\rho_m L}{A} \quad (3.16)$$

ULTRA GAIN BOOST CONVERTER FED BLDC MOTOR FOR FCEV APPLICATIONS

Where L is membrane thickness (cm), A denotes active area of membrane (cm²) and ρ_m is the membrane specific resistivity (ohm-cm) and is given as

$$\rho_m = \frac{181.6[1+0.03J+0.062(\frac{T}{303})^2(J)^{2.5}]}{[G-0.634-3J]\exp[4.18(1-\frac{303}{T})]} \quad (3.17)$$

Where G is water content of the membrane and J is current density and is expressed as

$$J = \frac{I_{FC}}{A} \quad (3.18)$$

Finally, the concentration overvoltage V_{CON} can be calculated from the following expression

$$V_{con} = -\frac{RT}{nF} \ln \left(1 - \frac{J}{J_{max}} \right) \quad (3.19)$$

Where F is Faraday's constant, R is universal gas constant and Jmax is maximum current density. A DC-DC converter is connected to the output of the fuel cell to maintain a constant voltage across the DC link. The design specifications of 1.26kW PEMFC are given in Table 3.1.

Table 3.1 1.26kW PEMFC parameter specifications

Parameter Description	Rating
Maximum power Pmax	1.26kw
Maximum Current Imax	52A
Maximum Voltage	24.23V
Temperature T	55°C
Number of Cells	42
Nominal airflow Rate	2400 lpm

3.7 VSI and BLDC motor

The 3-Φ inverter is used to convert the dc supply from boost converter to three phase ac and provides it to stator of the BLDC motor so that it can be controlled. At this point, the Insulated Gate Bipolar Transistor (IGBT) based VSI is used to designed for feeding the BLDC motor with dc link charge through converter. It can be able to controlled with two methods such as by controlling the dc supply voltage, the speed can be controlled or by using the PWM control in three phase inverter operation. The inverter is used for only dc-ac conversion and thereby energizing the stator coils in appropriate manner so that the BLDC motor will run smoothly. The hall sensors I ns mounted on

ULTRA GAIN BOOST CONVERTER FED BLDC MOTOR FOR FCEV APPLICATIONS

the motor which provides the hall signals which in turn is converted to EMFs for each phase and the switching of the inverter will be done accordingly.

3.8 BLDC motor Controller and commutation

In brush DC motor, the commutation occurs at brushes in which the reverse current flows but In BLDC motor, the commutation occurs with the help of switching sequences of three phase inverter and hence this termed as Electronic Commutation.

Table 3.2 Truth Table for BLDC drive with Hall Sensor

H _a	H _b	H _c	Emf a	Emf b	Emf c	Q1	Q2	Q3	Q4	Q5	Q6
0	0	0	0	0	0	0	0	0	0	0	0
0	0	1	0	-1	+1	0	0	0	1	1	0
1	11	0	-1	+1	0	0	1	1	0	0	0
0	1	1	-1	0	+1	0	1	0	1	1	0
1	0	0	+1	0	-1	1	0	0	0	0	1
1	0	1	+1	-1	0	1	0	0	0	0	0
1	1	0	0	+1	-1	0	0	1	0	0	1
1	1	1	0	0	0	0	0	0	0	0	0

So as to hall sensors are mounted on the motor for each 60 degrees and the generated Hall signal are processed with the help switching table shown below as Table 3.2 and hence the inverter operates under proper sequence in order to operate the BLDC motor.

3.9 Speed control system

A controller circuit is essential to operate and control the speed of a BLDC motor. There are many types of speed control system developed for controllers but the speed controllers have to modernize with the ages. However, they are generally classified as closed loop and open loop control systems, respectively. Closed loop techniques are used for high accuracy control system. Fig 3.5 shows a BLDC motor speed controller block diagram using two closed loop systems. In this case, the internal loop is used for tuning and sense the power supply polarity and the external loop is used to control the speed. The motor speed controller helps to adjust the voltage of the DC bus. To control the system, DC supply is required and its value depends on the motor speed (rpm) and its capacity.

This system also requires a controller, in which case a PID controller is used that ultimately controls the inverter output voltage. A sensor is an integral part of a

closed loop controller for controlling the speed of a motor. The primary function of the sensor is to convert the physical position and condition of the motor shaft into an equivalent electrical signal for the controller circuit. Typically, BLDC motor requires an AC-like voltage-waveform for its operation, so inverter circuit is used to convert the DC power supply voltage into an equivalent AC supply voltage for proper function.

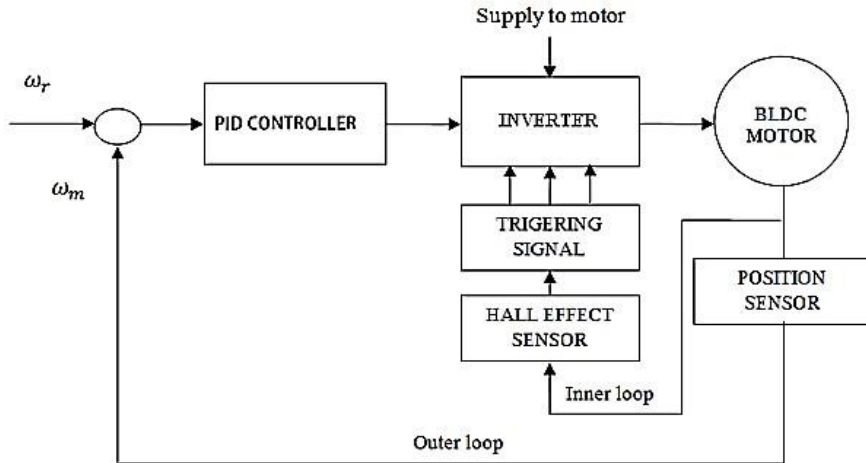


Fig 3.5 Block Diagram of BLDC Motor Speed Control

3.10 The Back Electro Motive Force (BEMF)

Typically, a 3-phase BLDC motor uses six electronic switches (power transistors) to produce 3-phase voltage simultaneously to a full-bridge configuration power converter. The transistors have a rotor position, which will be defined as the switching sequence. Most of the cases motor starter is monitoring by using three hall sensor devices.

The hall sensors provide the information to the decoder block for producing the sign of reference current signal vector to the back electromotive force (BEMF). To operate the motor in the opposite direction, the current is changed in reverse direction or the switching order of the controller is changed. The transistors have a rotor position, which will be defined as the switching sequence. Most of the cases motor starter is monitoring by using three hall sensor devices. The MATLAB simulation block diagram for generating the back EMF of the decoder is shown in Fig. 3.6. To operate the motor in the opposite direction, the current is changed in reverse direction or the switching order of the controller is changed. To operate the motor in the opposite direction, the current is changed in reverse direction or the switching order of the controller is changed. The current is changed in reverse direction or the switching order of the controller is changed. Similarly, Fig 3.7 shows the functional block diagram of the inverter switching for MATLAB simulation, and Table 3.2 shows the decoder

ULTRA GAIN BOOST CONVERTER FED BLDC MOTOR FOR FCEV APPLICATIONS

sequences of the proposed 3-phase PID controller for the BLDC motor to rotate in the counter clockwise motion.

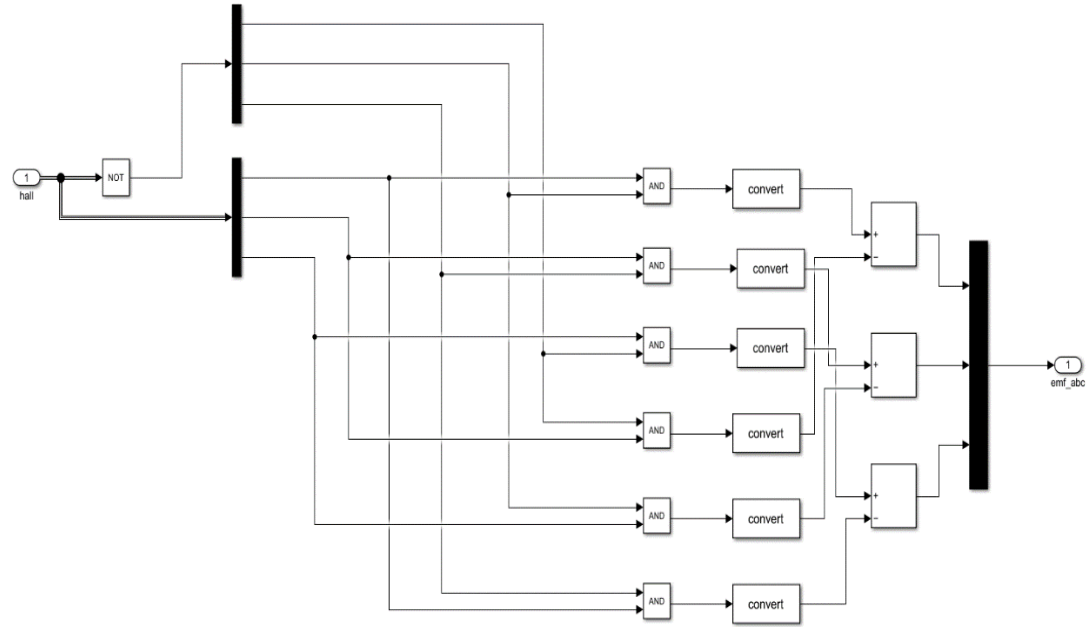


Fig 3.6 Back EMF of Decoder for MATLAB Drive.

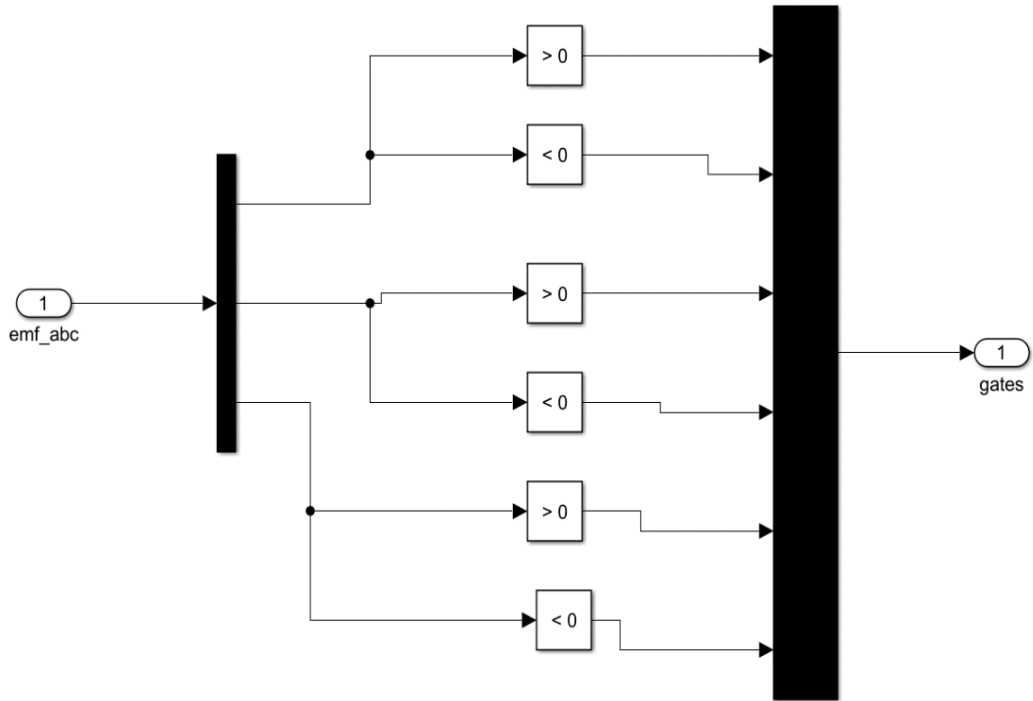


Fig 3.7 Inverter Switching for MATLAB Drive.

Fig 3.8 shows circuit diagram of proposed converter which is fed to the BLDC motor. A Fuel cell is a electrochemical device that converts chemical energy into electrical energy.

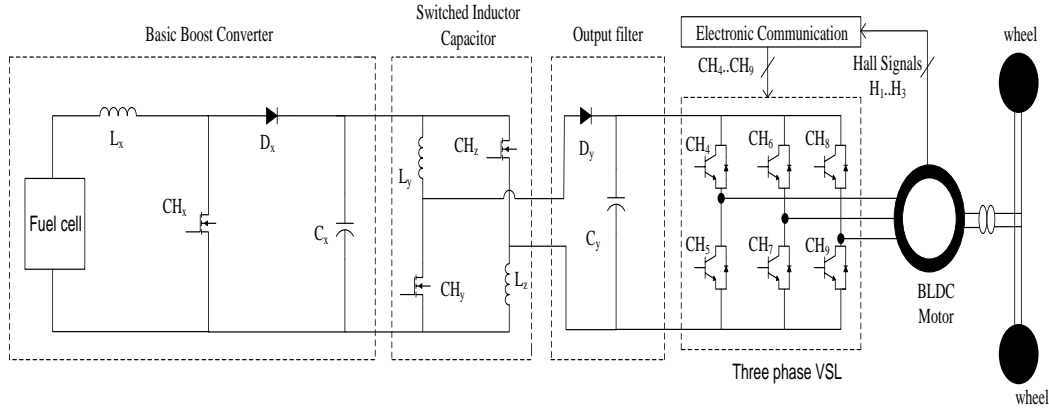


Fig 3.8 Circuit diagram of Proposed converter with BLDC Motor

Among all of these, PEMFCs are dominating the automobile industry due to their low operating temperature and the quick startup. The generated electrical energy from fuel cell i.e. voltage is given as input to ultra gain Boost converter.

In the Ultra-gain boost converter, the output of the basic boost converter is fed as the input to the switched inductor circuit, this circuit raises the voltage level and provides a sufficient voltage at the output side. The output voltage of the proposed converter is given to the BLDC Motor through an inverter for propulsion of the vehicle, this BLDC motor drives the wheels of a vehicle through the vehicle transmission system and switches of the VSI are controlled by using electronic commutation of BLDC motor.

3.11 Summary

This chapter clearly elaborates the detailed information about the design of the proposed circuit parameters. The principle of operation and the steady-state analysis of the converter in the continuous conduction mode are presented. Also explained the design of fuel cell and BLDC motor.

CHAPTER 4

RESULTS AND DISCUSSIONS

4.1 Introduction

An explanation of the Simulink model of the proposed converter is given in this chapter, which exhibits the output waveforms to support the claim of high gain and high efficiency.

Math Works has created Simulink (Simulation and Link) as an add-on to MATLAB. Multi-domain dynamic systems may be modelled and analysed using this graphical programming language.

Table 4.1 Simulation component values

Component	Description	Specification
V_{in}	Input Voltage	20-35 V
V_0	Output Voltage	100-350 V
L_x	Inductor	3 μ H
L_y, L_z	Inductors	3 μ H
C_x	Input Capacitor	260 μ F
C_y	Output Capacitor	260 μ F
D_x	Power Diode	BYE72EW-200
D_0	Output Diode	BYE72EW-200
P_0	Rated Output Power	2.5KW

From the table 4.1, For this converter the input voltage is 20V-35V. The projected converter is designed for an output power of 2.5KW, to reduce the converter size, it is advisable to take higher switching frequencies (f_s). The proposed converter contains five energy elements which includes three inductors and two capacitors. With the considerable current and voltage ripples on the inductors and capacitors respectively, the energy component values are calculated and are observed. The considerable current and voltage ripples on the inductors and capacitors respectively.

The proposed converter contains five energy elements which includes three inductors and two capacitors. The proposed converter contains five energy elements which includes three inductors and two capacitors. With the considerable current and voltage ripples on the inductors and capacitors respectively, the energy component

ULTRA GAIN BOOST CONVERTER FED BLDC MOTOR FOR FCEV APPLICATIONS

values are calculated and are observed. Fig 4.1 & Fig 4.2 are the simulation diagrams of the proposed converter and the whole proposed configuration.

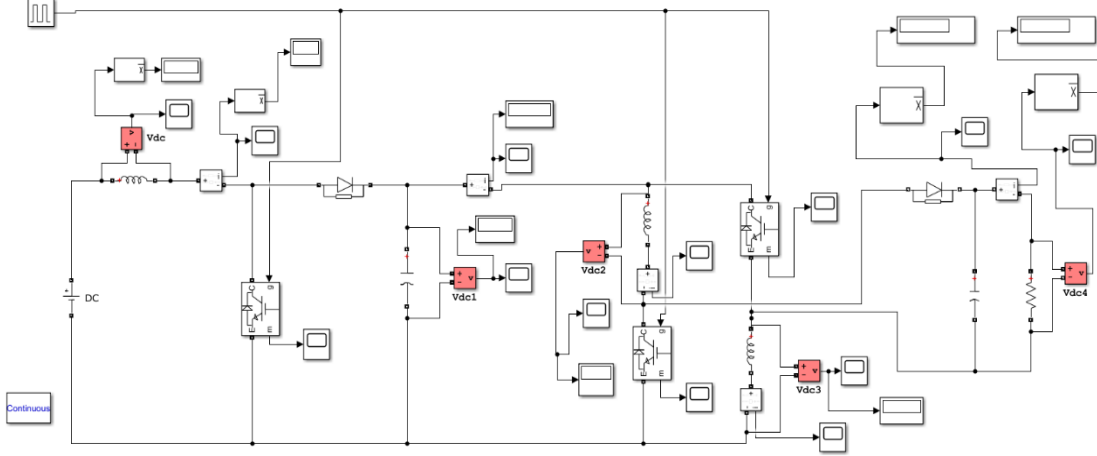


Fig. 4.1 Simulation diagram of the proposed converter

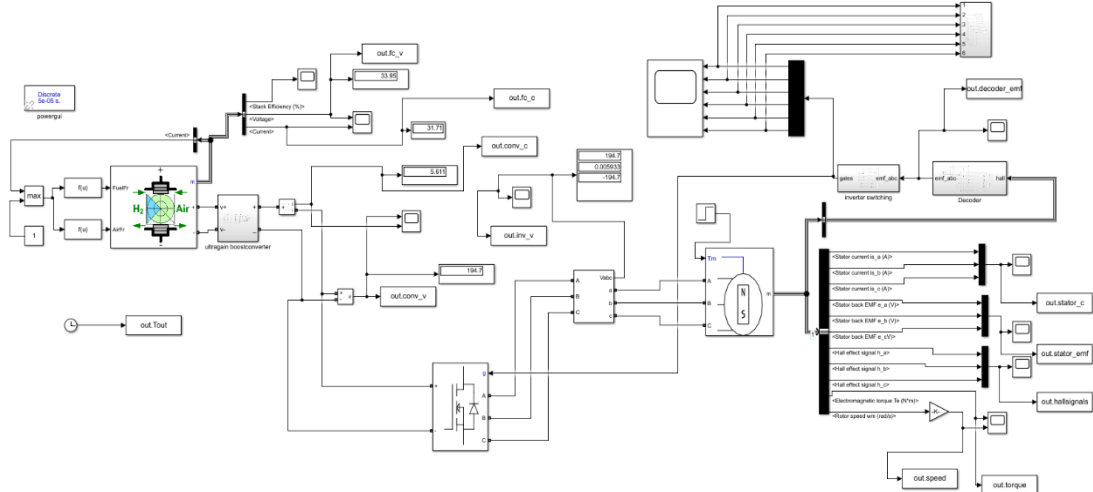


Fig 4.2 Simulation diagram of the whole proposed configuration

4.2 Simulation Waveforms of proposed converter

In this section, Using MATLAB software, simulated waveforms of various parameters such as switch voltage, waveforms, Capacitor voltage waveforms, diode voltage waveforms and output voltage waveforms are obtained clearly. By observing the nature of waveforms of proposed converter, its performance can be understood easily. Ripple content can be estimated. The simulation waveforms of proposed converter for different parameters are illustrated in below figures.

Fig 4.3 clearly shows the simulated capacitor voltage stress waveform of Proposed converter. The value of ripple content obtained with the simulation is equal

to theoretical analysis of the ripple value. The input capacitor voltage stress is simulated by using MATLAB software.

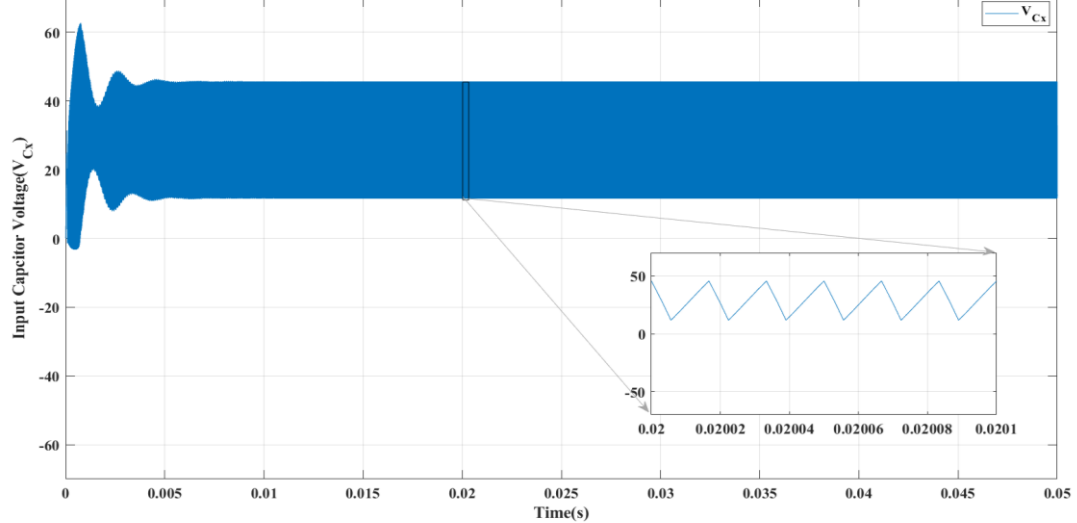


Fig 4.3 Simulated waveform of input capacitor voltage (V_{Cx})

By observing the nature of waveforms of proposed converter, its performance can be understood easily. Ripple content can be estimated. The possible solution for providing a higher voltage gain is the use of switched inductors or capacitors. These low rated components increase the overall efficiency of the system.

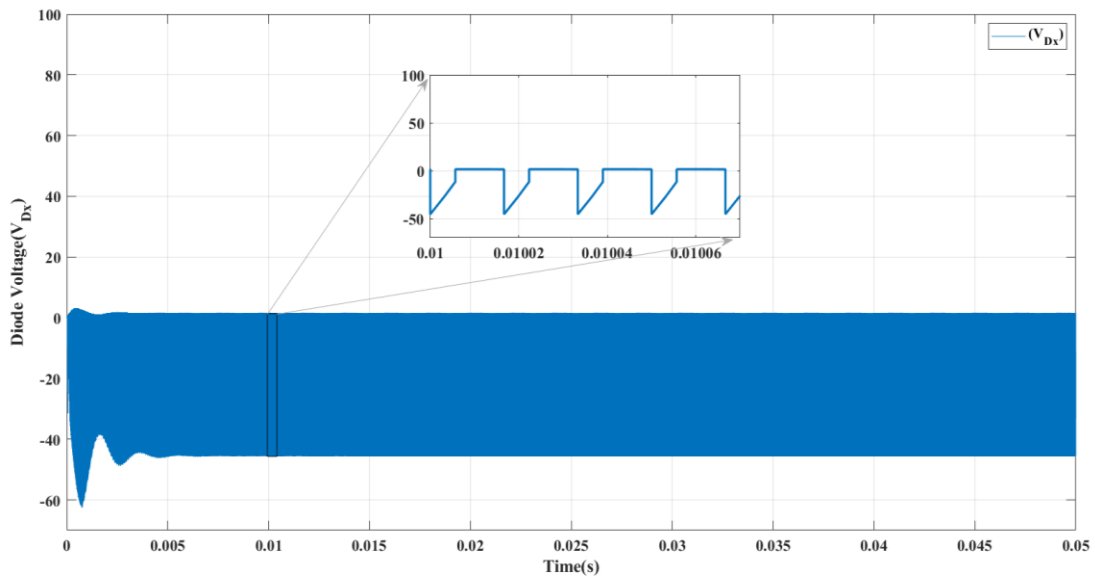


Fig 4.4 Simulated waveform of Diode voltage (V_{Dx})

Fig 4.4 clearly shows the simulated Diode voltage stress waveform of Proposed converter. We can say that Diode voltage stresses are lower in value of the Proposed converter. These are shown with negative values in the waveform.

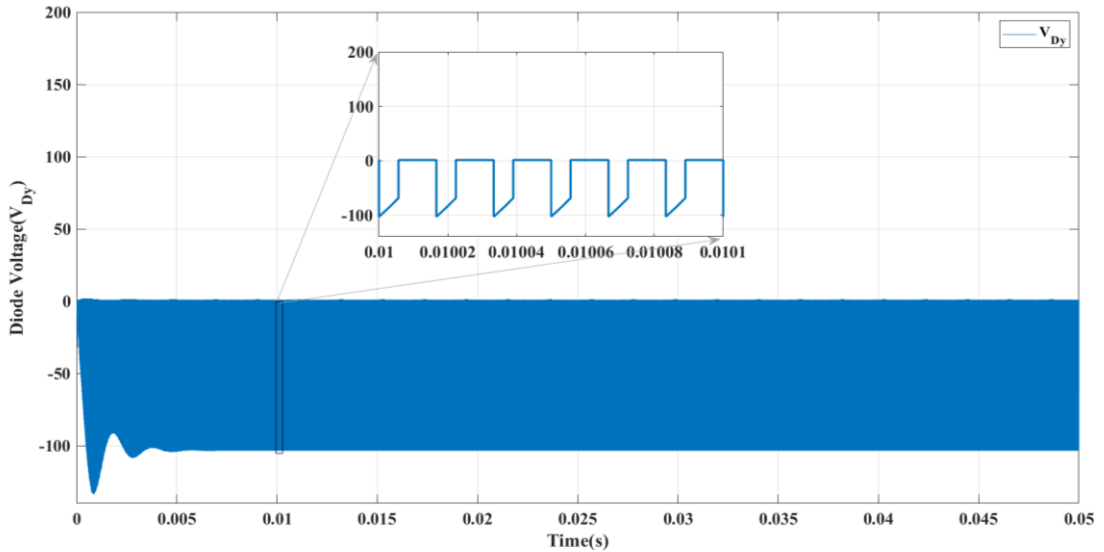


Fig 4.5 Simulated waveform of Diode voltage(V_{DY})

The fig 4.5 clearly shows the simulated Diode voltage stress waveform of Proposed converter. We can say that Diode voltage stresses are lower in value of the Proposed converter. These are shown with negative values in the waveform.. The possible solution for providing a higher voltage gain is the use of switched inductors or capacitors. These low rated components increase the overall efficiency of the system.

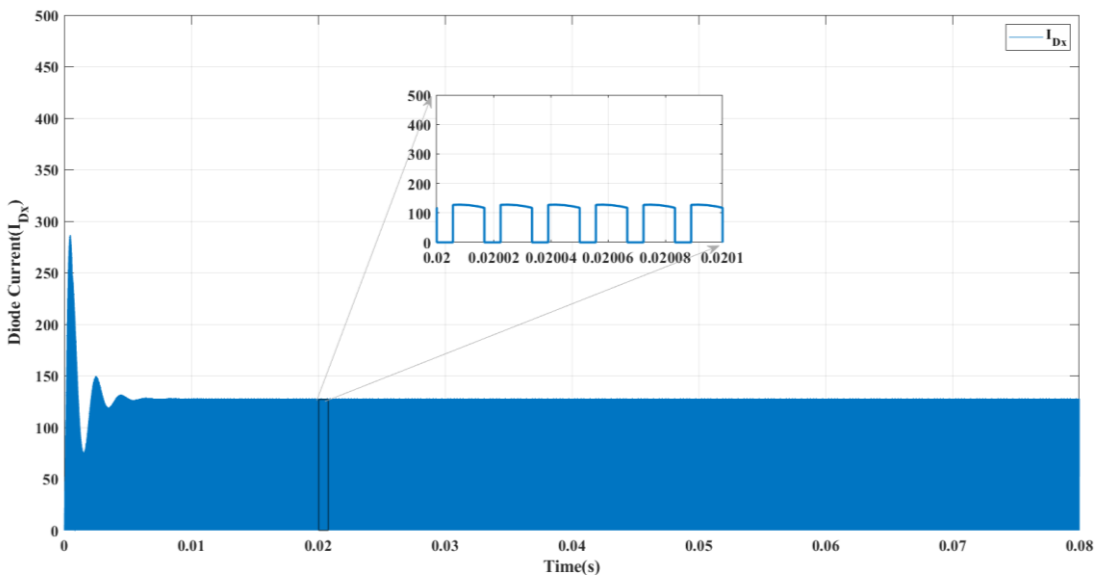


Fig 4.6 Simulated waveform of Diode current (I_{DX})

The fig 4.6 clearly shows the simulated Diode current stress waveform of Proposed converter. We can say that Diode current stresses are lower in value of the Proposed converter. The ripple value is low.

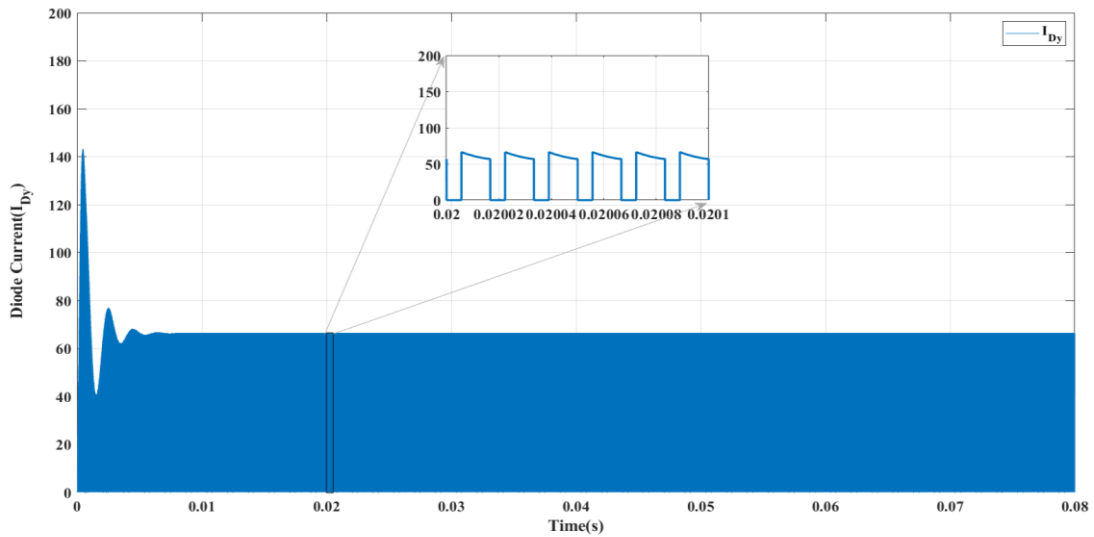


Fig 4.7 Simulated waveform of Diode current (I_{DY})

The fig 4.7 clearly shows the simulated Diode current stress waveform of Proposed converter. We can say that Diode current stresses are lower in value of the Proposed converter.

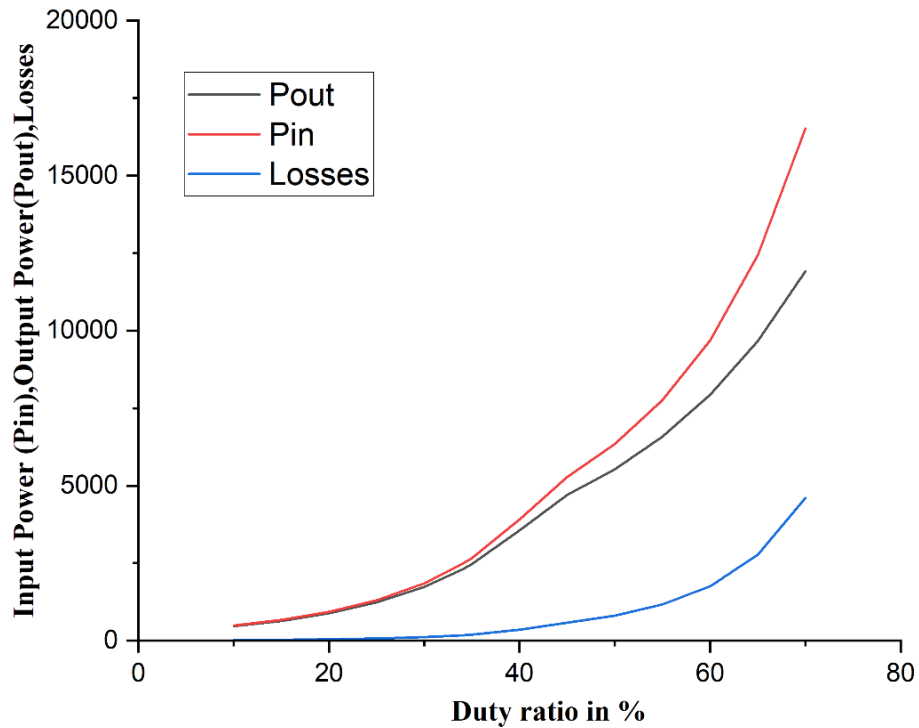


Fig 4.8 Input power P_{in} , Output power P_{out} , Losses

Fig 4.8 gives the input power, output power and power losses of the proposed converter. We know that input power – output power = losses. Losses should be lower in value in order to increase the efficiency. It can be observed that the losses are very low for the proposed converter for various duty ratios.

4.3 Comparison of Proposed Converter with Different Topologies

The merits & demerits of proposed converter can be clearly understood by plotting characteristics Curves such as output voltage vs duty ratio, diode stress vs duty ratio, voltage gain vs duty ratio, and different topologies. High-gain DC-DC converters also find their applications in fuel cells, electric vehicles, battery energy storage, automotive industries, and uninterrupted power supplies. The following are the comparison of the characteristics curves which helps us to know the performance level of proposed converter when compared to other different topologies. High-gain DC-DC converters also find their applications in fuel cells, electric vehicles, battery energy storage, automotive industries, and uninterrupted power supplies.

The proposed converter is suitable for different applications, such as Electric Vehicle applications and has some distinct advantages including a high step-up capability, low voltage stress and high efficiency. DC-DC converters are also referred to as linear or switching regulators, depending on the method used for conversion. There is a broad range of operating voltages for various electronic devices, such as ICs and MOSFETs, which necessitates providing voltage for each. High-gain DC-DC converters also find their applications in fuel cells, electric vehicles, battery energy storage, automotive industries, and uninterrupted power supplies. A Buck Converter provides a lower voltage than the original voltage, while a Boost Converter supplies a higher voltage. DC/DC converters can be designed to transfer power in only one direction, from the input to the output. However, almost all DC/DC converter topologies can be made bi-directional. A bi-directional converter can move power in either direction, which is useful in applications requiring regenerative braking.

The following are the comparison of the characteristics curves which helps us to know the performance level of proposed converter when compared to other different topologies in terms of various converter parameters and also simulated with various converter parameters. However, almost all DC/DC converter topologies can be made bi-directional.

The following are the comparison of the characteristics curves which helps us to know the performance level of proposed converter when compared to other different topologies. High-gain DC-DC converters also find their applications in fuel cells, electric vehicles, battery energy storage, automotive industries, and uninterrupted power supplies.

ULTRA GAIN BOOST CONVERTER FED BLDC MOTOR FOR FCEV APPLICATIONS

Table 4.2 Comparison values of proposed converter with different converter topologies

S.NO	Converter	No.of inductors	No. of capacitors	No.of diodes	No. of power switches	Total no. of components	Voltage gain
1	Boost	1	1	1	1	4	$1/(1-D)$
2	SL Boost	2	1	4	1	8	$(1+D)/(1-D)$
3	SC Boost	1	3	1	1	6	$1/(1-D)$
4	Dual-Switch High-Boost DC– DC Converter	1	3	4	2	10	$(3-2D)/(1-2D)$
5	Non isolated bidirectional DC– DC converter [23]	2	3	0	4	9	$1/(1-D)^2$
6	A New High-Gain DC-DC Converter [24]	2	2	2	2	8	$(1+D-D^2)/(1-D)^2$
7	Non isolated high step-up DC–DC converters	2	5	4	1	12	$(2+D)/(1-D)$
8	Single Switch High Step-Up DC– DC Converter	2	3	1	4	10	$(3+D)/2(1-D)$
9	Ultra voltage gain boost converter	3	2	2	3	10	$(1+D)/(1-D)^2$

The proposed converter is suitable for different applications, such as Electric Vehicle applications.

The comparison values of the proposed converter with the different converter topologies are mentioned in the table 4.2. The values are compared in terms of number of inductors, capacitors, Diodes, Components used. The values of Voltage gains of different converters are also mentioned. To operate a DC-to-DC converter, you must have a battery that is either higher or lower than the regulator output voltage. By using the smaller number of components, high voltage gain is achieved. For achieving or to maintain a consistent load voltage over the whole battery voltage range, the DC-to-DC converter must be able to function as a step-up or step-down voltage provider. By this the proposed converter has major advantages when compared to other converter topologies.

Fig 4.9 shows the output of different configurations. The voltage gain of various converter topologies are presented in comparison with the proposed converter. From the above we can clearly say that the voltage gain of the proposed converter is very large than the other DC-DC converter topologies. The voltage gain of various converter topologies are presented in comparison with the proposed converter. The main objective of the proposed converter is achieved using Boost converter which gains the voltage with lower voltage stresses and lower current stresses for different duty ratios which is used for Electric vehicle applications. Various converter topologies are presented in comparison with the proposed converter.

The proposed converter provides high voltage-gain while at the same time, imposing small voltage stresses on the active devices. Such features make the proposed converter to suitable well for electric vehicle applications. Gain of various converter topologies are presented in comparison with the proposed converter. The proposed converter is more efficient than other topologies.

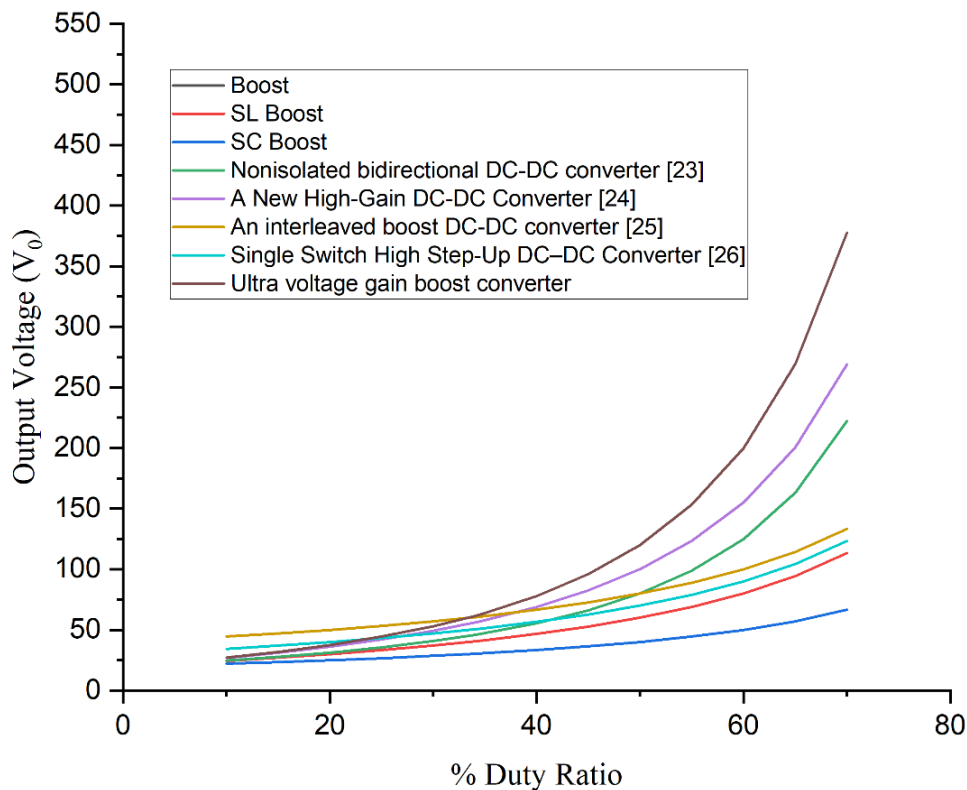


Fig 4.9 Output voltage (V_o)

From fig 4.10 It shows the Voltage gain values of different converters. The Boosting factor of various converter topologies are presented in comparison with the

proposed converter. "voltage gain" is regarding one of the main aspects regarding various types of Boost converters.

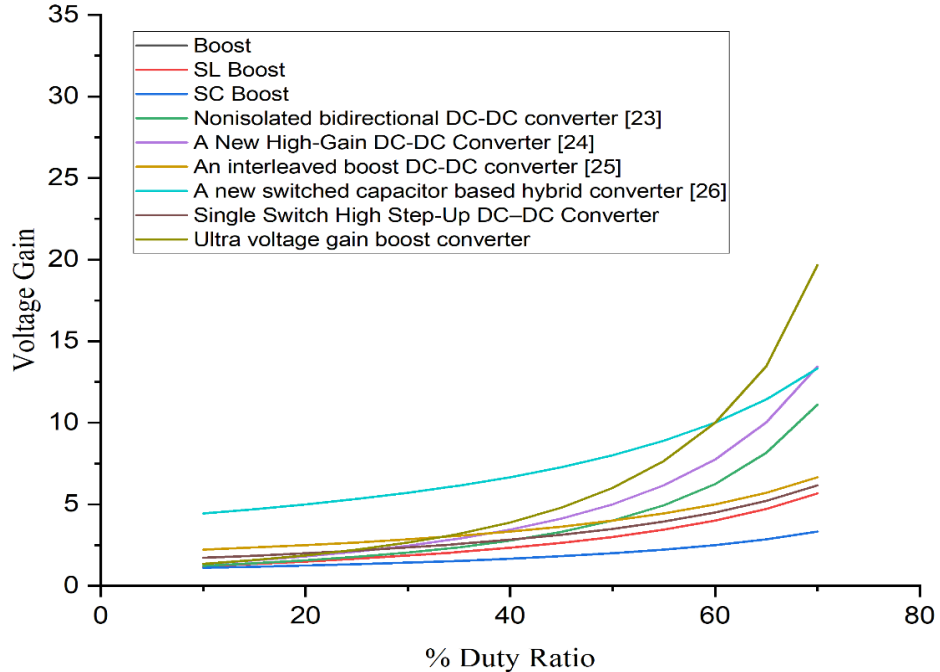


Fig 4.10 Voltage Gain

4.4 Simulation results of proposed configuration

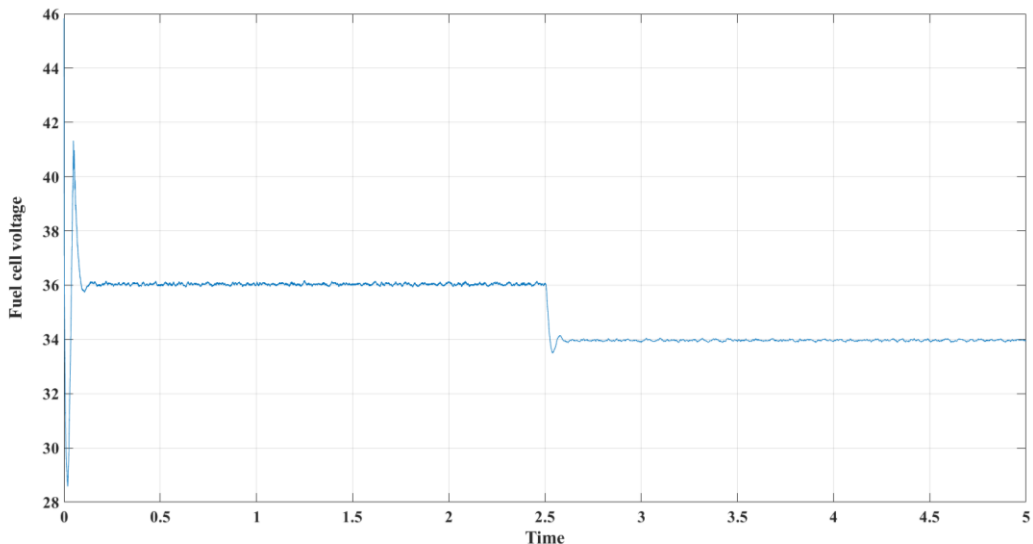


Fig 4.11 Fuel cell voltage vs time

The Fig 4.11 shows the fuel cell voltage. In this figure, the X and Y axis represented the time in second (sec) and the fuel cell generated voltage. The fuel cell voltage is 36V after 0.1 seconds and then is reduced to 34V after 2.5 seconds due to increase in the load torque. The output voltage of the fuel cell is used as the input of the converter.

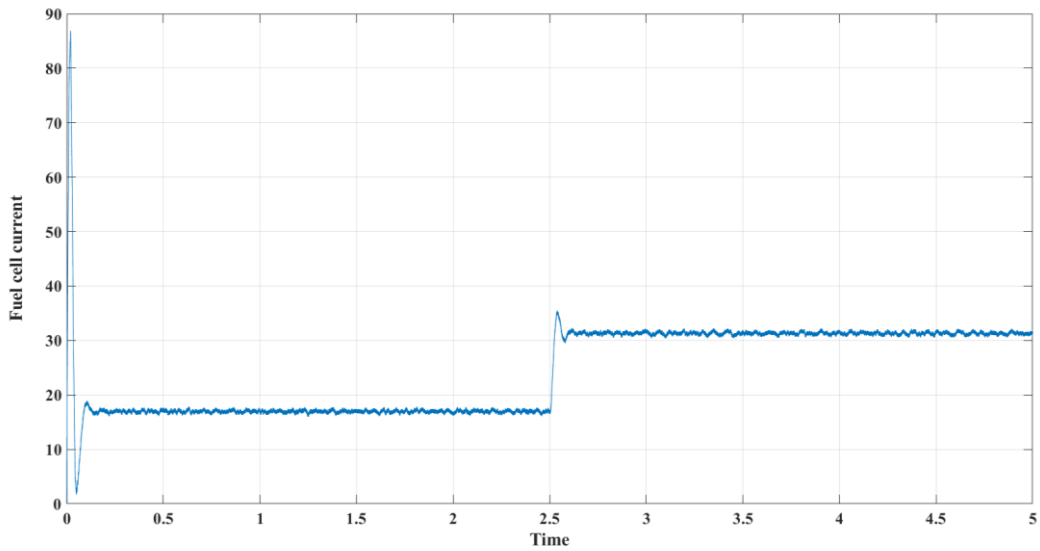
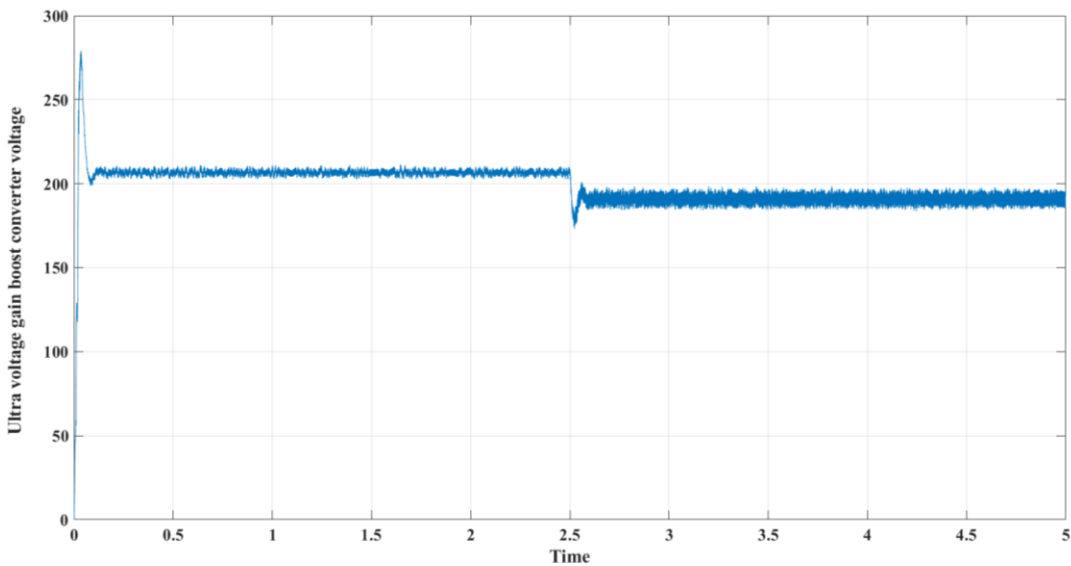


Fig 4.12 Fuel cell current vs Time

Fig 4.12 shows the generated fuel cell current which is at the input side. The x-axis and y-axis represent the time in second (sec) and the fuel cell current(amps). The fuel cell current after 0.1 seconds is approximately 18amps, then it is increased to 31amps respectively at 2.5 seconds due to increase in the load.



4.13 Boost Converter voltage vs Time

Fig 4.13 shows the ultra-gain boost converter voltage. The x-axis and y-axis represent the time in second (sec) and the boost converter voltage (volts). From the figure it is shown that the output voltage of ultra-gain boost converter is around 210V, which is approximately 5 times greater than fuel cell output voltage.

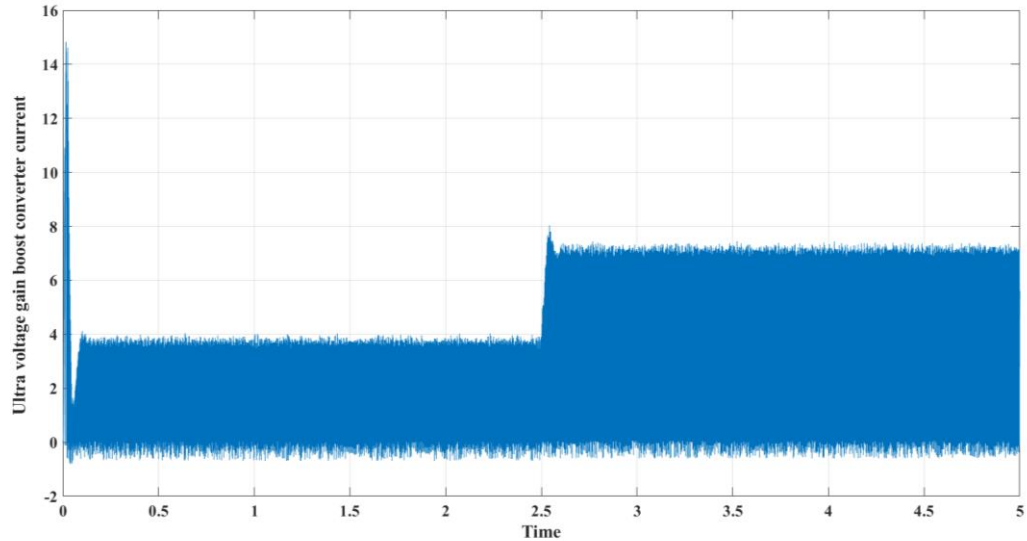


Fig 4.14 Boost converter Current vs Time

Fig 4.14 is about the ultra-gain boost converter current respectively. The x-axis and y-axis represents the time in second (sec) and ultra gain boost converter current (amps). As the step load increases at the load side, the current raised approximately to 7.5amps at 2.5 seconds.

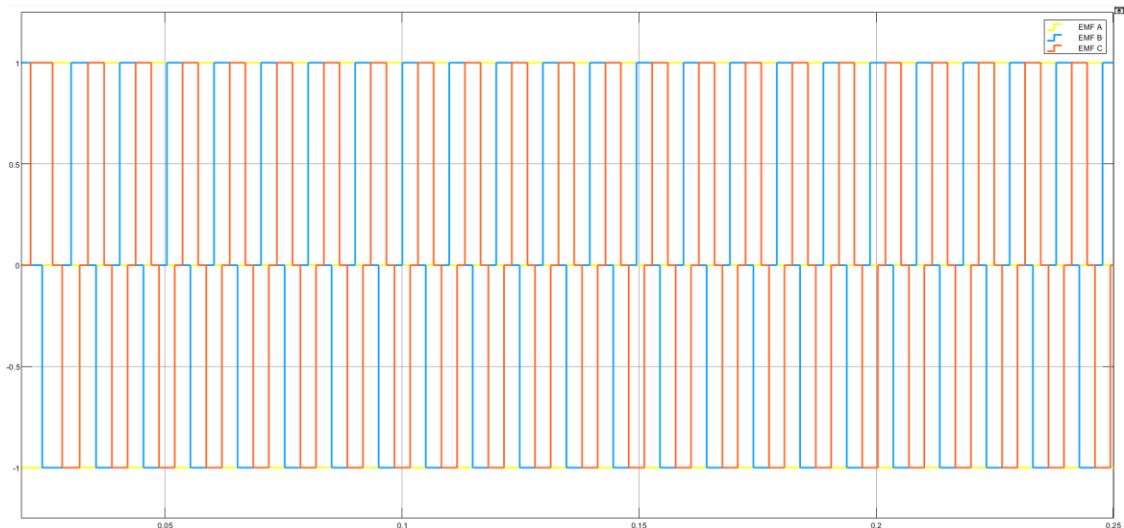


Fig 4.15 Decoder- EMF pulses of respective A, B & C Hall signals

Fig 4.15 represents the EMF pulses of respective A, B & C Hall signals. The x-axis and y-axis represents the time in second (sec) and EMF pulses of respective A, B & C Hall signals. Decoder decodes the respective A, B and C Hall signals as respective EMF pulses as shown in above figure. As shown in above EMF pulses vary in between 0 & 1 and 0 & -1 depending on the respective Hall signals.

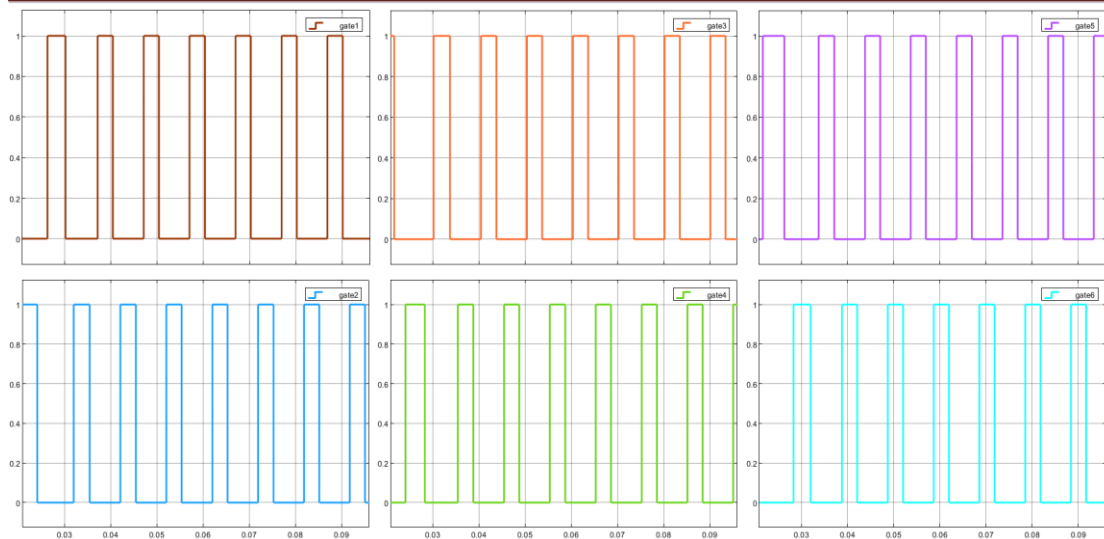


Fig 4.16 Gate Pulses Provided by Inverter- Switching Block

The fig 4.16 represents gate pulses provided by inverter switching block. The x-axis and y-axis represents the time in second (sec) and gate pulses. The gate pulses vary between 0 and 1. These are the six gate pulses that can be applied to the inverter six switches respectively.

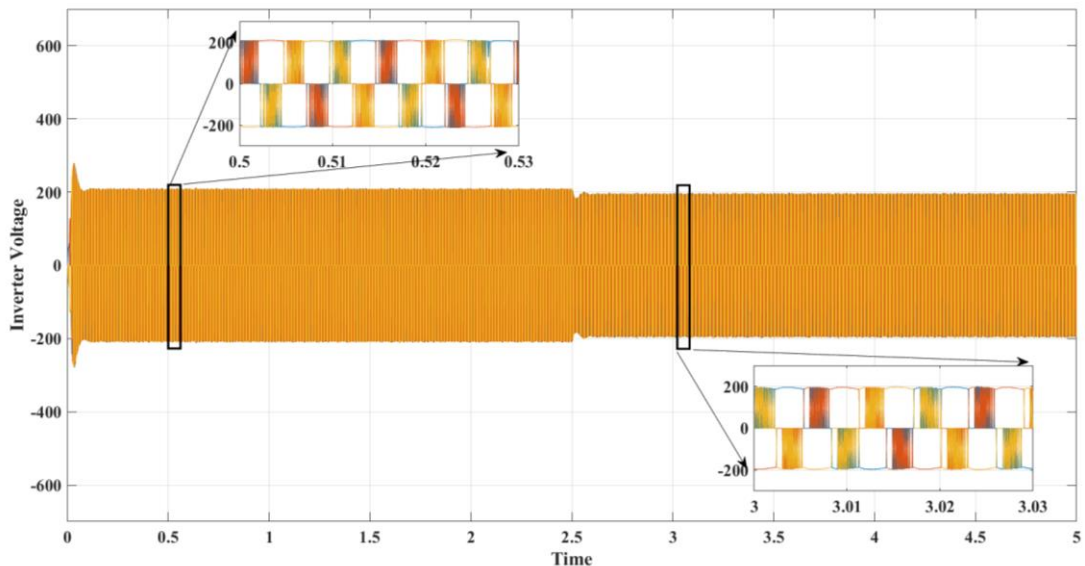


Fig 4.17 Inverter Output Voltage

Fig 4.17 represents the inverter output voltage respectively. The x-axis and y-axis represents the time in second (sec) and output voltage of the inverter. The output voltage of the inverter is between -200 and +200.

Fig 4.18 represents the hall signals provided by the Hall sensors(generally mounted on rotor) based on rotor position of BLDC motor.. The x-axis and y-axis

ULTRA GAIN BOOST CONVERTER FED BLDC MOTOR FOR FCEV APPLICATIONS

represents the time in second (sec) and hall signals. The width of the signals are different at all the times, where the signals vary between 0 and 1.

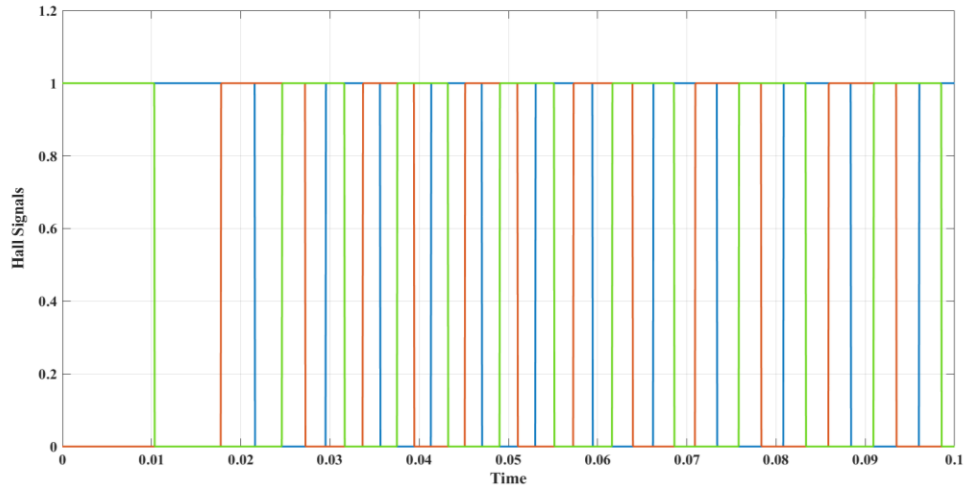


Fig 4.18 Hall Signals vs Time

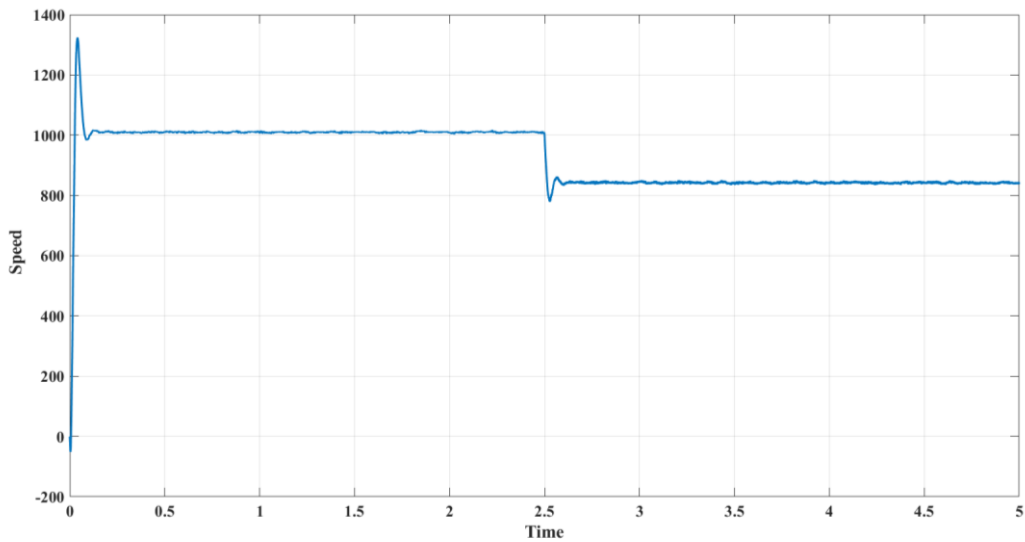


Fig 4.19 Speed Vs time

The performance of the designed brushless DC motor is shown in Fig 4.19. In this figure, the X and Y axis represented the time in second (sec) and the speed (rpm) of the BLDC motor. The graph represents the speed of BLDC motor varying with time. Upto 2.5 seconds, the speed is around 1000 rpm. At 2.5 sec, the load torque is suddenly increased, so the speed is decreased to 800 rpm. The speed characteristics play a vital role in analysing the performance of BLDC motor. The graph represents the speed of BLDC motor varying with time. Upto 2.5 seconds, the speed is around 1000 rpm Fig 4.20 shows the output torque response performance of the BLDC motor respectively.

ULTRA GAIN BOOST CONVERTER FED BLDC MOTOR FOR FCEV APPLICATIONS

In this figure, the X and Y axis represents the time in second (sec) and electromagnetic torque value in Newton-meter (Nm) of the BLDC motor.

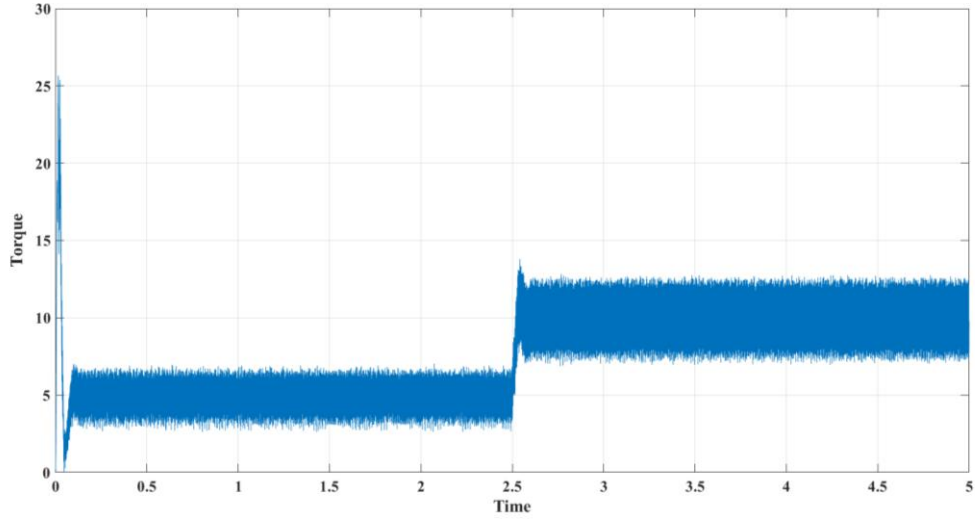


Fig 4.20 Torque vs Time

The load torque is suddenly raised from initial value 5 to value 10 at 2.5 sec.so, Electromagnetic torque waveform is also raised at 2.5 sec. It shows the applied torque value on BLDC motor. Torque characteristics play a vital role in analysing the performance of BLDC motor.

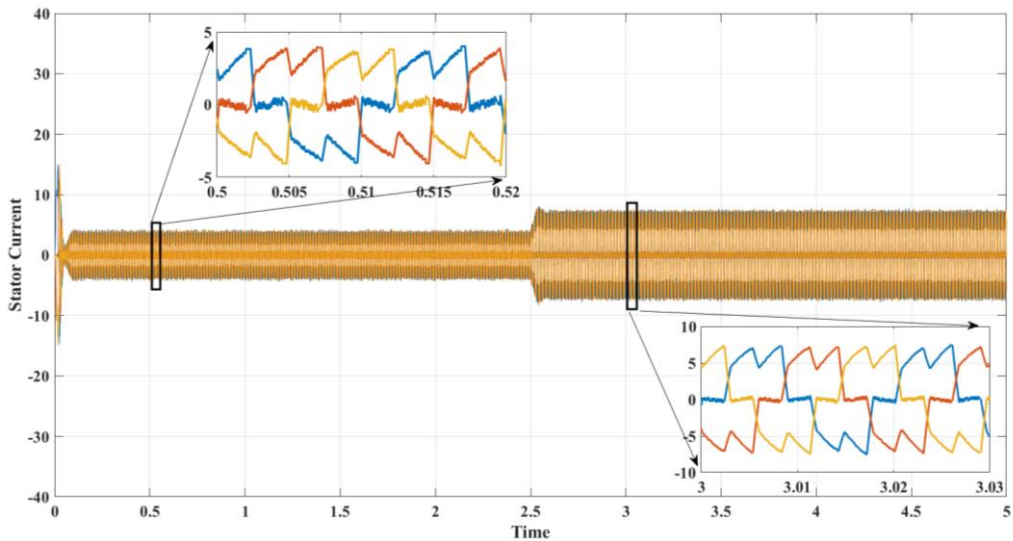


Fig 4.21 Stator Current vs Time

Fig 4.21 represents the stator current. The x-axis and y-axis represents the time in second (sec) and stator currents(amps) respectively. The currents of stator are between -4 and +4 and from 2.5seconds the stator currents ranges from -7 to +7. As the load torque is increased , stator currents also increased at 2.5 seconds. Different colours shows the respective A,B & C phases stator currents respectively.

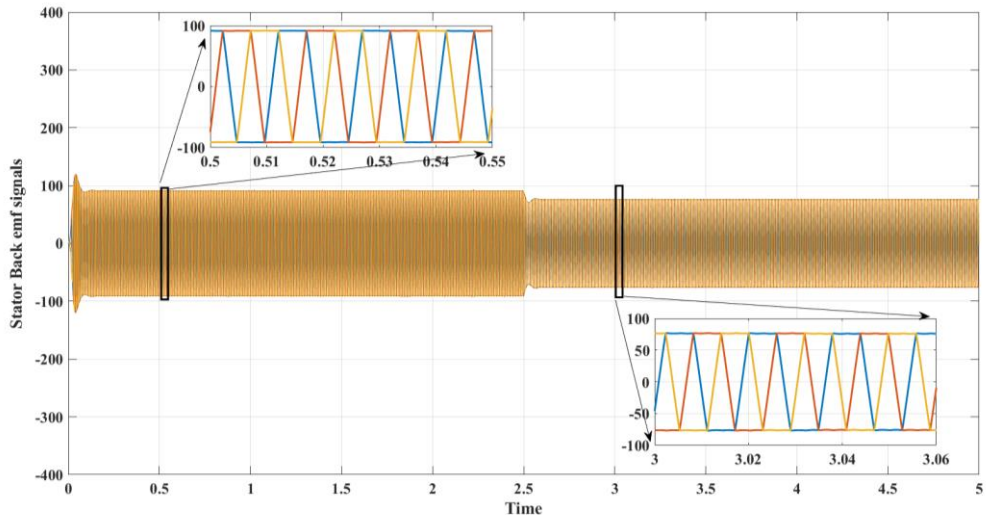


Fig 4.22 Stator Back emf signals Vs Time

Fig 4.22 shows the trapezoidal shaped Back EMF signals of A,B,C phases respectively. As the load torque is increased suddenly at 2.5 seconds, the Back EMF voltage is decreased at 2.5 seconds. In this figure, the X and Y axis represented the time in second (secs) and back emf value in Volt (V) of the BLDC motor. The 3-phase back emf voltages of the BLDC motor are illustrated by the figure, respectively. It is clear from the figure that the 3-phase back emf voltages are fixed $\pm 84V$.

4.5 Summary

Here the proposed converter is simulated using the MATLAB software using the theoretically designed specifications. The input, output voltage and currents waveforms are clearly illustrated along with their values comparison. Similarly, to show that the converter experiencing lower switching stresses, lower voltage and current stresses of all the switches are also represented clearly. The proposed structures are more suitable for modern applications in which it is desirable to achieve high voltage gains by using non-extreme duty-cycles.

CHAPTER 5

CONCLUSION AND FUTURE SCOPE

5.1 Conclusion

In this project, an Ultra Voltage gain DC-DC boost converter fed BLDC motor is proposed for FCEV applications. The proposed converter has reduced the fuel cell input current ripples and the voltage stress on the power semiconductor switches. The developed converter consisted of three switches, two diodes, and three inductors. A theoretical analysis of the converter demonstrated its high voltage-gain, low voltage and low current stress on its devices, and high efficiency. A three-phase BLDC motor controller has been successfully designed based on PID controller scheme and analyzed its performance. The Simulation results obtained were consistent with the theoretical analysis of the converter.

5.2 Future Scope

Fuel cells have the advantages of clean power generation, high reliability, high efficiency and low noise. The rapid advancements in fuel cell technologies play a vital role in development of Advanced Electric vehicles in future. The proposed converter has the features like increasing step-up gain voltage, continuous input current, increasing efficiency and a smaller number of components. Hence perfectly suitable for fuel cell system and Electric vehicle applications. In future BLDC motors can be well suited not only for FCEV vehicles but also for all types of Electric vehicles & for many other applications due to simple control, high reliability and high ruggedness etc.

5.3 POs & PSOs Attainments

After the completion of the project, the following POs and PSOs are attained PO1, PO2, PO3, PO4, PO5, PO7, PO8, PO9, PO10, PO12 PSO1, PSO2, PSO3, PSO

REFERENCES

- [1] Ye, Y., & Eric Cheng, K. W. (2014). Quadratic boost converter with low buffer capacitor stress. *IET Power Electronics*, 7(5), 1162–1170.
- [2] Shahin, A., Hinaje, M., Martin, J.-P., Pierfederici, S., Rael, S., & Davat, B. (2010). High Voltage Ratio DC–DC Converter for Fuel-Cell Applications. *IEEE Transactions on Industrial Electronics*, 57(12), 3944–3955.
- [3] F. L. Tufoli, D. de Souza Oliveira, R. P. Torrico-Bascope, and Y. J. A. Alcazar, “Novel nonisolated high-voltage gain DC–DC converters based on 3SSC and VMC,” *IEEE Trans. Power Electron.*, vol. 27, no. 9, pp. 3897–3907, Sep. 2012.
- [4] Li, W., Zhao, Y., Wu, J., & He, X. (2012). Interleaved High Step-Up Converter with Winding-Cross-Coupled Inductors and Voltage Multiplier Cells. *IEEE Transactions on Power Electronics*, 27(1), 133–143.
- [5] Bist, V., & Singh, B. (2014). An Adjustable-Speed PFC Bridgeless Buck–Boost Converter-Fed BLDC Motor Drive. *IEEE Transactions on Industrial Electronics*, 61(6), 2665–2677.
- [6] Singh, B., & Bist, V. (2015). A BL-CSC Converter-Fed BLDC Motor Drive with Power Factor Correction. *IEEE Transactions on Industrial Electronics*, 62(1), 172–183.
- [7] Ardi, H., Ajami, A., Kardan, F., & Nikpour, S. (2016). Analysis and Implementation of a Non-Isolated Bidirectional DC-DC Converter with High Voltage Gain. *IEEE Transactions on Industrial Electronics*, 1–1.
- [8] Kumar, J. S. V. S., & Rao, P. M. (2017). Design and simulation of front-end converter for fuel cell based electric vehicle applications. *2017 IEEE International Conference on Power, Control, Signals and Instrumentation Engineering (ICPCSI)*.
- [9] De Almeida, P. M., Valle, R. L., Barbosa, P. G., Montagner, V. F., Cuk, V., & Ribeiro, P. F. (2021). Robust Control of a Variable-Speed BLDC Motor Drive. *IEEE Journal of Emerging and Selected Topics in Industrial Electronics*, 2(1), 32–41.
- [10]. Jyotheeswara Reddy, K., & Sudhakar, N. (2018). High Voltage Gain Interleaved Boost Converter with Neural Network Based MPPT Controller for Fuel Cell Based Electric Vehicle Applications. *IEEE Access*, 6, 3899–3908.



[TESEA] Editor Decision

1 message

Revista UTB <revistautb@utb.edu.co>

Tue, Jun 13, 2023 at 3:19 AM

To: NAGI REDDY B <nagireddy208@gmail.com>, G. Vinay Kumar <vinayygt@gmail.com>, B. Vinay Kumar <bvinayraj226@gmail.com>, B. Jhansi <jhansireddybussa@gmail.com>, B. Sandeep <bajasandeep2@gmail.com>, K. Sarada <saradak@kluniversity.in>

NAGI REDDY B, G. Vinay Kumar, B. Vinay Kumar, B. Jhansi, B. Sandeep; K. Sarada:

We have reached a decision regarding your submission to Transactions on Energy Systems and Engineering Applications, "Fuel Cell Based Ultra-Voltage Gain Boost Converter for Electric Vehicle Applications".

Our decision is to: Accept Submission

The production editor will check your manuscript to make sure that it adheres to the style guidelines.

Your paper will be prepared for publication at this time. We will contact you again for approval of the galleys.

Thank you for your contribution to Transactions on Energy Systems and Engineering Applications. If you have any questions, please contact me at tesea@utb.edu.co.

Sincerely,

Andres Marrugo
Universidad Tecnológica de Bolívar
agmarrugo@utb.edu.co

Andres Marrugo
Editor

[Transactions on Energy Systems and Engineering Applications](#)



Article

Fuel Cell Based Ultra-Voltage Gain Boost Converter for Electric Vehicle Applications

B. Nagi reddy^{1,*}, G. Vinay Kumar², B. Vinay Kumar³, B. Jhansi⁴, B. Sandeep⁵ and Sarada K⁶

^{1,2,3,4,5} Department of Electrical and Electronics Engineering, Vignana Bharathi Institute of Technology, Hyderabad, India.

⁶ Department of Electrical and Electronics Engineering, Koneru Lakshmaiah Education Foundation.

* Correspondence: nagireddy208@gmail.com

Received: XX Month 202X; Accepted: XX Month 202X; Published: XX Month 202X

Abstract: By changing the transformer turn's ratio, high voltage gain can typically be achieved. However, transformer topologies have a few drawbacks such as high cost, design complexity and increased weight etc. The ultra-voltage gain boost converter suggested in this article is based on fuel cells. A higher output voltage is necessary for a basic EV system to generate propulsion for a vehicle. Switched inductors circuit is used in this article as an alternative to achieve high voltage gain. This switched inductor circuit helps the system to run more effectively overall by reducing size, weight, and cost. This transformer-less topology can thus boost the voltage levels while allowing the converter switching devices to operate under low voltage stress. The suggested design can generate larger voltage gain values even at low duty ratios. The fundamental boost converter's output serves as the input for the switched inductor circuit. This switched inductor circuit boosts voltage level while supplying more voltage to the output side. For applications requiring ultra-voltage gain in Electric Vehicles, the suggested converter is a serious contender. The EVs based on fuel cells produce minimum to zero pollution when compared to internal combustion engines. Space required is less by using this topology. To increase the output voltage and produce high voltage gain, a fuel cell-based ultra-high voltage gain boost converter may be employed. For the continuous conduction mode, the steady state investigation of the setup is described. The converter is theoretically verified and simulated using MATLAB software to show how the concept operates.

© 2022 by the authors. Published by Universidad Tecnológica de Bolívar under the terms of the [Creative Commons Attribution 4.0 License](#). Further distribution of this work must maintain attribution to the author(s) and the published article's title, journal citation, and DOI. <https://doi.org/10.32397/tesea.volX.nX.XXX>

1. Introduction

Present-day applications for DC-DC converters include photovoltaic energy systems, electric vehicle systems, and numerous industrial and automotive systems. Stepping up the voltage from a low level to a higher one is crucial for improving the performance of the working system such as an EV system; see Figure 1.

How to cite this article: B. Nagi reddy, G. Vinay Kumar, B. Vinay Kumar, B. Jhansi, B. Sandeep and Sarada K. Fuel Cell Based Ultra-Voltage Gain Boost Converter for Electric Vehicle Applications . *Transactions on Energy Systems and Engineering Applications*, X(X): XXX, 2022. DOI:10.32397/tesea.volX.nX.XXX

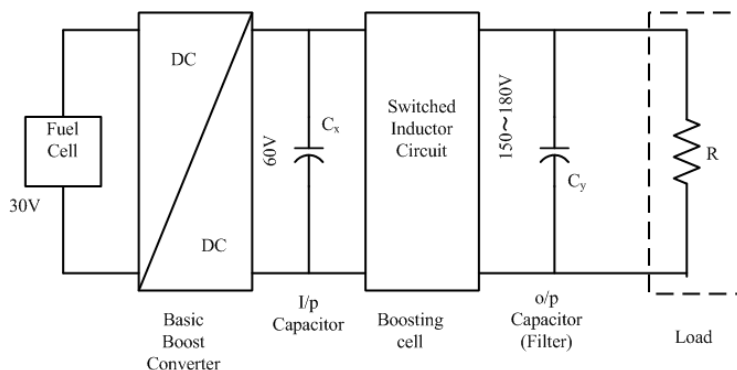


Figure 1. Fuel cell-based voltage gain dc-dc converter.

A higher output voltage is necessary for a basic EV system to generate propulsion for a vehicle. The series connection of cells or batteries will increase the output voltage. However, several hundreds of batteries are employed which might be a major challenge as the amount of space needed in the EV systems increases. The output voltage can be increased and high voltage gain achieved by using a fuel cell-based ultra-high voltage gain boost converter. This converter would make it possible to attain ultra-voltage gains with greater efficiencies under low voltage stresses while requiring less room and battery maintenance.

Fuel cell output voltage is basically DC in nature and it typically varies with load. They are consequently constantly linked to electrical power networks by means of suitable, controllable converter equipment. A typical boost converter should have an unlimited voltage gain. Practically speaking, however, this isn't the case because the converter also has conduction losses, switch voltage drops, and diode voltage drops. The converter is often set up to provide output voltages of around 400 V with input voltage levels between 18 and 50 V [1-5]. The power device's practical step-up performance is constrained by parasitic capacitance and inductance, conduction losses brought on by resistors, and diode voltage sag. The fact that the power switch may experience reverse recovery problems and magnetic saturation when activated during a high-duty cycle is another drawback of having such a high step-up ratio [6-8].

The cascading boost converter topology introduced can accomplish greater voltage gain without the need for a maximum duty cycle than the typical boost converter; even so, its switches are subjected to intense voltage and current stress. Another method for rising voltage gain is to use switched inductors and capacitors. [15-16]. The voltage gain of a switched converter topology is twice that of a typical step-up converter, however because semiconductors are used, a higher voltage stress is produced. In order to increase voltage gain and lessen the voltage and current stress on the switches, the voltage lift approach is utilized [17-18]. When the conversion ratio is high, a large number of diodes and capacitors are used. For limited topologies like linked inductors and flyback converters, the turns ratio in addition to the duty cycle has been employed to regulate the converter voltage gain. The necessary boost ratio is achieved at a medium duty cycle by which the overarching efficiency is increased. In methodologies like the flyback converter, there will be the leakage inductance which discharges energy. This energy causes increasing dissipations is an inevitable outcome. Such issues can be resolved by using passive clamp circuits or active clamp circuits. Without using any magnetic components, boosting is accomplished using switched capacitor converters [20-22]. Numerous articles are available in the literature on the design of high-gain, high-efficiency boost converters. [9-14]. By varying the transformer's turns ratio, topologies utilizing a transformer can produce high voltage gains. Transformers also provide separation between the input and output sides. Transformer-less topologies compete in terms of price, weight, and ease of design [12].

Boost converters with hard switching and switched capacitors, according to [22], have a low efficiency of less than 75%. The switched capacitor performs better when a resonance inductor is added [23-28].

Converters with inductors can adjust their duty cycle to boost a wide range, but the boosting range of the converter being compared is somewhat limited in comparison. The ultra-voltage gain boost converter is proposed in this paper. The proposed converter can be used for different purposes, including fuel cell-based systems. The converter's use of a switched inductor circuit increases step-up capability. The proposed converter attains high voltage gains and higher output voltages even for low duty ratio values. Because of this, the suggested converter is appropriate for use in electric vehicle applications. A 20V output from the fuel cell serves as the converter's input voltage. The voltage obtained from the converter would be in the range of 50-120V for a low duty ratio value, say D=0.5. The advantages of the proposed ultra-gain boost converter include improved efficiency, decreased voltage stress on active elements, and high step capacity.

A new proposal for an ultra-voltage gain high step-up voltage and low stresses in dc-dc converters is made. The paper consists of the following sections:- About Fuel cell, Modelling of Fuel cell, Fuel cell based EV system, Operation and Design analysis of Proposed ultra gain boost converter, Simulated waveforms, Results and Conclusion.

2. Fuel Cell

Since a fuel cell effectively produces the power by means of chemical energy of hydrogen, a fuel cell energy system is used as the converter's input. Compared to older technologies that rely on combustion, fuel cells have many advantages. These work with higher efficiencies, in excess of 60%. Compared with the internal combustion engines, hydrogen fuel cells are the most popular fuel cells because they emit only water, produce very little heat, and have very low emissions (see Figure 2). One benefit of fuel cells over batteries is that they don't self-discharge and don't need to be recharged. They need fuel and oxygen to operate continuously, but as long as these inputs are available, they can continuously generate electricity. A cathode (or anode) and an anode (or cathode) are sandwiched around an electrolyte to form a fuel cell. Air is introduced into the cathode, while fuel such as hydrogen, is introduced into the anode. To generate electricity, hydrogen fuel cells use a catalyst at the anode to divide hydrogen molecules into protons and electrons, which then move in opposite directions to the cathode. Electric current is produced as the electrons move through an external circuit. To create heat and water, protons in the anode react with oxygen and electrons at the cathode.

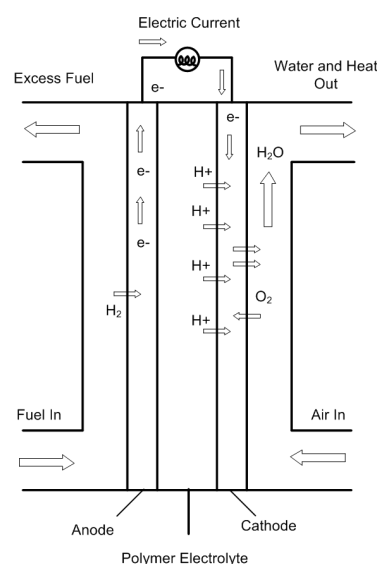
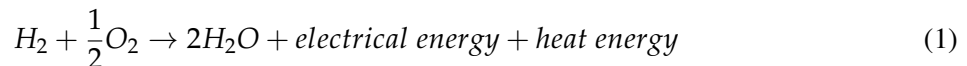


Figure 2. Basic hydrogen fuel-cell

3. Fuel-cell modelling

Hydrogen-based chemical energy is transformed into electrical energy via fuel cells, which are electrochemical devices. Without the need of thermal or electromechanical mechanisms, oxygen and hydrogen are both transformed into water and power. Under the electric field, the fuel cell's anode and cathode may settle. Ions can readily migrate across electrodes after settling. Overall, the anode and cathode oxidation and reduction reactions compose the Proton exchange membrane fuel cell (PEMFC) basic chemical reaction. Hydrogen oxidizes at the anode to produce protons and electrons. At the cathode, water is produced by two protons and two electrons. (1) refers to the entire chemical reaction.



The voltage generated from the fuel cell is given by

$$V_{FC} = E_{Nernst} - V_{act} - V_{ohmic} - V_{con} \quad (2)$$

Where V_{act} is used for modeling the activation losses and is given by

$$V_{act} = A \cdot \ln \left(\frac{i_{FC} + i_n}{i_0} \right) \quad (3)$$

The voltage drop due to Ohmic losses is given as:

$$V_{Ohm} = R_m (i_{FC} + i_n) \quad (4)$$

The concentrations losses are expressed as:

$$V_{Con} = -B \cdot \ln \left(1 - \frac{i_{FC} + i_n}{i_1} \right) \quad (5)$$

Figure.3 shows the electrical equivalent circuit that was utilized to simulate the fuel cell.

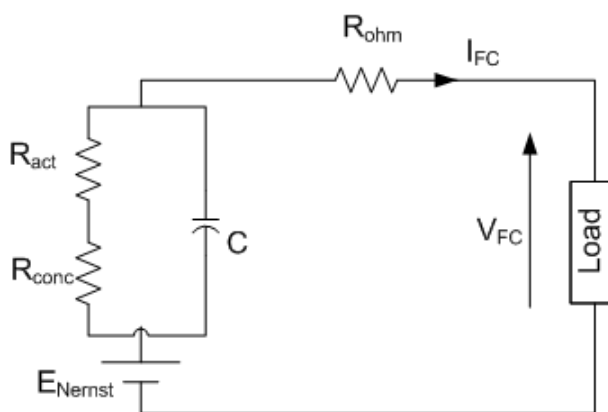


Figure 3. Electrical equivalent circuit

Figure.3 shows the electrical equivalent circuit that was utilized to simulate the fuel cell. Compared with the internal combustion engines, fuel cells emit very little to zero emissions. As a result, the most alluring distributed generation system resources for power delivery are fuel cells. To start a car quickly, batteries must be connected in parallel or series with the fuel cells. Low DC voltage is produced at the

fuel cell stack's output. Number of fuel cells must be added to the stack or a step-up converter must be used to generate higher DC voltages. Instead of using more fuel cells, this configuration uses a basic boost converter cascaded with a switched inductor circuit.

4. Fuel-cell based EV system

DC-DC converters can only transfer power in one direction, from input to output. But, it is possible to make all the DC-DC configurations bidirectional, though. A bidirectional topology is beneficial for applications which needs regenerative braking because it can transfer power in either direction. By adjusting the duty ratio, it is possible to control the amount of power flow from the input to the output. Usually, this is done to keep constant power or to regulate the input current, output voltage, and current. Converters built on transformers might offer isolation between the input and the output. Transformer topology does have some disadvantages like complexity, high cost, and heavy weight. The switched inductor circuit serves as the converter's boosting cell. These inexpensive, light-weight, and compact components with low ratings aid in raising the voltage to higher levels. The switched inductor circuit receives the output of the fundamental boost converter as its input. By increasing the voltage level, this circuit also delivers a sufficient voltage at the output side. Through the controller, the output voltage is further fed to the traction motor. As shown in Figure 4, the controller regulates the traction motor's speed and torque. Through the transmission system, the traction motor propels the wheels of a car.

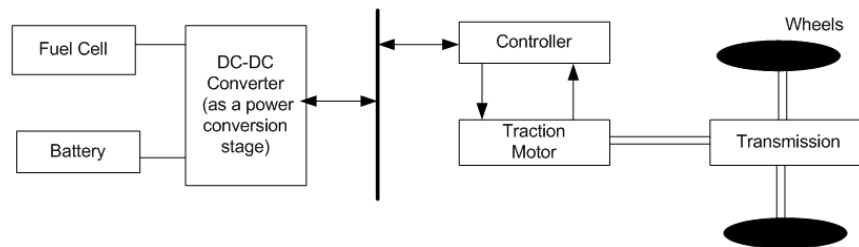


Figure 4. Basic block diagram of fuel cell fed electric vehicle

5. Proposed Ultra voltage gain Boost converter

The suggested converter's circuit configuration is shown in Figure 5. The converter that is being proposed is basically composed of three elements. First is the basic boost converter configuration, second is the switched inductor circuit and finally, third is the output filter capacitor. The proposed configuration includes three switches, two capacitors, three inductors, and two diodes. To the switched inductor circuit, the fundamental boost converter circuit is cascaded. To prevent output voltage ripple, the output filter capacitor is connected at the output side. In this context, the load denoted by the symbol "R" is thought of as a traction motor that drives the wheels of an electric vehicle. The three switches are switched ON and OFF at the same time. The switches and the two diodes in the circuit complement each other. While the switches are open, the inductor current has a clear path to follow. Inductors are charged when the switches are in the ON position, and their energies are released to the output load when they are in the OFF position.

The converter functions in continuous conduction mode. In CCM, the inductor current flows from end to end and it never reaches zero due to which the inductor partially discharges prior to the switching cycle. The parameters are taken to be ideal in order to make it easier to analyse the converter, and a small-ripple factor is employed in the following analysis. Figure 6 displays the waveforms corresponding to the proposed converter. The following sections discuss two different operating modes:

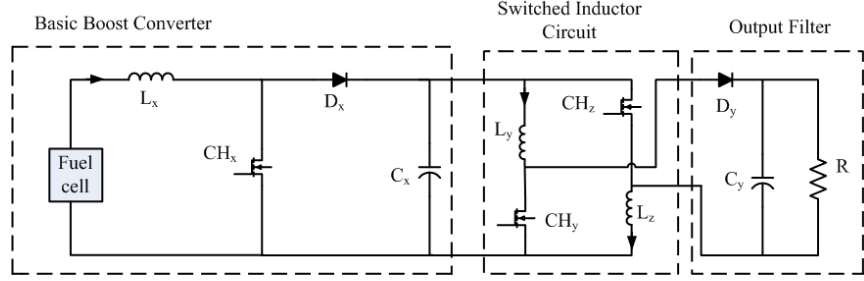


Figure 5. The proposed configuration

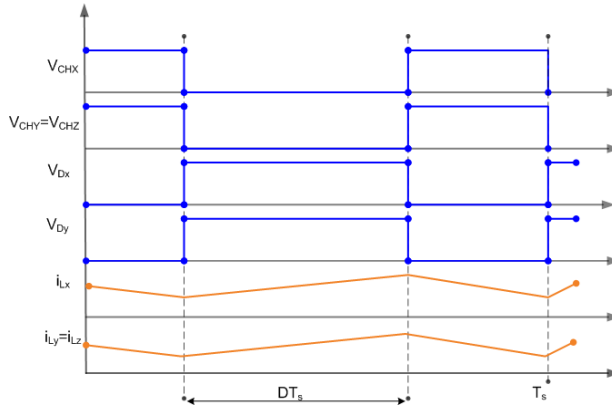


Figure 6. The converter's optimal key waveforms

5.1. Mode-1

In this mode, all three switches are turned on at once. Figure 7 below illustrates how this mode-1 is configured. Reverse biased diodes D_X and D_Y operate in this mode. The input dc source charges the inductor L_X , while the capacitor C_X charges the inductors L_Y and L_Z . The two capacitors, C_X and C_Y release the energy. While C_Y releases its energy to the load side, input capacitor C_X releases its energy to the inductors L_Y and L_Z . In this mode, the inductors L_Y and L_Z charge simultaneously. The following are the characteristic equations for this mode of operation:

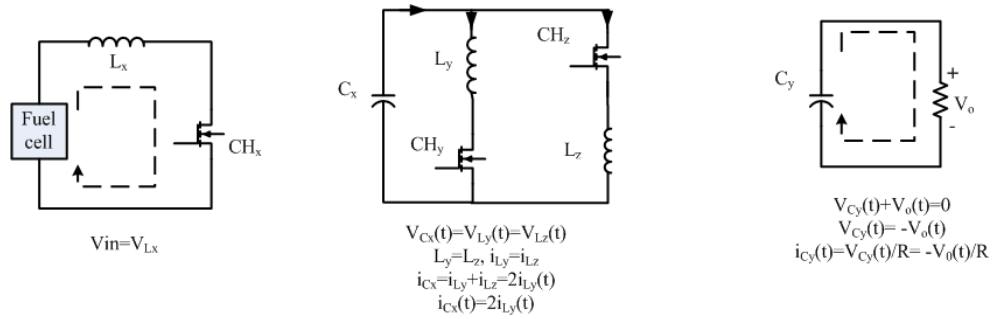


Figure 7. The configurations of mode 1

5.2. Mode-2

Inside this method of operation, all three switches are toggled off at the same time. Figure 8 depicts the configuration of this mode-2. In this mode the energy from the inductors L_Y and L_Z is discharged to the output capacitor C_Y and the output load, while the inductor L_X discharges its energy into the capacitor C_X .

Two diodes are activated in this mode, they function as free-wheeling diodes and give the inductor currents a continuous path. In this mode, the inductors L_Y and L_Z are connected in series. The characteristics equations for this mode of operation are as follows:

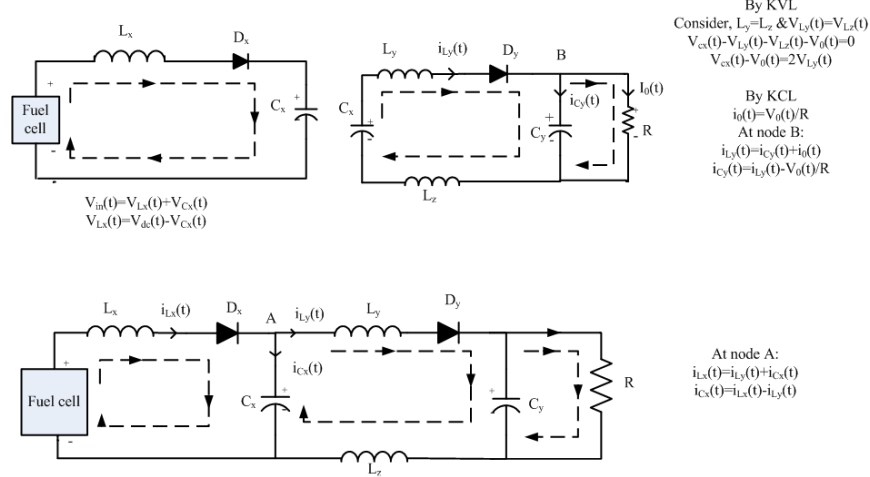


Figure 8. The configurations of mode 2

From the voltage-second balance principle, the steady state voltage of input capacitor C_X is calculated as follows:

$$V_{in}(t) T_{on} + (V_{in}(t) - V_{CX}(t)) T_{OFF} = 0 \quad (6)$$

$$(t) T_{on} = -V_{in}(t) T_{OFF} + V_{CX}(t) T_{OFF} \quad (7)$$

$$V_{in}(t) (T_{on} + T_{OFF}) = V_{CX}(t) T_{OFF} \quad (8)$$

$$V_{CX}(t) = \frac{V_{in}(t) (T_{on} + T_{OFF})}{T_{OFF}} \quad (9)$$

$$V_{CX(avg)} = V_{in} \left(\frac{T_{total}}{T_{total} - T_{ON}} \right) \quad (10)$$

$$V_{CX(avg)} = V_{in} \left(\frac{1}{1 - D} \right) \left(\because \frac{T_{on}}{T_{total}} = D \right) \quad (11)$$

From the loop equations in mode1 and mode 2 configurations,

$$V_{CX(avg)} = V_0 \left(\frac{1 - D}{1 + D} \right) \quad (12)$$

Equation 11 provides the voltage gain of the converter based on the information above.

$$\frac{V_0}{V_{in}} = \frac{1 + D}{(1 - D)^2} \quad (13)$$

Tables 1 and 2, respectively, show each element's voltage and current stresses. Each element is stressed at a lower voltage than that of the output voltage. As a result, this topology has a significant advantage. It aids in our decision-making process when selecting low-rated devices, increasing the system's overall

effectiveness. Tables 1 and 2 display the voltage and current stresses placed on each component, respectively. The benefit of this design is that each component has a voltage stress that is lower than the output voltage. The system's overall effectiveness is increased because it allows us to choose devices that have low ratings.

Switching Device	Voltage Stress at Peak
CH_x	$V_o(1 - D)/(1 + D)$
CH_y	$V_o/(1 + D)$
CH_z	$V_o/(1 + D)$
D_x	$V_o(1 - D)/(1 + D)$
D_y	$2V_o/(1 + D)$

Table 1. The switching devices' voltage stresses.

Switching Device	RMS Current Stress
CH_x	$I_{in}\sqrt{D}$
CH_y	$(1 - D)\sqrt{D}I_{in}/2$
CH_z	$(1 - D)\sqrt{D}I_{in}/2$
Free-Switch Diodes	Average Current Stress
D_x	$I_{in}(1 - D)$
D_y	$(1 - D)^2 I_{in}/2$

Table 2. The switching devices' current stresses.

5.3. Inductor L_x design

The L_x current in an inductor is shown in Figure 9. I_1 stands for the inductor L_x current's average value, and Δi_{Lx} is the difference between the peak and average currents.

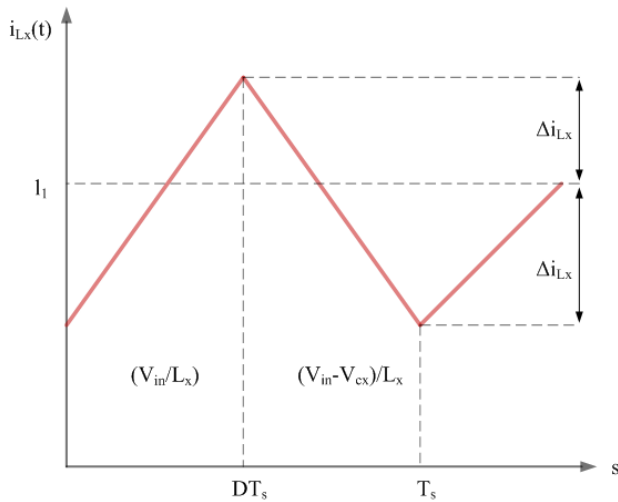


Figure 9. The inductor L_x current

The ripple of inductor L_x is given for the first interval of the switching cycle,

$$2\Delta iL_x = \left(\frac{V_{in}}{L_x} \right) DTs \quad (14)$$

$$L_x = \left(\frac{V_{in}}{2\Delta iL_x} \right) DTs \quad (15)$$

5.4. Inductor L_y and L_z

Similar to the current through the L_z , Figure 10 represents the inductor L_y current waveform. It is stated as the difference between the average current and peak current of the inductor, and it stands in for the average value of the L_y current. When the first interval of the switching cycle is taken into account, the inductor L_y 's ripple is taken into account.

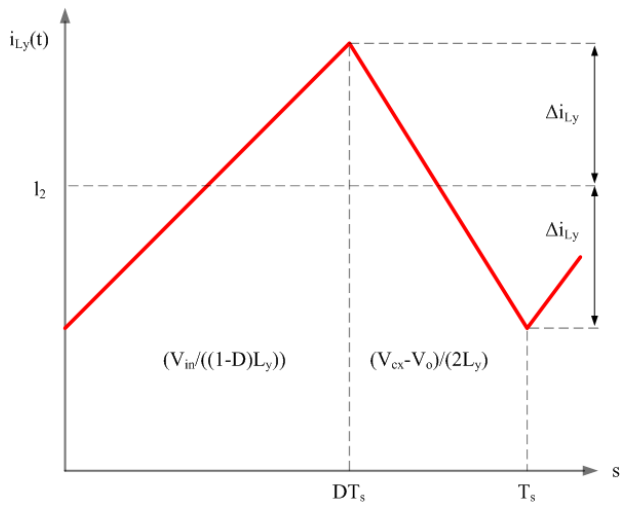


Figure 10. The inductors L_y and L_z currents

$$2\Delta iL_y = \left(\frac{V_{in}}{L_y} \right) \left(\frac{DTs}{1-D} \right) \quad (16)$$

$$L_y = L_z = \left(\frac{V_{in}}{2\Delta iL_y} \right) \left(\frac{DTs}{1-D} \right) \quad (17)$$

Equation (17) states that the input voltage V_{in} , duty cycle D, sample time Ts , and inductor current ripple i_{L_y} all have an impact on the inductance of inductors L_y and L_z .

5.5. Capacitor C_x design

Similar to capacitor C_y , capacitor C_x 's design is complex; without the dc components, its current is the same as that of inductor L_x (see figure 10). Figure 11 shows the capacitor voltage as it approaches its maximum and minimum limits at the two zero crossing points of its current waveforms. The greatest ripple of the capacitor's C_x voltage and total charge q have the following relationship:

$$q = C_x(2\Delta V_c) \quad (18)$$

where ΔV_{c_x} which is the difference between the capacitor's average and maximum voltage values.

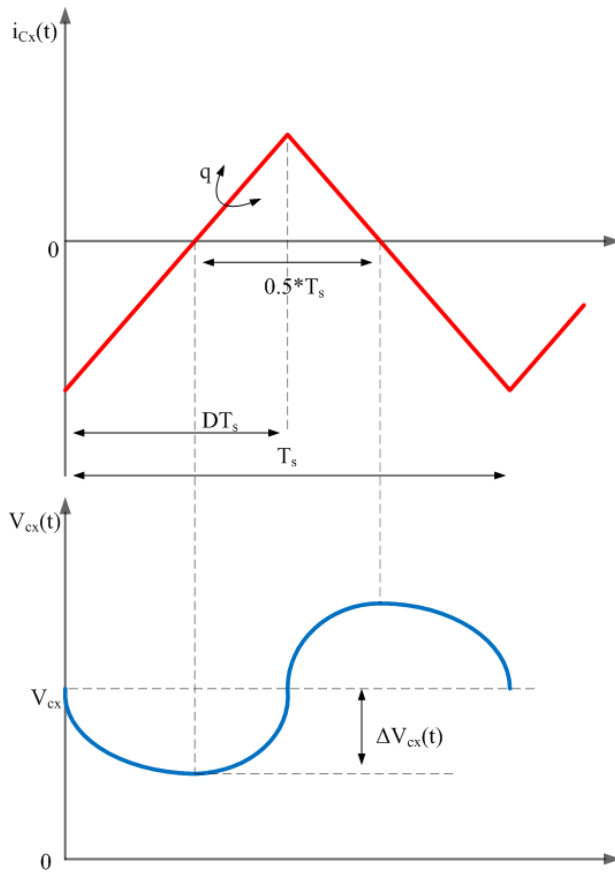


Figure 11. Current and voltage across the capacitor C_x

The capacitor's symmetry determines the current waveform, and the charge q value is determined by embedding the shaded portion of the C_x current:

$$q = \frac{1}{2} \Delta i_L \frac{T_s}{2} \quad (19)$$

Equation (18) is replaced by Equation (19), and the voltage ripple peak amplitude solution is obtained.

$$\Delta v_x = \frac{\Delta i_L T_s}{8C_x} \quad (20)$$

$$C_x = \frac{\Delta i_L T_s}{8\Delta V C_x} \quad (21)$$

The capacitor value is influenced by the sampling interval, the permitted ripple on the capacitor C_x , and the current ripple of the inductor L_x .

5.6. Output Capacitor C_y

The quantity of ripple allowed on the capacitor's C_y voltage limits the converter's output voltage ripple. To keep the converter output voltage ripple within the permitted range, capacitor C_y must be constructed. Figure 12 shows the capacitor C_y voltage along with the mean capacitor voltage \bar{V}_o and the discrepancy between the median wage and peak capacitor voltages V_o . By taking into account the first switching cycle duration, the ripple of capacitor C_y is determined.

$$\Delta v_o = \left(\frac{V_o}{2RC_y} \right) DT_s \quad (22)$$

$$\Delta C_y = \left(\frac{V_o}{2\Delta V_o} \right) DT_s \quad (23)$$

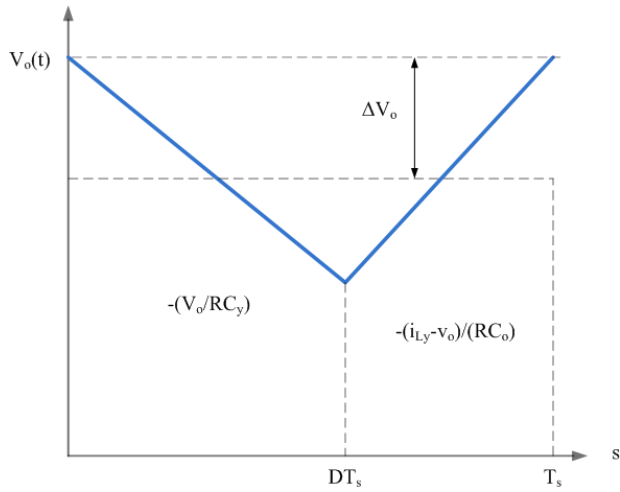


Figure 12. The capacitor C_y output voltage

Equation (23) shows how the capacitor C_y 's value is influenced by the output voltage V_o , duty cycle D, sampling time T_S , and capacitor voltage ripple V_o .

6. Results

To confirm the suggested converter's functionality and properties, it is simulated using MATLAB software. The table below provides the MATLAB Simulation parameters needed to create the suggested converter.

Component	Description	Specification
V_{in}	Input voltage	20V
V_o	Output voltage	60V
L_x	Inductor	11.33μH
L_y, L_z	Inductors	20.83μH
C_x	Input Capacitor	20.83μF
C_y	Output Capacitor	34μF
R_o	Resistor	1.44Ω
$M(D) = V_o / V_{in}$	Gain	3
D	Duty Ratio	0.34
F_s	Switching Frequency	60000Hz
P_o	Rated Output Power	2500W

Table 3. simulation component values.

From the above table 3, the input voltage is 20V. The proposed converter is designed for a 2.5KW output power; higher switching frequencies (f_s) are recommended to reduce converter size. Higher switching

frequencies (f_s) are not necessary for the proposed simulation, though; the design takes the frequency of 60 kHz into consideration. Three inductors, two capacitors, and five energy elements make up the proposed converter. The energy component values are calculated and observed using significant current and voltage ripples on the inductors and capacitors, respectively.

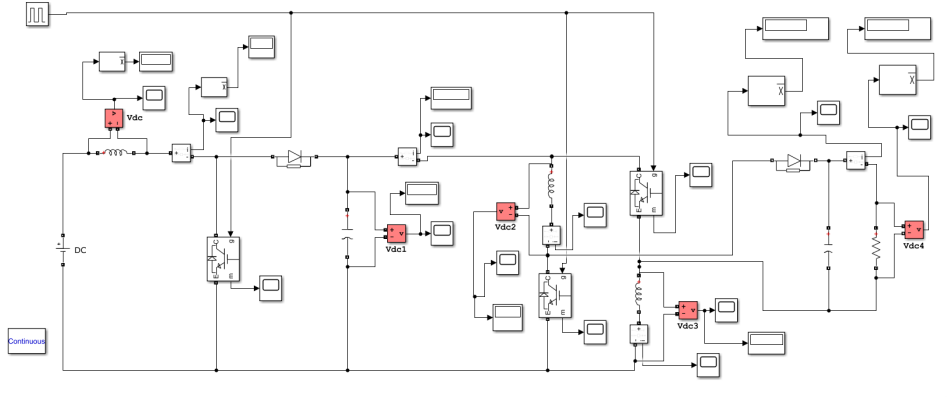


Figure 13. Simulation diagram of the proposed converter

Figure 13 shows the results of a MATLAB simulation used to assess the viability and validity of the suggested ultra-voltage gain boost converter. The description of the system components listed in table 3 is used in MATLAB simulation. The duty ratio is set at 0.34, the input side voltage is 20V, and the evaluated output side voltage across the converter is approximately 60V in the case study depicted in the following figure. The waveforms of switches voltage stresses are clearly displayed in Figures 14 and 15. While switches CH_x and CH_y experience different voltage stresses, CH_y and CH_z experience similar voltage stresses. Compared to switch voltage stresses across CH_y and CH_z the switch voltage stress across CH_x has a lower value.

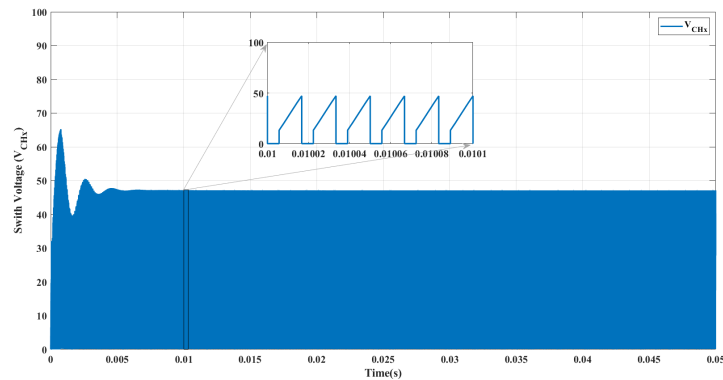


Figure 14. switch CH_x voltage stress waveform

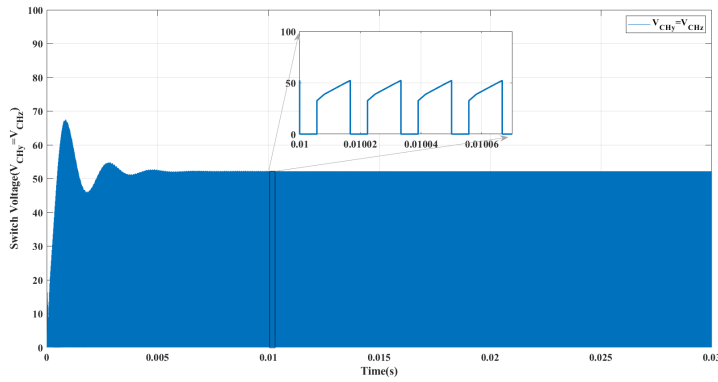


Figure 15. switch CH_y and CH_z voltage stress waveforms

Figure 16 shows the simulation results of voltage stress waveform across capacitor CH_x of the designed converter. The charging and discharging of capacitor CH_x is observed in the simulated waveform and it is deduced that theoretical analysis of the ripple value is exactly similar to the value of ripple content obtained through simulation. Figure 17 shows the simulation results of input current waveform at Duty ratio D=0.34.

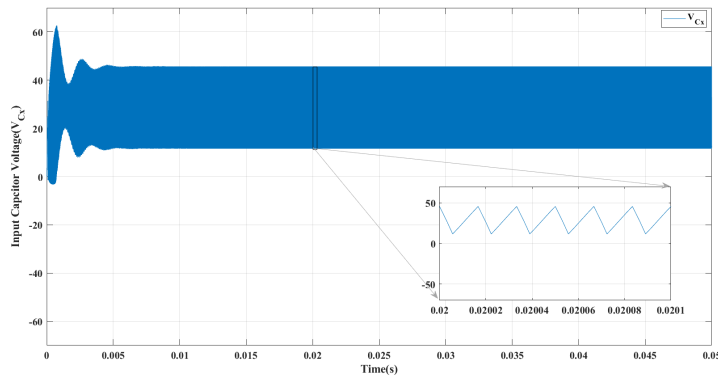


Figure 16. Input capacitor CH_x voltage stress waveform

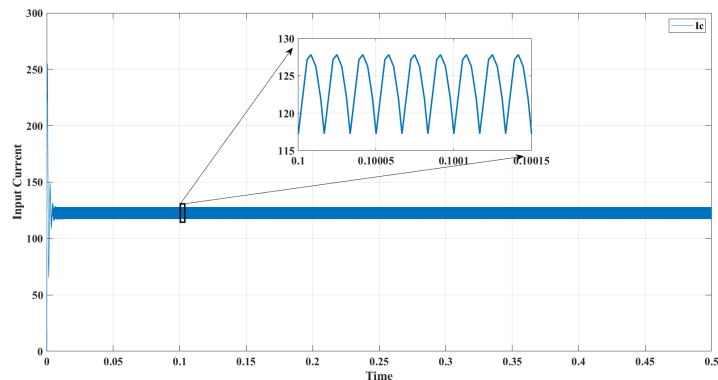


Figure 17. Input current waveform

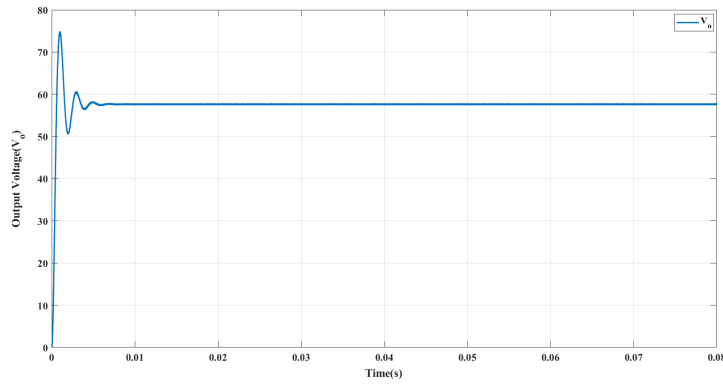


Figure 18. Output voltage waveform

Figure 18 clearly shows the suggested model's predicted output voltage waveform. When the input voltage is 20V and the duty ratio is set to 0.34, the theoretical output voltage is roughly 60V. The simulation produced an output voltage value of 60V. The output voltage derived through theoretical analysis is equivalent to it.

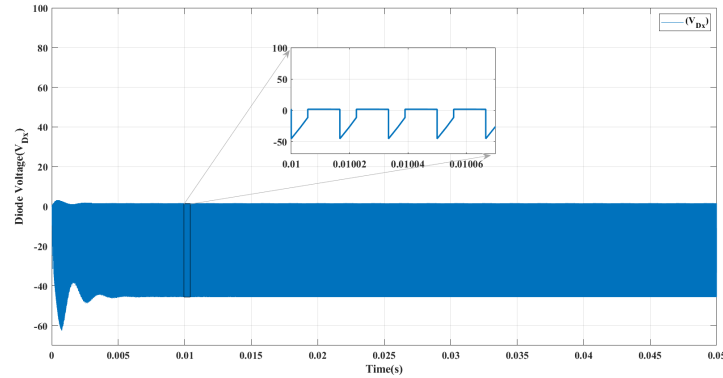


Figure 19. Diode D_X voltage stress waveforms

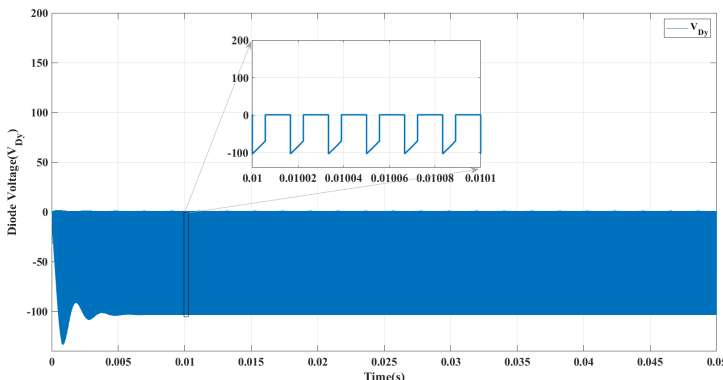


Figure 20. Diode D_Y voltage stress waveforms

Figures 19 and 20 show simulated Diode voltage stress waveforms of the suggested converter. Diode voltage stresses are lower in value and are shown with negative values.

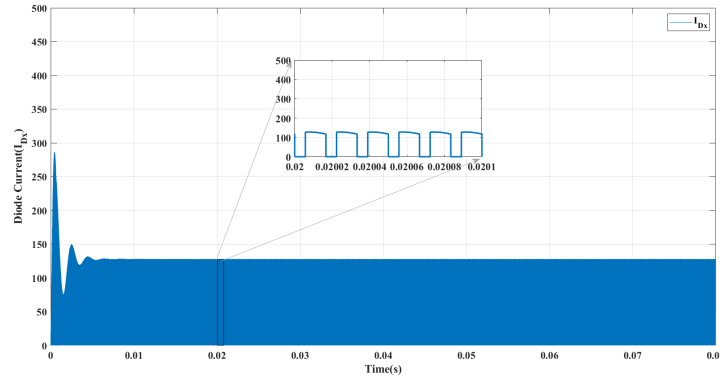


Figure 21. Diode D_X current stress waveform

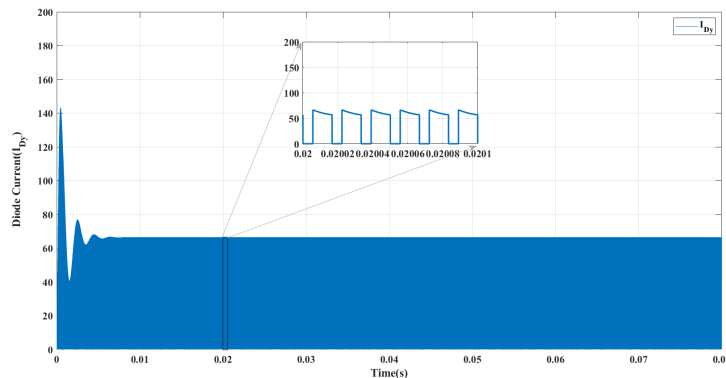


Figure 22. Diode D_Y current stress waveform

Figure 21 and 22 show simulated diode current stress waveforms of the suggested converter. For proper demonstration, a steady-state segment with few complete cycles is exhibited in the figures. Diode current stresses are lower in value.

Analysis is done on the converter's performance in terms of output power, output voltage, output current, and efficiency. The table presents the simulated values of different parameters for various duty ratios. From performance table 4, it is clear that for varied duty ratios, the suggested converter maintains higher efficiency. As the value of the duty ratio increases, losses increase, and efficiency slightly drops.

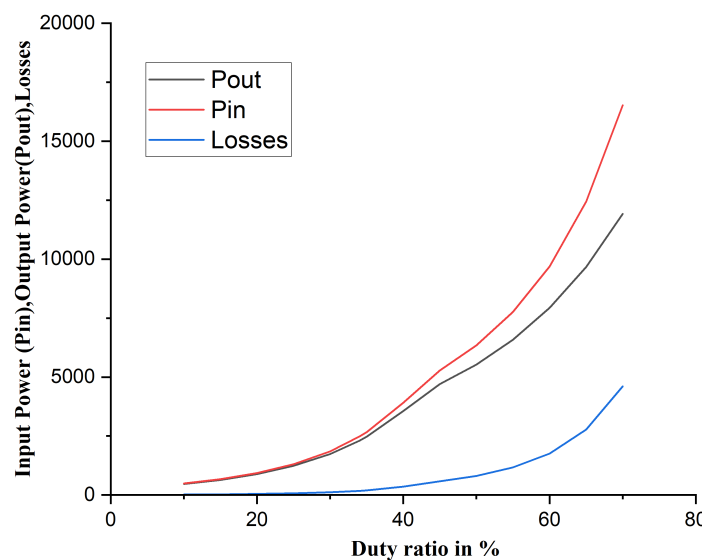
Table 5 gives the comparison between theoretical and simulated values of switch voltage stresses for various duty ratios. Upto 50% duty ratio, the theoretical values are almost equal to the simulated values. Beyond 50% duty ratio, the switch voltage stresses increase exponentially.

To understand clearly the characteristics of the designed converter, the graphs of various parameters concerning duty ratio are plotted (figures 23-27) and they clearly show how the specific parameter changes with respect to changes in duty ratios.

D	V_o	I_o	P_o	P_{i_n}	% η
10	25.9	18.03	468.23	489.6	95.6
15	30.38	21.09	640.71	671	95.4
20	35.66	24.77	883.29	928.4	95.1
25	42.11	29.25	1231.71	1301.4	94.6
30	49.97	34.7	1733.9	1847.6	93.8
34	57.56	34.97	2300.67	2476	92.91
35	59.67	41.44	2472.7	2668	92.6
40	71.59	49.72	3559.4	3912	90.9
45	82.26	57.12	4698.6	5276	89.05
50	89.24	61.98	5531	6340	87.7
55	97.34	67.6	6580.1	7752	84.8
60	106.9	74.2	7931.9	9692	81.8

Table 4. Performance of Proposed converter.

D	$V_{CH_X}(T)$	$V_{CH_X}(S)$	$V_{CH_y}(T)$	$V_{CH_y}(S)$	$V_{CH_z}(T)$	$V_{CH_z}(S)$
10	22.22	22.28	24.69	24.18	24.69	24.18
15	23.52	23.69	27.68	26.82	27.68	26.82
20	25	24.9	31.25	30.38	31.25	30.38
25	26.66	26.6	35.55	34.8	35.55	34.8
30	28.57	27.2	40.81	39.8	40.81	39.8
34	30.30	30.35	45.91	44.1	45.91	44.1
35	30.76	32.5	47.33	45.4	47.33	45.4
40	33.33	35.5	55.55	53.7	55.55	53.7
45	36.36	40.4	66.11	60.7	66.11	60.7
50	40	41.12	80	67.42	80	67.42
55	44.44	46	98.76	70.76	98.76	70.76
60	50	54.4	125	77.2	125	77.2

Table 5. Switch voltage stresses of proposed converter.**Figure 23.** Power vs duty ratio.

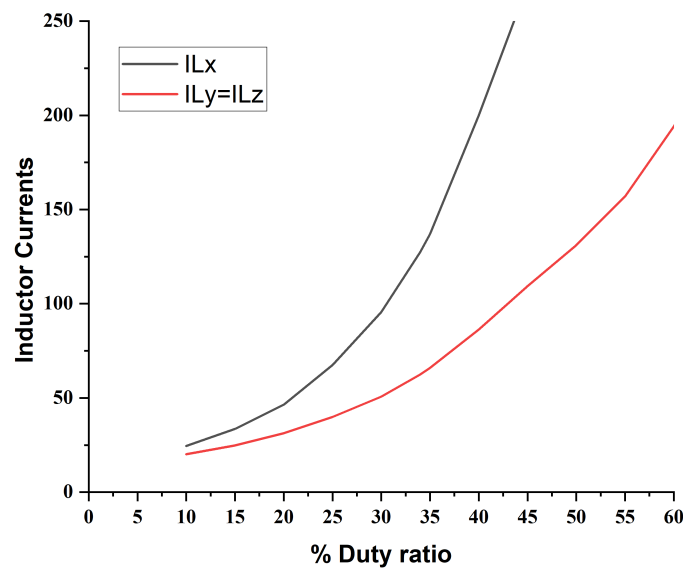


Figure 24. Inductor currents vs duty ratio.

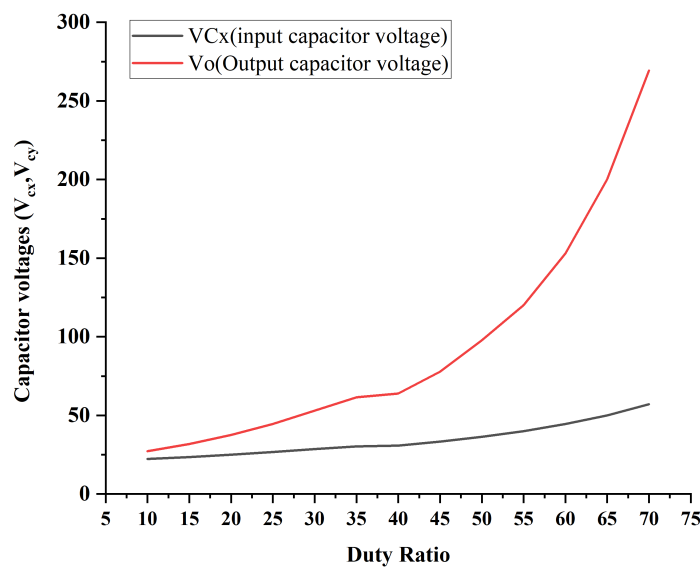


Figure 25. Capacitor voltages vs duty ratio.

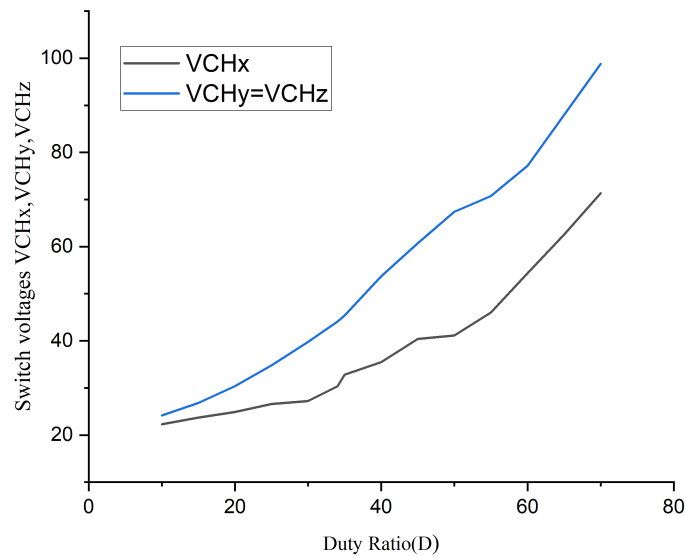


Figure 26. Switch voltages vs duty ratio.

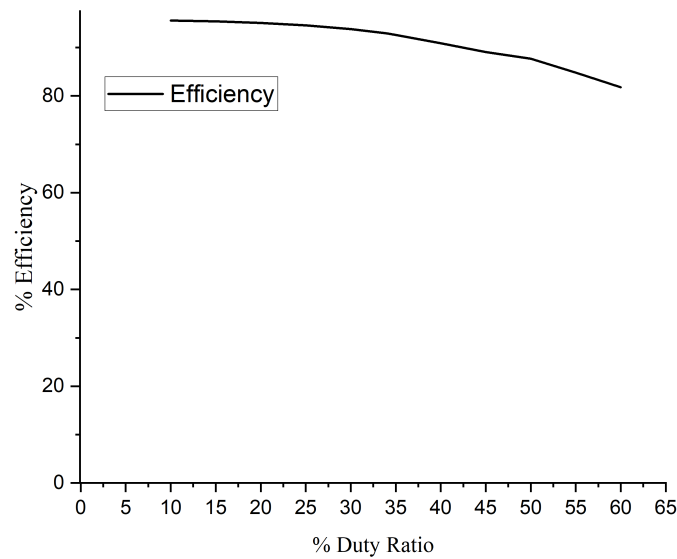


Figure 27. Efficiency vs duty ratio.

In terms of the quantity of energy elements, switches, diodes, and voltage gain, Table 6 compares the performance of the proposed converter with that of existing topologies. A graph of the voltage gain in response to the converters' duty ratio can be seen in Figures 28 and 29. It may be concluded that the suggested converter generates a high boost factor when compared to other converters for the same duty ratio. Table 6 demonstrates that the typical boost converter's applications are restricted since it cannot provide

a high voltage gain. The proposed boost converter produces a high boost factor i.e.; $(1 + D)/(1 - D)^2$ when compares the traditional boost converter. The energy elements present are low-rated components that reduce the cost, and size of the converter.

S.No	Converter	No.of Inductors	No.of Capacitors	No.of Diodes	No.of Power switches	Total No.of Components	Voltage Gain
1	Boost	1	1	1	1	4	$1/(1 - D)$
2	SL Boost	2	1	4	1	8	$(1 + D)/$ $(1 - D)$
3	SC Boost Non-isolated bidirectional DC-DC converter [25]	1	3	1	1	6	$1/(1 - D)$
4	A New High-Gain DC-DC Converter [26]	2	3	0	4	9	$1/(1 - D)^2$
5	An interleaved boost DC-DC converter [27]	2	2	2	2	8	$(1 + D - D^2)/$ $(1 - D)^2$
6	Non-isolated high step-up DC-DC converters [28]	2	3	4	2	11	$2/(1 - D)$
7	Ultra-voltage gain boost converter	2	5	4	1	12	$(2 + D)/$ $(1 - D)$
8		3	2	2	3	10	$(1 + D)/$ $(1 - D)^2$

Table 6. Comparison values of proposed converter with different converter topologies.

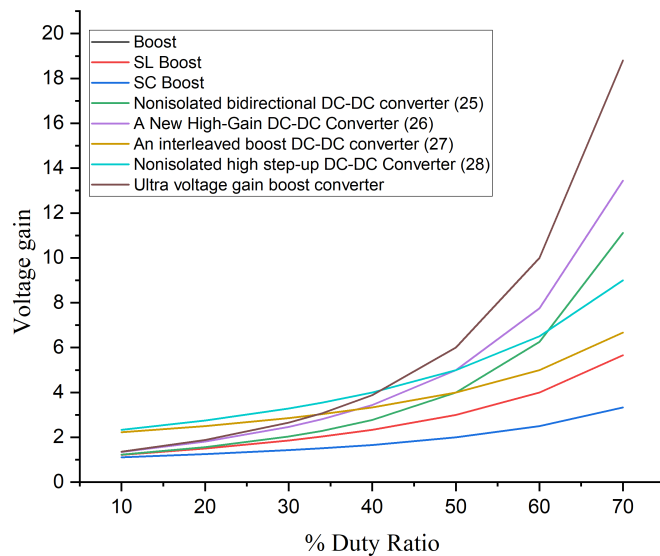


Figure 28. Voltage gain comparison between the suggested converter and different topologies.

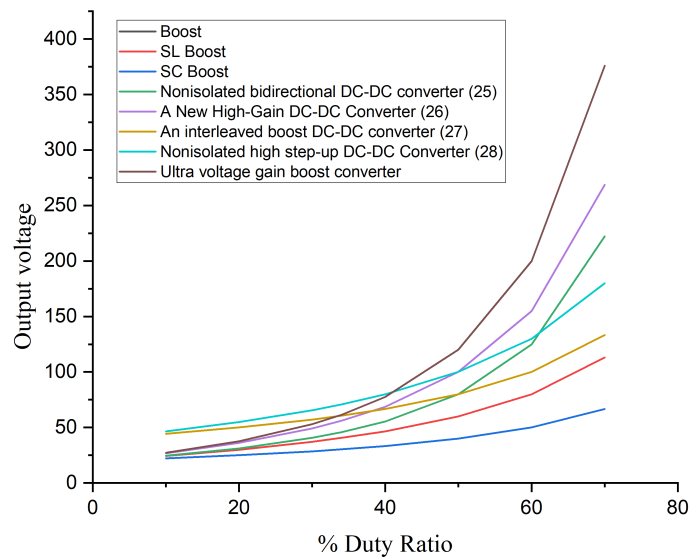


Figure 29. Comparison of the proposed converter's output voltage to that of other topologies.

Figures 28 and 29 depict characteristic curves like voltage gain and output voltage of different topologies to help us determine the proposed converter's level of performance. The suggested converter's output voltages have higher duty ratios than those of any existing converter topologies. The key advantage of the suggested converter is a larger voltage gain at lower voltage and current strains. The output voltage and voltage gain of the suggested converter are high when compared to alternative topologies.

7. Conclusion

A fuel cell based ultra-voltage gain boost converter for electrical vehicle applications is proposed. Three switches, two diodes, two capacitors, and three inductors make up the designed configuration. The performance of the proposed converter in continuous current mode for steady state condition is analyzed. The proposed boost converter may be seen to deliver considerable voltage gain even at low duty ratios. When compared to the topologies that are currently in use, the suggested converter has reduced voltage and current stresses. Therefore, the efficiency of the proposed converter is high for various duty ratios. The theoretical interpretation is provided to support the experimental findings. The converter that is being proposed has characteristics like increased step-up gain voltage, continuous input current, increasing efficiency, and fewer components. Hence, it is suitable for fuel-cell systems and Electric vehicle applications.

References

- [1] P. T. Bankupalli, S. Ghosh, L. Kumar, and S. Samanta, "Fractional order modeling and two loop control of PEM fuel cell for voltage regulation considering both source and load perturbations," *Int. J. Hydrog. Energy*, vol. 43, no. 12, pp. 6294–6309, Mar. 2018, doi: 10.1016/j.ijhydene.2018.01.167.
- [2] A. W. Al-Dabbagh, L. Lu, and A. Mazza, "Modelling, simulation and control of a proton exchange membrane fuel cell (PEMFC) power system," *Int. J. Hydrog. Energy*, vol. 35, no. 10, pp. 5061–5069, May 2010.
- [3] Nagi Reddy, B., Kosika, S.P., Gadham, M.P., Banoth, J., Banoth, A., Goud, S. B: Analysis of positive output buck-boost topology with extended conversion ratio. *J. Energy Syst.* 6(1), 62–83 (2022)
- [4] Alamri, B.; Alahmadi, A. "Family of transformer less quadratic boost high gain dc-dc converters". *Energies* 2021, 14, 4372.
- [5] Barbosa, E.A.O.; Carvalho, M.R.S.D.; Rodrigues Limongi, L.; Cavalcanti, M.C.; Barbosa, E.J.; Azevedo, G.M.D.S. "High-gain high-efficiency dc–dc converter with single-core parallel operation switched inductors and rectifier voltage multiplier cell". *Energies* 2021, 14, 4634.
- [6] Pereira, A.V.C.; Cavalcanti, M.C.; Azevedo, G.M.; Bradaschia, F.; Neto, R.C.; Carvalho, M.R.S.D."A novel single-switch high step-up dc–dc converter with threewinding coupled inductor". *Energies* 2021, 14, 6288.
- [7] Souza, L.C.; Morais, D.C.; Silva, L.D.S.D.C.E.; Seixas, F.J.M.D.; Arenas, L.D.O. "DC-DC 3SSC-a-based boost converter: Analysis, design, and experimental validation". *Energies* 2021, 14, 6771.
- [8] Gholizadeh, H.; Gorji, S.A.; Afjei, E.; Sera, "D. Design and implementation of a new cuk-based step-up DC–DC converter". *Energies* 2021, 14, 6975.
- [9] Chub, A.; Vinnikov, D.; Blaabjerg, F.; Peng, F.Z. "A review of galvanically isolated impedance-source DC-DC converters". *IEEE Trans. Power Electron.* 2016, 31, 2808– 2828.
- [10] Abdel-Rahim, O.; Chub, A.; Blinov, A.; Vinnikov, D. "New high-gain noninverting buck-boost converter". In Proceedings of the IECON 2021–47th Annual Conference of the IEEE Industrial Electronics Society, Toronto, ON, Canada, 13 October 2021; pp. 1–6.
- [11] Ojeda-Rodríguez, Á.; González-Vizuete, P.; Bernal-Méndez, J.; Martín-Prats, M.A. "A survey on bidirectional dc/dc power converter topologies for the future hybrid and all electric aircrafts". *Energies* 2020, 13, 4883.
- [12] De Souza, A.F.; Tofoli, F.L.; Ribeiro, E.R. Switched capacitor dc-dc converters: A survey on the main topologies, design characteristics, and applications. *Energies* 2021, 14, 2231.
- [13] Forouzesh, M.; Siwakoti, Y.P.; Gorji, S.A.; Blaabjerg, F.; Lehman, B. Step-up DC-DC converters: A comprehensive review of voltage-boosting techniques, topologies, and applications. *IEEE Trans. Power Electron.* 2017, 32, 9143–9178.

- [14] Andrade, A.M.S.S.; Martins, M.L.D.S. "Quadratic-boost with stacked zeta converter for high voltage gain applications". IEEE J. Emerg. Sel. Top. Power Electron. 2017, 5, 1787–1796.
- [15] Ai, J.; Lin, M. "Ultra large gain step-up coupled-inductor dc-dc converter with an asymmetric voltage multiplier network for a sustainable energy system". IEEE Trans. Power Electron. 2017, 32, 6896–6903.
- [16] Zhang, Y.; Gao, Y.; Zhou, L.; Sumner, M. "A switched-capacitor bidirectional dc-dc converter with wide voltage gain range for electric vehicles with hybrid energy sources". IEEE Trans. Power Electron. 2018, 33, 9459–9469.
- [17] Axelrod, B.; Berkovich, Y.; Ioinovici, A. Switched-capacitor/switched-inductor structures for getting transformer less hybrid DC-DC pwm converters. IEEE Trans. Circuits Syst. 2008, 55, 687–696.
- [18] Young, C.-M.; Chen, M.-H.; Chang, T.-A.; Ko, C.-C.; Jen, K.-K. Cascade Cockcroft–Walton Voltage Multiplier Applied to Transformer less High Step-Up DC-DC Converter. IEEE Trans. Ind. Electron. 2013, 60, 523–537.
- [19] Andrade, A.M.S.S.; Hey, H.L.; Schuch, L.; da Silva Martins, M.L. Comparative Evaluation of Single Switch High-Voltage Step-Up Topologies Based on Boost and Zeta PWM Cells. IEEE Trans. Ind. Electron. 2018, 65, 2322–2334.
- [20] De Paula, W.J.; Júnior, D.O.O.; Pereira, D.D.; Tofoli, F.L. "Survey on non-isolated high-voltage step-up dc-dc topologies based on the boost converter". IET Power Electron. 2015, 8, 2044–2057
- [21] Waradzyn, Z.; Stala, R.; Mondzik, A.; Penczek, A.; Skala, A.; Pirog, S. "Efficiency Analysis of MOSFET-Based Air-Choke Resonant DC-DC Step-Up Switched Capacitor Voltage Multipliers". IEEE Trans. Ind. Electron. 2017, 64, 8728–8738.
- [22] Cervera, A.; Evzelman, M.; Peretz, M.M.; Ben-Yaakov, S. "A high-efficiency resonant switched capacitor converter with continuous conversion ratio". IEEE Trans. Power Electron. 2015, 30, 1373–1382.
- [23] Stala, R.; Waradzyn, Z.; Mondzik, A.; Penczek, A.; Skała, "A. DC-DC high stepup converter with low count of switches based on resonant switched-capacitor topology". In Proceedings of the 2019 21st European Conference on Power Electronics and Applications (EPE'19 ECCE Europe), Genova, Italy, 2–5 September 2019; pp. P.1–P.10.
- [24] Shoyama, M.; Naka, T.; Ninomiya, T. "Resonant switched capacitor converter with high efficiency". In Proceedings of the 2004 IEEE 35th Annual Power Electronics Specialists Conference 2004, Aachen, Germany, 20–25 June 2004; Volume 5, pp. 3780–3786.
- [25] Ardi, H.; Ajami, A.; Kardan, F.; Avilagh, S.N. "Analysis and implementation of a nonisolated bidirectional DC-DC converter with high voltage gain". IEEE Trans. Ind. Electron. 2016, 63, 4878–4888.
- [26] Ahmad, J.; Zaid, M.; Sarwar, A.; Lin, C.-H.; Asim, M.; Yadav, R.K.; Tariq, M.; Satpathi, K.; Alamri, B. "A New High-Gain DC-DC Converter with Continuous Input Current for DC Microgrid Applications". Energies 2021, 14, 2629.
- [27] R. Gules, L. L. Pfitscher, and L. C. Franco, "An interleaved boost DC-DC converter with large conversion ratio," in Proc. IEEE Int. Symp. Ind. Electron., 2003, pp. 411–416.
- [28] G. Wu, X. Ruan, and Z. Ye, "Nonisolated high step-up DC-DC converters adopting switched-capacitor cell," IEEE Trans. Ind. Electron., vol. 62, no. 1, pp. 383–393, Jan. 2015.